CHARACTERIZING THE MICROBIAL RESPONSE TO PLASTIC AND BIOPLASTIC DEBRIS IN THE MARINE ENVIRONMENT

A Dissertation

By

LEE J. PINNELL

BS, University of Waterloo, 2009
MS, University of Waterloo, 2011

Submitted in Partial Fulfillment of the Requirements of the Degree of

DOCTOR OF PHILOSOPHY

in

MARINE BIOLOGY

Texas A&M University-Corpus Christi
Corpus Christi, Texas

December 2019

December 2019

CHARACTERIZING THE MICROBIAL RESPONSE TO PLASTIC AND BIOPLASTIC DEBRIS IN THE MARINE ENVIRONMENT

A Dissertation

By

LEE J. PINNELL

This dissertation meets the standards for scope and quality of
Texas A&M University-Corpus Christi and is hereby approved.

Dr. Jeffrey W. Turner, PhD
Chair

Dr. Christopher E. Bird, PhD
Committee Member

Dr. Jeremy L. Conkle, PhD
Committee Member

Dr. Michael S. Wetz, PhD
Committee Member

Dr. Patrick Crowley, PhD
Graduate Faculty Representative

December 2019

ABSTRACT

Plastic is the most abundant type of debris found in the marine environment, commonly representing between 60-95% of all marine debris. Plastic debris accumulation is greatest in urbanized coastal zones and closed bays or lagoons with limited flushing, and benthic environments are the final resting place for the majority of this debris, as biofouling leads to the sedimentation of floating plastics and many plastics have higher densities than seawater. However, the impact of plastic debris on benthic microbial communities is largely unknown. Similarly, the impact of bioplastics, which are promising alternatives for mitigating plastic pollution, is virtually unknown. The goal of this study was to characterize how benthic microbial communities respond to the deposition of both plastic (polyethylene terephthalate; PET) and bioplastic (polyhydroxyalkanoate; PHA) in coastal marine sediments. The microbial community colonizing ceramic served as a biofilm control while the free-living microbial community in the overlying water served as a non-biofilm control. Findings showed that biofilm communities (i.e. PET, PHA, and ceramic) were taxonomically distinct in comparison to free-living communities. Further, the PET and ceramic communities were indistinguishable. By contrast, bioplastic selected for a distinct microbial community that was enriched for depolymerases and dominated by sulfate-reducing microorganisms (SRM). Successional patterns demonstrated that the PHA-associated communities remained atypical and dominated by SRM throughout a 424-day microcosm. The isolation and whole-genome sequencing of individuals from PHA-associated biofilms led to the discovery of *Bacillus* strains capable of degrading PHA and reducing sulfate. The results presented here clearly demonstrate that plastic was not colonized by a unique microbial community whereas bioplastic was. Additionally, culture-independent and culture

dependent experiments showed that the PHA-associated microbial community was capable of PHA degradation and sulfate reduction. Given that SRM mediate carbon mineralization in coastal sediments, bioplastic loading and the subsequent enrichment of SRM could unintendedly alter sediment biogeochemistry. Future scientific investigation and government legislation should consider the microbial response to plastic as well as bioplastic loading when developing legislation and best-management practices related to plastic pollution.

ACKNOWLEDGEMENTS

I'd like to start by thanking my amazing spouse, Dr. Tracy Smith, who will no longer (unless something goes horribly wrong) be able to lord her doctorate over me! In all seriousness though, without her support while I jetted off to winterless South Texas from the Great White North this wouldn't have been possible. Harvey said it best, "Me lobe yoy long time". I'd also like to thank the rest of my family and friends for their support throughout the past four years.

A massive thank you to my supervisor Dr. Jeff Turner for his encouragement, advice, and dedication to me and our entire lab. Your leadership has made these four years of work not only bearable, but incredibly enjoyable and rewarding. Additionally, thank you to Drs. Chris Bird, Jeremy Conkle, and Mike Wetz for your advice and support throughout.

Thank you to the entire staff of the Center for Coastal Studies and Dr. Paul Zimba for providing my great office space, numerous trips to the field, and support throughout this whole process. Specifically, I'd like to thank Bobby, Jay, and Baxter for some very interesting, if nothing else, boat trips. Long live Chuck Mangione.

Last but not least, a huge thank you to my lab and office mates. In no particular order, Nicole, Megan, Rachel, Morgan, Joey, Wade, Christian, Hailey, Sandra, Giulia – thank you for making coming to work fun and not really like work at all. Paxton – thanks for nothing. Someday, I hope you all acquire the skills to rise to the level of 27X Hate Ball champion.

Support for this study was provided by the Natural Sciences and Engineering Research Council of Canada, the Texas General Land Office, Texas Sea Grant, and the Texas Research and Development Fund.

And now for something completely different.

TABLE OF CONTENTS

LIST OF FIGURES

FIGURES PAGE

LIST OF TABLES

TABLES PAGE

INTRODUCTION

Plastic pollution in marine environments

The mass production of plastics in the 1940s was celebrated as the dawn of a new era – the Age of Plastic (Thompson et al., 2009b). The benefits of plastic were obvious: it's inexpensive, lightweight, durable, and corrosion-resistant. The prolific use of plastic has spurred a greater than 500-fold increase in plastic manufacturing annually since 1950 (Thompson et al., 2009b). However, the detriments associated with the loading of natural environments with plastic waste were not anticipated. Recent studies have estimated that 5.5 billion tons of plastic waste have entered natural environments (Geyer et al., 2017). In 2010 alone, between 5.3 and 14.0 million tons of plastic waste entered the oceans (Jambeck et al., 2015). As a result, our oceans are now awash with over 5 trillion pieces of floating plastic debris weighing approximately 270,000 tons (Eriksen et al., 2014).

Plastic is the most prominent type of anthropogenic debris found in marine environments, representing between 60-95% of all marine debris (Moore, 2008). The abundance of plastic debris strongly correlates ($r^2 > 0.97$) with human habitation (Barnes, 2005), but plastic has been found in even the most remote locations. For example, plastic debris has been found on the remote uninhabited oceanic islands of Antarctica within the Southern Ocean (Convey et al., 2002). The vast majority of plastic debris found in remote locations originates from land and is carried there by ocean currents (Barnes et al., 2009; Galgani, 2015). Within the open ocean, plastic debris accumulates in eddies and convergences (Shaw and Mapes, 1979). For example, it has been well documented that plastic debris accumulates in oceanic gyres, with the density of debris reaching 5,114 g km^{-2} in the North Pacific Gyre (Moore et al., 2001). However, the

accumulation of plastic waste is greatest in coastal seas, bays, and lagoons surrounded by densely populated coastlines (Eriksen et al., 2014). In particular, closed bays and lagoons with limited flushing (i.e. limited exchange with larger water bodies) are sinks for the accumulation of plastic debris (Barnes et al., 2009).

There are numerous sources of plastic debris, which are broadly defined as either land-based or ocean-based. Land-based sources are responsible for approximately 80% of plastic debris in the marine environment (Li et al., 2016a), with the major source being improper waste disposal (Derraik, 2002). For example, researchers have found that improper solid waste disposal and accidental spillage during handling and other processes were responsible for large quantities of plastic debris on beaches (Redford et al., 1997; Derraik, 2002). Other land-based sources include effluent from wastewater treatment plants and leachate from landfills (Browne et al., 2010). Ocean-based sources represent the remaining 20% of marine plastic debris, of which commercial fishing gear is the only major contributor (Li et al., 2016a). Approximately 640,000 tons of discarded fishing gear is estimated to be added to the marine environment each year, representing roughly 10% of all marine debris (Good et al., 2010). There is considerable evidence demonstrating that the level of fishing activity correlates with the amount of plastic debris in the marine environment (e.g. Cunningham and Wilson, 2003; Edyvane et al., 2004; Ribic et al., 2010; Li et al., 2016a).

Plastic debris is commonly divided into three broad classes based on size: macroplastic (>200 mm), mesoplastic (5-200 mm), and microplastic (<5 mm). Microplastics, in particular, have received considerable interest due to their overwhelming abundance in marine environments and their small size, which makes them accessible to a larger range of marine organisms (Law and Thompson, 2014). Early reports of what we now call microplastics

described large quantities of resin pellets found along the eastern seaboard of the United States in the early 1970s (Colton et al., 1974). Microplastics have now been found in virtually every part of the marine environment including coastal sediments (Claessens et al., 2011; Mohamed Nor and Obbard, 2014), deep-sea sediments (Van Cauwenberghe et al., 2013; Woodall et al., 2014), surface water (Thompson et al., 2004; de Lucia et al., 2014), sub-surface water (Desforges et al., 2014; Kanhai et al., 2018), and arctic sea ice (Obbard et al., 2014). The abundance of microplastics in marine environments has consistently increased (Thompson et al., 2004) and their composition has shifted from being made up of mostly resin pellets to fragmented pieces of larger plastic debris (Ryan, 2008; Ryan et al., 2009).

Microplastics are generally classified into two categories: primary or secondary. Primary microplastics are manufactured for use in clothing and a variety of consumer care products like cosmetics, body wash, and toothpaste (Derraik, 2002; Fendall and Sewell, 2009). Primary microplastics also include resin pellets, which serve as feedstock for the manufacture of plastic products. These resin pellets frequently enter the oceans as a result of accidental losses during transport or run-off from processing and manufacturing facilities (Andrady, 2011). Secondary microplastics are created through the photo-degradation and subsequent fragmentation of larger plastic debris (Moore, 2008; Barnes et al., 2009). The five types of microplastics most frequently encountered in the marine environment are polypropylene (PP), low-density polyethylene (LDPE), polyvinyl chloride (PVC), high-density polyethylene (HDPE), and polyethylene terephthalate (PET) (Andrady, 2011).

PET is of great concern in the coastal bend of Texas as the world's largest PET manufacturing facility will be commissioned in May 2020 (Acosta, 2019). Additionally, there is already a high concentration of plastic manufacturing plants along the Texas coast and Texas

shipped more plastic than any other state in 2017 (Plastics Industry Association, 2018). PET is a semi-crystalline thermoplastic polyester with average specific gravity of 1.37 (Müller et al., 2001; Andrady, 2011). Its high mechanical strength, low permeability to gases, and aesthetic appearance make it an excellent industrial plastic. There are two major uses of PET: 1) the use of PET fibers in the textile industry to produce clothing, upholstery, and sheets, and 2) the use of PET resin pellets as feedstock to manufacture packaging and beverage containers (Kint and Muñoz-Guerra, 1999; Gupta and Bashir, 2002). The demand for bottle-grade PET has surpassed the demand for fibers in North America and western Europe (Gupta and Bashir, 2002). To supply the high demand, 56 million tons of PET were manufactured in 2013 (Yoshida et al., 2016), but only 29% of available PET is recycled (National Association for PET Container Resources, 2018). As a result of this improper disposal, PET debris has become a ubiquitous pollutant in marine environments across the globe (World Economic Forum - Ellen MacArthur Foundation, 2016).

The lifespan of petroleum-based plastics like PET in the marine environment is mainly due to their recalcitrant nature, which is the product of condensation polymerization reactions during the manufacturing process that form high-energy bonds between petroleum-derived monomers (Kint and Muñoz-Guerra, 1999). While plastics are highly resistant to degradation, microbial enzymes capable of breaking their high-energy bonds have been identified (Wei and Zimmermann, 2017). A bacterium capable of degrading PET (*Ideonella sakaiensis* 201-F6) was isolated from a PET-bottle recycling factory (Yoshida et al., 2016). It produces two enzymes capable of hydrolyzing PET and the reaction intermediate mono(2-hydroxyethyl) terephthalic acid (Yoshida et al., 2016). Microorganisms capable of degrading plastics may be restricted to highly polluted sites as previous reports have described microorganisms originating from plastic-

contaminated soils (Orr et al., 2004; Sivan et al., 2006; León-Zayas et al., 2019), landfills (Esmaeili et al., 2013; Gajendiran et al., 2016), waste-water facilities (Mukherjee et al., 2016), and recycling facilities (Yoshida et al., 2016). To date, microorganisms from the marine environment capable of degrading plastics are limited to two strains originally isolated from seawater that degraded PE following extensive enrichment culturing in the laboratory (Sudhakar et al., 2008).

Impact of plastic on marine organisms

The detrimental effects of plastic on a wide variety of marine organisms are well documented and the two major areas of concern are entanglement and ingestion. Entanglement is a serious threat to sea turtles (Nelms et al., 2015), seals (Page et al., 2004; Boren et al., 2006; Lawson et al., 2015), seabirds (Schrey and Vauk, 1987; Votier et al., 2011), fish (Degange and Newby, 1980), and whales (Winn et al., 1979; Neilson et al., 2009). Entanglement accounts for 13-29% of mortalities in gannets in the North Sea and it is one of the major causes of sea turtle mortality in northern Australia and the Mediterranean Sea (Casale et al., 2010; Jensen et al., 2013). Seals, especially juvenile seals, are susceptible to entanglement as they are attracted to floating debris (Derraik, 2002; Lawson et al., 2015). Once entangled, an animal may drown, incur wounds, or experience a reduced ability to catch prey or avoid predators (Laist, 1997). For all marine animals, the threat of entanglement, primarily through discarded fishing gear (Derraik, 2002; Stelfox et al., 2016) remains a significant concern.

There is a vast body of literature on the ingestion of plastic debris by marine organisms and the problems associated with it have been described worldwide. The shape and coloration of plastic fragments in marine environments causes them to be mistaken for food by various marine

animals (Moser and Lee, 1992). For example, plastic pellets resembling fish eggs have been ingested by fish (Carpenter et al., 1972). Microplastics are especially susceptible to being ingested due to their small size, and are mistaken for food by both fish and suspension-feeding biota such as zooplankton, crustaceans, and bivalves (Browne et al., 2008; Boerger et al., 2010; Cole et al., 2013; Devriese et al., 2015). While ingestion rates vary between species and locations, it is clear that ingestion occurs throughout the food web from the aforementioned zooplankton up to large pelagic fishes, seabirds, and marine mammals (Denuncio et al., 2011; Choy and Drazen, 2013; Wilcox et al., 2015; Schuyler et al., 2016).

Some of the earliest reports of plastic ingestion by marine organisms were focused on seabirds, with multiple plastic fragments found in the stomachs of albatrosses on Pacific islands near Hawaii in the late 1960s (Kenyon and Kridler, 1969). In the northwestern Atlantic, a fourteen-year study during the 1970s and 1980s found that 21 of 38 seabird species had ingested plastic (Moser and Lee, 1992). A more recent study spanning four years sampled 1,295 northern fulmars (*Fulmarus glacialis*) from the North Sea and found that 95% of them had plastic in their stomachs, which on average contained 35 particles and weighed 0.31 g (van Franeker et al., 2011). A 2019 study that took place in the Indian Ocean revealed that 79% of shearwaters and 59% of petrels ingested plastic (Cartraud et al., 2019). Interestingly, while a lower proportion of petrels ingested plastic, they ingested higher amounts of plastic per bird than the shearwaters. An alarming trend is that the ingestion rates by seabirds are increasing and a model has predicted that by 2050 99% of all seabird species will have ingested plastic (Wilcox et al., 2015).

Plastic ingestion by zooplankton has been described in marine environments worldwide, including the Pacific Ocean (Desforges et al., 2015), the Atlantic Ocean (Cole et al., 2013), and the South China Sea (Sun et al., 2017). Research on zooplankton from the northeast Atlantic

determined that thirteen species of copepods had the ability to ingest plastic beads ranging in size from 1.7 – 30.6 μm (Cole et al., 2013). In the northeast Pacific, the amounts of ingested microplastic ranged from 0.026 ± 0.005 particles per copepod to 0.058 ± 0.01 particles per euphausiid, and that zooplankton located closer to shore ingested higher levels of plastic (Desforges et al., 2015). While using a different scale to quantify ingestion, the study in the South China Sea also demonstrated that zooplankton at higher trophic levels exhibited higher rates of plastic ingestion (Sun et al., 2017). Regardless of study location, findings indicated that marine zooplankton ingest plastic, which can have a negative impact on their function and health.

Studies investigating the ingestion of microplastic debris by crustaceans and mollusks have reported very high rates of ingestion. For example, microplastic was found in the stomachs of 83% of a commercially important European crustacean (*Nephrops norvegicus*) sampled in the Firth of Clyde off the western coast of Scotland (Murray and Cowie, 2011). Similarly, 63% of brown shrimp (*Crangon crangon*) sampled in the North Sea contained microplastics in their stomach, with an average of 1.23 ± 0.99 microplastics per shrimp (Devriese et al., 2015). In mollusks, the presence of microplastics has been observed in both wild and cultured populations (De Witte et al., 2014; Mathalon and Hill, 2014; Van Cauwenberghe and Janssen, 2014). In the North Sea, averages of 0.36 ± 0.07 and 0.47 ± 0.16 particles$\times g^{-1}$ were observed in mussels (*Mytilus edulis*) and oysters (*Crassostrea gigas*), respectively (Van Cauwenberghe and Janssen, 2014). Mussels from the west coast of Scotland were found to contain between 1.05 ± 0.66 and 4.44 ± 3.03 particles$\times g^{-1}$, which is considerably higher than the mussels from the North Sea (Courtene-Jones et al., 2017b). In mussels from the eastern coast of Canada, higher amounts of plastic were detected in cultured mussels versus wild mussels, with 75 and 34 plastic fragments

per mussel found in cultured and wild mussels, respectively (Mathalon and Hill, 2014). The majority of studies focused on crustaceans and bivalves have been conducted in coastal systems, but interestingly, similar rates of plastic ingestion have been reported in deep-sea benthic invertebrates (Courtene-Jones et al., 2017a).

Ingestion of microplastics by marine fish has been extensively documented, but levels of ingestion vary between fish species and sampling location. A study investigating rates of ingestion of three demersal commercial fish species examined over 200 fish and demonstrated that 17.5% of the fish ingested microplastics with an average of 1.56 ± 0.5 particles per fish (Bellas et al., 2016). In cod (*Gadus morhua*) sampled from the English Channel, a much higher rate of 33% was reported (Foekema et al., 2013). Another study examined a semi-pelagic species of seabream in the Mediterranean Sea and reported that 57.8% of all sampled fish stomachs (n = 195) contained microplastics (Nadal et al., 2016). Also within the Mediterranean Sea, larger pelagic fish like swordfish and tuna have been shown to ingest microplastics, with rates ranging from 12.5% to 32.4% (Romeo et al., 2015). An open-ocean study investigated microplastic ingestion by 27 species of mesopelagic fish (n = 141) from the North Pacific Subtropical Gyre and reported that 9.2% of fish stomachs contained plastic (Davison and Asch, 2011). As a whole, this study estimated that mesopelagic fishes in the North Pacific ingest between 12,000 – 24,000 tons of plastic per year. In coastal environments, research has shown that three species of catfish (n = 180) ingested plastic at rates ranging from 18% to 33% (Possatto et al., 2011) and that 7.2% of two drum species (n = 569) contained plastic in their stomachs (Dantas et al., 2012). A robust study investigating 69 different estuarine fish species (n = 2,233) found an average ingestion rate of 1.06 ± 0.30 particles per fish and concluded that microplastic ingestion occurred regardless of

fish size and functional group (Vendel et al., 2017). Clearly, microplastic ingestion is widespread amongst marine fishes.

Studies have estimated that over half of the world's sea turtles have ingested plastic (Schuyler et al., 2016). Oceanic-stage sea turtles are at a greater risk of plastic ingestion than coastal turtles, and herbivorous or gelatinovorous species are also more likely to ingest plastic (Schuyler et al., 2014). For example, 83% of oceanic-stage loggerheads sampled near the North Atlantic Subtropical Gyre were reported to have ingested plastic (Pham et al., 2017), but a study in the Adriatic reported lower ingestion rates, with 35.2% of loggerheads containing plastic debris in their stomachs (Lazar and Gračan, 2011). Of all sea turtles, oceanic leatherback and green turtles are believed to be at the highest risk for both lethal and sublethal effects from plastic ingestion (Schuyler et al., 2016). As in the case with seabirds, the probability of turtles ingesting plastic is expected to increase over time (Schuyler et al., 2016).

Plastic ingestion by cetaceans has also been reported, with ingestion being documented for at least 26 species (Baird and Hooker, 2000). Multiple reports of manatee mortalities as a result of plastic ingestion have been reported in Florida, with ingestion rates being estimated at 14.4% for the Florida manatee (*Trichechus manatus latirostris*) (Laist, 1987; Beck and Barros, 1991). Various species of whales including humpback (Besseling et al., 2015), pygmy sperm (Tarpley and Marwitz, 1993), orca (Baird and Hooker, 2000), True's beaked (Lusher et al., 2015), and Blainville's beaked (Secchi and Zarzur, 1999) have been described ingesting plastic. As the largest animals in the ocean, whales tend to ingest the largest fragments of plastic, which typically causes death by obstructing their stomach compartments (Tarpley and Marwitz, 1993).

An issue further compounding the concerns of plastic ingestion is the leaching of chemical additives and adsorbed chemicals into marine organisms. Many plastics contain

additive plasticizers like phthalates and nonylphenol that could be transferred to organisms if ingested (Koch and Calafat, 2009; Oehlmann et al., 2009). Further, because of their hydrophobic surface, plastics represent an adsorbent for organic compounds and heavy metals in seawater (Rios et al., 2007; Holmes et al., 2014; Rochman et al., 2014). A wide variety of chemicals, including aldehydes, ketones, esters, acids, peresters, and peracids are capable of adsorbing to plastics (Rjeb et al., 2000; Teuten et al., 2007). This issue is of particular concern for microplastics as their larger surface area to volume ratio increases contact between plastic and organism (Browne et al., 2008). The interaction between plastic and these substances could cause them to be transported into organisms (Mato et al., 2001; Rochman et al., 2013). Importantly, chemicals adsorbed to plastic are released much faster within an organism's gut than in seawater, which may be attributed to a lower pH and a higher temperature in the gut (Bakir et al., 2014). Plastics can therefore be considered a vehicle for the transport of toxic chemicals into marine food webs.

Impact of plastic on marine microorganisms

Microorganisms rapidly colonize and form biofilms on biotic and abiotic surfaces in marine environments (Dang and Lovell, 2016). As such, marine microbial communities are commonly distinguished as free-living or particle-associated (DeLong et al., 1993; Crump et al., 1999; Hollibaugh et al., 2000). A particle-associated lifestyle is thought to provide microorganisms with increased nutritional resources and environmental stability (Azam et al., 1994). Detrital aggregates, in particular, are hotspots of microbial diversity that are fundamentally distinct in comparison to free-living communities (DeLong et al., 1993; Crump et al., 1999). Particles are also habitats of enhanced enzyme activity (Karner and Herndl, 1992;

Kellogg and Deming, 2014) that contribute to the rapid turnover of particulate organic matter (Biddanda and Pomeroy, 1988; Azam and Long, 2001) and it is clear that particle-associated microorganisms play an important role in biogeochemical processes (Ploug et al., 1999; Seymour et al., 2017).

Plastic pollution has introduced a new surface for microbial colonization and biofilm formation (Zettler et al., 2013; Oberbeckmann et al., 2014). The majority of studies assessing the impact of plastic on marine microorganisms have focused primarily on floating plastic debris of unknown origin collected at random with neuston nets (Lobelle and Cunliffe, 2011; Zettler et al., 2013; Bryant et al., 2016; Kirstein et al., 2016; Pedrotti et al., 2016; Didier et al., 2017). A study on plastic surveys of the marine environment found that 41 of 50 (82%) reviewed papers sampled plastic via neuston nets (Conkle et al., 2018). Given that the colonization of abiotic surfaces is nonspecific and shaped by the surrounding environment (Dang and Lovell, 2016), the unknown life history of the plastic associated with this type of sampling makes it challenging to decipher and understand plastic-microorganism interactions.

Plastic, like all surfaces in the marine environment, is rapidly colonized by microorganisms. For example, research has demonstrated that biofilms developed within seven days on floating plastic debris in the English Channel (Lobelle and Cunliffe, 2011). The biofilm formation coincided with changes to the physiochemical properties of the plastic, with submerged plastic becoming less hydrophobic and more neutrally buoyant over time (Lobelle and Cunliffe, 2011). Several studies have characterized the pelagic microbial colonization of plastic in ocean gyres (Carson et al., 2013; Zettler et al., 2013; Bryant et al., 2016). In the North Pacific Gyre, a study reported that microplastic biofilms were dominated by pennate diatoms and species of *Bacillus* (Carson et al., 2013). Moreover, free-living diatom abundance was correlated

with microplastic abundance. A separate study in the North Pacific Gyre reported an increased concentration of Chl *a* and an increased abundance of nitrogenase genes in microplastic-associated biofilms (Bryant et al., 2016). Together, these studies suggest that plastic debris may enhance primary production in this otherwise oligotrophic gyre.

Studies investigating the occurrence of pathogenic microorganisms within the biofilms formed on plastic debris have become more prevalent in recent years. The concept of pathogens hitchhiking on floating plastic debris was originally introduced in earlier studies aimed at characterizing the overall microbial community attached to plastic debris when they discovered the presence of potential pathogens such as *Vibrio* (Zettler et al., 2013). Since then, numerous studies have argued that plastic debris is enriched for pathogenic microbial species. *Vibrio*, in particular, has been established as a member of the biofilms formed on plastic debris in numerous studies (Zettler et al., 2013; Foulon et al., 2016; Keswani et al., 2016; Kirstein et al., 2016; Oberbeckmann et al., 2016). Other opportunistic pathogens, including *E. coli*, *Bacillus* species, *Pseudomonas* species, and Campylobacteraceae have also been identified as members of plastic biofilms (McCormick et al., 2014; Van der Meulen et al., 2014; Jiang et al., 2018). The presence of these pathogens in plastic-associated biofilms has led to the belief that plastic debris represents a reservoir for pathogens (Vethaak and Leslie, 2016), but whether pathogens are overrepresented on plastic surfaces versus other inert surfaces remains unknown.

One of the first studies to describe the structure of marine microbial communities forming biofilms on plastic debris demonstrated that the plastic-associated microbial community was taxonomically different than the free-living microbial community in the surrounding seawater (Zettler et al., 2013). Further research reported that plastic-associated microbial communities differed functionally from free-living microbial communities. Specifically, plastic-

associated microbial communities contained higher abundances of secretion system, chemotaxis, and nitrogen fixation genes (Bryant et al., 2016). However, as described previously, the taxonomic and functional differences between particle-associated and free-living microbial communities is a well-known dichotomy in microbial ecology (e.g. Biddanda and Pomeroy, 1988; Karner and Herndl, 1992; DeLong et al., 1993; Crump et al., 1999; Hollibaugh et al., 2000; Kellogg and Deming, 2014). By contrast, understanding of plastic-associated microbial communities versus biofilm controls is a critical knowledge gap.

Few studies assessing the interactions between marine microorganisms and plastics have included biofilm controls. The first utilized glass slides as an inert biofilm control for the colonization of pieces of PET bottles in the surface waters of the North Sea (Oberbeckmann et al., 2014). While using less robust methods than later studies, this study found there was no significant different between denaturing gradient gel electrophoresis (DGGE) community profiles between glass and PET (Oberbeckmann et al., 2014). A more recent study by the same group used 16S rRNA gene sequencing to provide a more complete picture of the microbial colonization of PET bottles and glass microscope slides in the surface waters of the North Sea (Oberbeckmann et al., 2016). The structure of the microbial communities colonizing the plastic differed significantly from the free-living community and varied with season and sampling station, suggesting that colonization was driven by conventional marine biofilm processes. Further, the microbial community colonizing the PET was indistinguishable from the community colonizing the glass biofilm control, suggesting that floating plastic debris acted as a raft for microbial biofilms, but it did not recruit and maintain a plastic-specific community. The PET biofilms did, however, contain a small number of enriched taxa, such as Cryomorphaceae and Alcanivoraceae, to suggest that specific taxa may interact with plastic debris.

Similarly, few studies have characterized microbe-plastic interactions in benthic systems (Harrison et al., 2014; De Tender et al., 2015; Nauendorf et al., 2016). The transport of plastic debris to benthic systems is facilitated by sinking; debris with a density higher than seawater (1.02 g cm^{-3}) sink immediately while floating debris lose buoyancy with biofouling (Barnes et al., 2009; Andrady, 2011). Sinking is therefore an important process and benthic systems are sinks for plastic debris accumulation (Thompson et al., 2004; Van Cauwenberghe et al., 2015). In these coastal marine environments, benthic microorganisms play an invaluable role in ecosystem processes (Klump and Martens, 1981), so understanding how benthic microorganisms are responding to plastic debris is paramount. A previous study showed that microorganisms rapidly colonize pelagic and benthic plastic debris (Harrison et al., 2014). Said study also demonstrated that the structure of the plastic-associated microbial communities converged over time regardless of sediment type (Harrison et al., 2014). However, that study was unable to show that plastic was colonized by a unique microbial community as its experimental design did not incorporate a biofilm control.

Regulatory and industrial solutions to plastic loading

Marine plastic pollution has been a growing concern for decades. While not aimed specifically at plastic, one of the first attempts to combat marine debris was the 1973 International Convention for the Prevention From Ships (MARPOL 73/78) (Xanthos and Walker, 2017). In 1988, a complete ban on disposal of plastics at sea was agreed upon by 134 countries, but the legislation was seemingly widely ignored. According to a 1997 estimate, 6.5 million tons of plastic was still discarded from ships per year (Clark, 1997) and the tonnage of plastic in the ocean has continued to increase (Xanthos and Walker, 2017). This increasing trend

is largely the result of the improper disposal of plastic waste on land and recent legislation has focused on mitigating land-based sources of plastic pollution.

Historically, legislative measures (e.g. levies and bans) have focused on the reduction or elimination of single-use plastics such as plastic bags. Governments across the globe have attempted to curb their use by banning their sale, charging for their use, or taxing the stores that use them (Xanthos and Walker, 2017). While these methods have been met with only limited success in North America, several countries in Asia, Africa, and Europe have successfully banned or implemented levies on plastic bag usage (Dikgang et al., 2012; Poortinga et al., 2013; O'Brien and Thondhlana, 2019). Importantly, India and China, two of the largest of producers of plastic waste entering the oceans, have also banned plastic bags (Xanthos and Walker, 2017). However, plastic bag usage remains very high among street vendors and small stores in China (Block, 2013).

Legislation aimed at reducing the use of microbeads has rapidly increased in the past few years. The province of Ontario passed legislation banning the manufacture of microbeads in 2015 (Legislative Assembly of Ontario, 2015). The United States implemented similar legislation that banned the manufacturing of cosmetics containing microbeads effective July 1, 2017, with no more sales allowed after July 1, 2019 (United States Congress, 2015). According to this act, microbeads are considered to be any particle less than 5 mm in size that are intended to be used to exfoliate or cleanse any part of the human body. It remains unclear whether microbeads intended for uses other than exfoliating or cleansing are banned, and therefore this act may not eliminate all microbead manufacturing (Conkle et al., 2018). Given the recent nature of these bans and the uncertainty surrounding their implementation and enforcement, their

impact on plastic pollution and the marine environment remains unknown (Xanthos and Walker, 2017).

As of 2018, more than 60 countries approved bans or levies against single-use plastics according to the United Nations Environmental Program (U.N.E.P., 2018). These bans and levies have resulted in over 140 regulations being passed into law at national and local levels, and the European parliament recently approved a ban on the top ten most abundant single-use plastics (E.U., 2018). Despite these efforts, there is still not adequate information to draw strong conclusions about the impact of these legislative actions. Up to 20% have had little to no impact and a lack of data has hindered impact assessments for more than 50% of these actions (U.N.E.P., 2018). In their 2018 report, the United Nations provides a ten-step roadmap to guide governments in directing legislation aimed at the reduction of plastic pollution including the promotion of biodegradable alternatives.

The promotion of alternatives includes the increased production and use of bioplastic. The term bioplastic encompasses both bio-based plastics and biodegradable plastics (European Bioplastics, 2018). A parallel aim of the legislative actions described in the previous paragraph is the increased production and use of bioplastic, and the growth of an innovative bioeconomy. For instance, Antigua and Barbuda legislated, as part of their plastic bag ban, that the materials used to manufacture bioplastic alternatives are to be kept tax free (U.N.E.P., 2018). In particular, bioplastics like polyhydroxyalkanoates (PHAs), that are both bio-based and biodegradable, have received considerable attention due to their reduced carbon footprint and enhanced waste management (European Bioplastics, 2018).

In recent years, PHAs have been considered strong candidates to replace petroleum-based plastics (Nehra et al., 2017). PHAs have material properties similar to those of petroleum-based

plastics, and have high a potential for use in household, medical, industrial, and other applications (Albuquerque et al., 2007). As a result, their industrial production was predicted to quadruple from 2018 to 2023 (Chinthapalli et al., 2019). PHAs are a diverse group of linear polyesters composed of ester bonds between the carboxyl group of one monomer and the hydroxyl group of neighboring monomers (Verlinden et al., 2007). They are broadly classified into two groups: short-chain length (3 – 5 carbon atoms) and medium-chain length (6 – 14 carbon atoms). More than 100 distinct monomers have been identified (Li et al., 2016b), but the most common and well-studied is poly-(3-hydroxybutyrate) (PHB). PHB is a short-chain length PHA that is highly crystalline and shares some mechanical properties with polypropylene (Antipov et al., 2006), but it is less permeable due to its low thermal stability and brittleness (Matsusaki et al., 2000). While PHB has been the target of most research efforts, other variants are also generating considerable research interest (Nehra et al., 2017).

Impact of bioplastic on marine microorganisms

At least 75 genera of microorganisms synthesize PHAs as intracellular energy storage compounds during periods of excess carbon coupled with nutrient limitation (Ishizaki et al., 2001; Reddy et al., 2003). Whether a microorganism synthesizes short- or medium-chain length PHAs is the determined by its metabolism and the substrate specificity of its PHA synthase enzyme (Solaiman and Ashby, 2005). For instance, the synthase of *Alcaligenes eutrophus* can only polymerize 3-hydroxyalkanoic acids made up of less than six carbon atoms, but species of *Pseudomonas* can polymerize 3-hydroxyalkanoic acids longer than six carbon atoms and can therefore accumulate medium-chain length PHAs (Anderson and Dawes, 1990). Microorganisms can accumulate incredibly high levels of PHA under certain environmental conditions. For

example, intracellular PHA granules can account for up to 80% of biomass in *Ralstonia eutropha* (Hawas et al., 2016). The level of accumulation varies between taxonomic groups, but multiple lineages are capable of using several different carbon sources for PHA production (Bharti and Swetha, 2016).

The prevalence of natural PHA has selected for a phylogenetically diverse and widely distributed taxon of PHA-degrading microorganisms (Emadian et al., 2017). While most have been isolated from soil or compost, members from diverse genera (e.g. *Alcaligenaceae, Alteromonadaceae, Bacillaceae, Comamonadaceae, Enterobacteriaceae, and Pseudoalteromonadaceae*) within the marine environment are capable of degrading PHAs (Mukai et al., 1993; Mergaert et al., 1995; Kita et al., 1997; Leathers et al., 2000; Volova et al., 2010). For example, strains of *Enterobacter*, *Bacillus*, and *Gracibacillus* from tropical coastal sediments were capable of degrading two forms of PHA under aerobic conditions (Volova et al., 2010). Two studies from vastly different environments (the North Sea and coastal waters around Puerto Rico) suggested strains of *Pseudoalteromonas* play a significant role in the degradation of PHA in marine environments (Mergaert et al., 1995; Leathers et al., 2000). A recent study comparing degradation in anaerobic sludge and seawater showed that members of *Clostridiales, Gemmatales, Phycisphaerales, and Chlamydiales* were associated with PHA degradation in seawater (Wang et al., 2018).

Several studies have quantified the degradation of PHA in marine environments (Sridewi et al., 2006; Thellen et al., 2008; Volova et al., 2010; Wang et al., 2018). A recent meta-study, utilizing PHA degradation data from multiple studies, calculated a mean biodegradation rate of 0.04 – 0.09 $mg_X day^{-1} cm^{-2}$, which translates to a 1.5 – 3.5 year lifespan for a PHA water bottle (Dilkes-Hoffman et al., 2019). The location of PHA in the water column (i.e. pelagic versus

benthic) was shown to affect the rate of degradation (Dilkes-Hoffman et al., 2019), with benthic bioplastic degrading faster than pelagic bioplastic (Mayer, 1990). This distinction could reflect the role of oxygen in PHA degradation, but oxygen has not been discussed as a limiting factor in marine-based studies (Dilkes-Hoffman et al., 2019). Temperature has been considered in previous marine degradation studies, with higher temperatures supporting higher rates of degradation. The degradation of samples incubated *in situ* was faster in warmer summer months (Mergaert et al., 1995) while a lab-based study suggested that colder temperatures slowed degradation rates (Thellen et al., 2008). Despite the numerous studies characterizing PHA degradation in marine environments, no one environmental factor has emerged as the key to degradation rates and further study is needed to understand the effects of individual and synergistic parameters (Dilkes-Hoffman et al., 2019).

In marine environments, the sedimentation of PHA will likely play an important role in its degradation as the density of PHA is greater than seawater (Dilkes-Hoffman et al., 2019). In benthic habitats, abiotic forces like UV degradation and wave action would be minimized (Gewert et al., 2015), but degradation by benthic microorganisms would be enhanced. Additionally, seeing that marine sediments are commonly anoxic, the PHA would be exposed to a taxonomically distinct group of microorganisms that range from facultative to obligate anaerobes.

Few studies have investigated the microbial response to bioplastic in marine sediments. One study compared the colonization rates of plastic and bioplastic bags at the sediment-water interface in a coastal region of the Mediterranean Sea and revealed that the plastic types were colonized at similar rates (Eich et al., 2015). The authors also demonstrated that the composition of diatoms differed between plastic and bioplastic surfaces. An *in vitro* study that incubated

plastic and bioplastic bags in sediment from the Baltic sea found that the biodegradable bags were colonized faster than PE counterparts (Nauendorf et al., 2016). Interestingly, the bioplastic bags were colonized five times faster under aerobic conditions and eight times faster under anaerobic conditions. This suggests that anaerobic marine microorganisms may preferentially colonize bioplastic. However, no degradation of either plastic or bioplastic was observed in either of these benthic studies, and the authors proposed that the lack of degradation was a result of either the preferential use of another carbon source or a lack of abiotic degradation initiators (Nauendorf et al., 2016).

Next-generation sequencing technologies, such as metagenomics, have rarely been used when assessing bioplastic-microbe interactions in marine sediments and therefore, the community composition of bioplastic biofilms remain unknown. Two early, culture-dependent studies demonstrated that the addition of PHA was correlated with sulfide production in anoxic sediments (Mas-Castellà et al., 1995; Urmeneta et al., 1995). A separate study identified a sulfate-reducing microorganism (SRM) capable of degrading PHB under anaerobic conditions (Çetin, 2009), suggesting that the deposition of PHB in marine sediments could impact sedimentary biogeochemical processes. The microorganism was as a strain of *Desulfotomaculum* from the Firmicutes group of SRM (Müller et al., 2014) and after 60 days of incubation, it produced as mass loss of 10% (Çetin, 2009). To date, this is the only known SRM proven capable of independently degrading PHA. In a scenario where bioplastic use and pollution are more common, understanding its impact on sedimentary processes like dissimilatory sulfate reduction (DSR) will be paramount.

Dissimilatory sulfate reduction in coastal sediments

In anoxic sediments, DSR is the dominant terminal process in the mineralization of organic matter, responsible for degrading up to 50% of all organic matter in coastal sediments (Jørgensen, 1982). A common pathway for DSR is shared amongst known SRM, beginning when the uptake of sulfate is mediated by ATP sulfurylase (SAT/MET3) to form adenosine-5'-phosphosulfate (APS). The APS is then reduced to sulfite by adenylyl-sulfate reductase (Apr) and the final step is the further reduction of sulfite to H_2S by the dissimilatory sulfite reductase (Dsr) complex (Purdy et al., 2002; Santos et al., 2015). The distribution, abundance, and diversity of SRM in the environment are commonly studied through the detection of genes encoding these enzymes (i.e. functional markers) in the DSR pathway (Wagner et al., 2005; Müller et al., 2014). The richness of these genes in many environments is dominated by novel sequences that represent a large number of microorganisms from unknown phylogenies (Müller et al., 2014).

A diverse group of microorganisms make up the known SRM, which are broadly divided into four groups: 1) Gram-negative mesophilic, 2) Gram-positive spore-forming, 3) thermophilic bacterial, and 4) thermophilic archaeal (Castro et al., 2000). While a large number of SRM belong to the Deltaproteobacteria, members from Actinobacteria, Firmicutes, Nitrospirae, Euryarchaeota, Crenarchaeota, and a large number of unclassified environmental lineages are also considered SRM (Müller et al., 2014). Within coastal marine sediments, members of *Desulfovibrionaceae, Desulfobacteraceae,* and *Desulfobulbaceae* have been identified as the dominant SRM and typically constitute 5-20% of the overall microbial community (Devereux et al., 1996; Purdy et al., 1997; Purdy et al., 2003). While numerous studies have characterized the

diversity and abundance of SRM within marine sediments, data describing the involvement of SRM in plastic and bioplastic colonization and degradation is a critical knowledge gap.

Future research into plastic and bioplastic microbial interactions

The majority of plastic-microbe and bioplastic-microbe research has assessed differences between plastic-associated (i.e. particle-associated) and free-living microbial community structure. Thus, little is known about differences between plastic-associated, bioplastic-associated, and other particle-associated microbial communities. Additionally, little is known about how plastic- and bioplastic-associated microbial communities function. Depolymerases, lipases, esterases, and cutinases can facilitate the biodegradation of both plastics and bioplastics (Sivan et al., 2006; Volova et al., 2010; Sharon and Sharon, 2017), but whether these enzymes are enriched on plastic and bioplastic surfaces remains unknown. Understanding how plastic- and bioplastic-associated microbial communities function will advance our understanding of plastic pollution in marine environments and assess the efficacy of using bioplastics as a replacement for petroleum-based plastics. Moreover, a functional understanding of these microbial communities will advance understanding of how their metabolism may impact biogeochemical processes such as sedimentary carbon mineralization.

CHAPTER 1:

SHOTGUN METAGNOMICS REVEALS THE BENTHIC MICROBIAL RESPONSE TO PLASTIC AND BIOPLASTIC IN A COASTAL MARINE ENVIRONMENT

This chapter published as Pinnell LJ., and Turner JW. (2019). Shotgun metagenomics reveals the benthic microbial community response to plastic and bioplastic in a coastal marine environment. *Front. Microbiol.* 10:1252. doi: 10.3389/fmicb.2019.01252

Abstract.

Plastic is incredibly abundant in marine environments but little is known about its effects on benthic microbiota and biogeochemical cycling. This study reports the shotgun metagenomic sequencing of biofilms fouling plastic and bioplastic microcosms staged at the sediment-water interface of a coastal lagoon. Community composition analysis revealed that plastic biofilms were indistinguishable in comparison to a ceramic biofilm control. By contrast, bioplastic biofilms were distinct and dominated by sulfate-reducing microorganisms (SRM). Analysis of bioplastic gene pools revealed the enrichment of esterases, depolymerases, adenylyl sulfate reductases (*aprBA*), and dissimilatory sulfite reductases (*dsrAB*). The nearly 20-fold enrichment of a phylogenetically diverse polyhydroxybutyrate (PHB) depolymerase suggests this gene was distributed across a mixed microbial assemblage. The metagenomic reconstruction of genomes identified novel species of *Desulfovibrio, Desulfobacteraceae, and Desulfobulbaceae* among the abundant SRM, and these genomes contained genes integral to both bioplastic degradation and sulfate reduction. Findings indicate that bioplastic promoted a rapid and significant shift in benthic microbial diversity and gene pools, selecting for microbes that participate in bioplastic degradation and sulfate reduction. If plastic pollution is traded for bioplastic pollution and sedimentary inputs are large, the microbial response could unintentionally affect benthic biogeochemical activities through the stimulation of sulfate reducers.

Introduction.

Microorganisms rapidly colonize and form biofilms on biotic and abiotic surfaces in marine environments (Dang and Lovell, 2016). As such, marine microbial communities are commonly distinguished as free-living or particle-associated (DeLong et al., 1993; Crump et al., 1999; Hollibaugh et al., 2000). A particle-associated lifestyle is thought to provide microorganisms with increased nutritional resources and environmental stability (Azam et al., 1994). Detrital aggregates, in particular, are hotspots of microbial diversity that are fundamentally distinct in comparison to free-living communities (DeLong et al., 1993; Crump et al., 1999). Particles are also habitats of enhanced enzyme activity (Karner and Herndl, 1992; Kellogg and Deming, 2014) that contribute to the rapid turnover of particulate organic matter (Biddanda and Pomeroy, 1988; Azam and Long, 2001) and it is clear that particle-associated microorganisms play an important role in biogeochemical processes (Ploug et al., 1999; Seymour et al., 2017).

Plastic pollution has introduced a new surface for microbial colonization and biofilm formation (Zettler et al., 2013; Oberbeckmann et al., 2014). A recent global assessment of all mass produced plastics estimated that 4.9 billion tons of plastic waste was discarded in landfills or natural environments (Geyer et al., 2017). Oceans serve as a sink for said waste with an estimated 4.8 to 12.7 million metric tons entering the oceans annually (Jambeck et al., 2015; Geyer et al., 2017). And it is clear that marine microorganisms colonize and form biofilms on floating plastic debris and it is also clear that plastic-associated microbial communities are distinct compared to free-living communities (Bryant et al., 2016; Oberbeckmann et al., 2016).

Several studies have characterized pelagic microbe-plastic interactions (Carson et al., 2013; Zettler et al., 2013; Bryant et al., 2016) but relatively few studies have characterized

microbe-plastic interactions in benthic systems (Harrison et al., 2014; De Tender et al., 2015; Nauendorf et al., 2016). In the North Pacific Gyre, a previous study reported that microplastics were colonized by diatoms (Carson et al., 2013) and a separate study reported an increased concentration of Chl *a* and an increased abundance of nitrogenase genes in microplastic biofilms (Bryant et al., 2016). By contrast, understanding of benthic microbe-plastic interactions are limited. The transport of plastic debris to benthic systems is facilitated by sinking; debris with a density higher than seawater (1.02 g cm^{-3}) sink immediately while floating debris lose buoyancy with biofouling (Barnes et al., 2009; Andrady, 2011). Sinking is therefore an important process and benthic systems are sinks for plastic debris accumulation (Thompson et al., 2004; Van Cauwenberghe et al., 2015).

In coastal regions, benthic microorganisms support primary producers in the overlying water column by the remineralization of organic-rich debris (Klump and Martens, 1981). The remineralization of carbon in anoxic coastal sediments is predominantly carried out via sulfate reduction (Jørgensen, 1977). The microbial pathway for dissimilatory sulfate reduction involves the reduction of sulfate to sulfite by sulfate adenyltransferases (Sat) and adenylyl-sulfate reductases (AprBA), followed by the reduction of sulfite by sulfite reductases (DsrAB) (Anantharaman et al., 2018). Climate warming and eutrophication are expanding the distribution of anoxic sediments worldwide (Vigneron et al., 2018) and recent studies have clearly shown that sulfate- and sulfite-reducers are more abundant, diverse and widespread that previously believed (Müller et al., 2014; Anantharaman et al., 2018; Hausmann et al., 2018; Vigneron et al., 2018; Zecchin et al., 2018). Yet the effect plastic pollution may have on sulfate-reducing microorganisms (SRM) is an open question.

In 2018, the United Nations Environmental Program reported that more than 60 countries approved bans or levies on single-use plastics (U.N.E.P., 2018). In the same year, the European Parliament approved a ban on the top ten single-use plastics and called for a reduction in single-use plastics (E.U., 2018). The proposal states "this systemic change and material substitution will also promote bio-based alternatives and an innovative bioeconomy". In the wake of legislative actions and increased public awareness, the production of bioplastics such as polyhydroxyalkanoate (PHA) is predicted to increase tenfold (Aeschelmann and Carus, 2015). If bioplastic is similarly discarded, the subsequent increase in bioplastic waste entering the oceans will introduce yet another surface for microbial colonization and while some research has investigated the response of marine organisms to bioplastic (Eich et al., 2015; Pauli et al., 2017), little is known about how microorganisms respond to bioplastic versus petroleum-based plastic.

The aim of this study was to characterize the microbial communities and individuals that form biofilms on plastic (polyethylene terephthalate; PET) and bioplastic (PHA) in a coastal benthic habitat. For comparative purposes, ceramic pellets were included as a biofilm control. This study was primarily designed to address two questions. Does the introduction of either plastic or bioplastic select for a distinct microbial community compared to a biofilm control, and does this introduction promote a significant shift in taxa or enzyme pools with implications for polymer degradation or biogeochemical cycling? We hypothesized that the PET biofilms would be indistinguishable from the ceramic biofilms whereas the introduction of PHA would select for the growth of a distinct microbial assemblage involved in polymer degradation and biogeochemical cycling.

Materials & Methods.

Site description

The Laguna Madre (Texas, USA) is a large coastal lagoon in the northern Gulf of Mexico (NGOM). The lagoon is divided into two sections: Upper Laguna Madre (ULM) and Lower Laguna Madre (LLM). The microcosms described in this study were deployed adjacent to a dredge material island at 27°32'39.0"N and 97°17'07.7"W in the ULM (Figure 1).The ULM is 76 km in length, 6 km in width, has an average depth of 0.8 m, and is separated from the NGOM by the Padre Island National Seashore (Tunnell, 2002). The dredge material island itself is remote to the nearest population center (Corpus Christi, TX) and is therefore relatively free of plastic pollution.

Figure 1. Map of sampling location showing the Upper Laguna Madre (ULM) along the northwestern Gulf of Mexico (Texas, USA) with the sampling site labeled.

Sample deployment and collection

A microcosm was designed to circumvent the challenges of isolating preexisting plastic debris from heterogeneous sediment samples. A microcosm also permitted the inclusion of a ceramic biofilm control. Briefly, 6.0 g of ceramic pellets (Lyman Products, Middletown, CT, USA), 3.0 g of PET pellets (M&G Chemicals, Ettelbruck, Luxembourg), and 3.0 g of PHA pellets (Doctors Foster and Smith, Rhinelander, WI, USA) were deployed in triplicate inside custom made microbial capsules (MicroCaps; Figure S2) at the sediment-water interface for 28 days (May 24, 2016 to June 21, 2016). All pellets were approximately 3-4 mm in diameter and therefore, the PET and PHA pellets were considered microplastics (Andrady, 2011). MicroCaps utilized 315 µm Nitex mesh to contain the pellets and permit the exchange of water, nutrients, bacteria, and some grazers but limit the entry of larger organisms. The microcosms and triplicate 1 L seawater samples (also from the sediment-water interface) were collected at the end of the exposure. All samples were stored on ice and processed immediately upon return to the laboratory, with the extraction procedure starting within two hours of sample collection. Substrates were washed three times with 25 mL of 0.22 µm filter-sterilized, site-specific seawater to remove any organisms not part of the biofilm. Seawater (100 mL) was pre-filtered through 315 µm Nitex mesh and the microbial community was collected by membrane filtration on a 0.22 µm polycarbonate filter (Millipore Sigma, Burlington, MA, USA) in triplicate. Environmental parameters from the start and end of the exposure period were collected using a 6920 V2-2 Multi-Parameter Water Quality Sonde (YSI, Yellow Springs, OH, USA) and varied minimally: water temperature (28.56-29.28 °C), salinity (37.78-40.28), pH (8.35-8.47), and DO (8.30-5.68 mg L^{-1}).

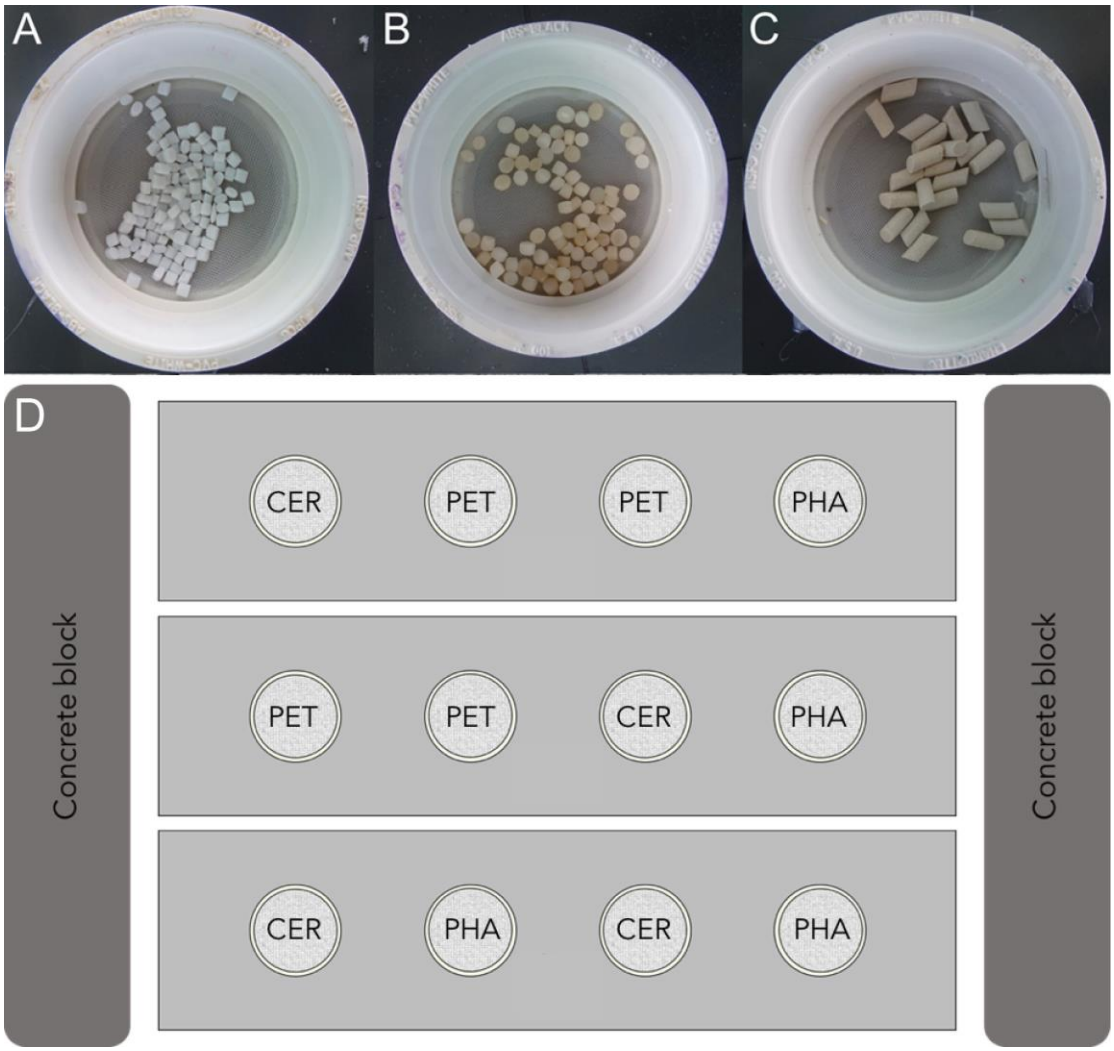

Figure 2. Example of the sampling device designed for this experiment. Each sampling device (D) consisted of a PVC frame containing four MicroCaps: A) polyethylene terephthalate (PET), B) polyhydroxyalkanoate (PHA), or C) ceramic pellets. A total of twelve MicroCaps (n=4 of each sample type) were deployed at the water-sediment interface using a randomized experimental design as shown in panel D.

DNA isolation

Genomic DNA was isolated in triplicate for each sample type (seawater, ceramic, PET, and PHA) using a modified version of a high-salt and sodium dodecyl sulfate-based method (Zhou et al., 1996). The only modification from the original procedure was that instead of 5.0 g

soil, DNA was isolated from a quartered 0.22 µm polycarbonate filter (seawater), 6.0 g of ceramic pellets, 3.0 g of PET, or 3.0 g PHA pellets. Due to their higher density, 6.0 g of ceramic was approximately equal in volume to 3.0 g of either plastic type. Following isolation, DNA was quantified (ng μL^{-1}) and assayed for quality (A_{260}/A_{280} and A_{260}/A_{230}) using a BioPhotometer D30 (Eppendorf, Hamburg, Germany) and the 'ds_DNA' methods group with default settings. Final DNA concentrations were verified using a Qubit Fluorometer (Thermo Fisher Scientific, Waltham, MA, USA). The DNA was stored in the dark at -20 ºC prior to sequencing.

Metagenome sequencing

Metagenomic library preparation and sequencing was carried out by Molecular Research LP (Shallowater, TX, USA). A total of 12 metagenomes were sequenced: three seawater, three ceramic, three PET, and three PHA. Libraries were prepared using the Nextera XT DNA Library Preparation Kit (Illumina Inc., San Diego, CA, USA) and diluted to 10.0 pM. The average library size was determined using an Agilent 2100 Bioanalyzer (Agilent Technologies, Santa Clara, CA, USA). Sequencing was performed on the Illumina HiSeq 2500 platform using 2x150 bp paired-end read chemistry. The DNA concentration (ng μL^{-1}) and average size (bp) of the sequencing libraries, and the number of sequence reads produced are reported in Supplemental Table 1. Raw sequence reads were submitted to the European Nucleotide Archive and the European Bioinformatics Institute's (EBI) Metagenomics Pipeline (Mitchell et al., 2016) version 3.0, which includes an automated workflow for read processing. Briefly, overlapping reads were merged with SeqPrep (John, 2011), low quality reads and adapter sequences were trimmed using trimmomatic (Bolger et al., 2014), and reads less than 100 bp were removed using BioPython (Cock et al., 2009). Identification of the 16S rRNA reads was performed using rRNASelector

(Lee et al., 2011) and FragGeneScan (Rho et al., 2010) was used to find reads containing predicted coding sequences (pCDS) greater than 60 nucleotides in length. The number of sequenced reads ranged from 26 860 030 to 36 522 626, with an average of 30 888 258 reads per sample. Following quality control and merging, the number of remaining reads ranged from 11 273 807 to 22 918 149, with an average of 16 270 447 processed reads per sample.

Table 1. Library preparation and sequencing information.

Sample type	**Final library [DNA] (ng μL^{-1})**	**Average library size (bp)**	**Reads generated**
Seawater 1	4.40	523	32,009,126
Seawater 2	4.48	484	26,860,030
Seawater 3	5.06	568	31,981,354
Ceramic 1	5.40	1001	30,229,962
Ceramic 2	7.12	1469	30,021,626
Ceramic 3	7.28	1420	29,251,312
PET 1	6.66	1516	36,278,178
PET 2	4.80	458	30,133,310
PET 3	5.00	1086	27,764,482
PHA 1	4.44	1516	29,795,160
PHA 2	5.16	458	29,812,234
PHA 3	3.06	1086	36,522,626

Abbreviations: PET, polyethylene terephthalate; PHA, polyhydroxyalkanoate

Microbial community composition

Operational taxonomic units (OTUs) were assigned using the QIIME (Caporaso et al., 2010) version 1.9 closed-reference OTU picking protocol and the SILVA 128 SSU 97% database (Quast et al., 2013) with reverse strand matching enabled. Beta-diversity was analyzed using weighted UniFrac (Lozupone et al., 2011) values calculated in QIIME. Permutational Multivariate Analysis of Variance (PERMANOVA) was used to test for significant differences

between communities using Primer 7 with the PERMANOVA+ package (Clarke and Gorley, 2015) (PRIMER-E Ltd., Plymouth, UK). PERMANOVA was performed using 999 permutations based on the weighted UniFrac from the beta-diversity analysis in QIIME. Due to the low number of unique permutations possible for pair-wise tests, Monte Carlo simulations were used to generate p-values for all pair-wise comparisons.

Enrichment of alpha/beta-hydrolases

Predicted coding sequences (pCDS) from each of the 12 metagenomes were aligned against a modified database (turnerlab.tamucc.edu/research/databases) of protein sequences from the ESTHER database of alpha/beta-hydrolases (Hotelier et al., 2004). Proteins included in the modified database were restricted to depolymerases, esterases, lipases, and cutinases as these were previously implicated in plastic-microbe interactions (Yoshida et al., 2016). To reduce redundancy within the database, CD-HIT (Clarke and Gorley, 2015) version 4.7 was used to cluster protein sequences with default settings. The modified database used here included 10 protein families containing a total of 1 079 protein sequences. Alignments were performed using the command-line version of blastp, as implemented in BLAST+ (Camacho et al., 2009) version 2.6.0, with an expect value (e-value) cutoff of 10^{-5}, a minimum alignment length of 30 amino acids, and a minimum percent identity of 50%. To visualize the effect of sample type on hydrolase profiles, proportions of positive alignments were normalized to the total number of positive alignments per sample, and a hierarchical cluster analysis based on a Bray-Curtis resemblance matrix was performed. To test for significant differences among profiles, a similarity profile analysis (SIMPROF) (Clarke et al., 2008) using 999 permutations and a

significance level of 0.05 was performed in Primer 7. Additionally, the abundance of protein sequences was normalized to the total pCDS and compared between all samples (n=12).

Relatedness of polyhydroxybutyrate (PHB) depolymerases

Processed reads for each of the PHA samples (n=3) were co-assembled using MEGAHIT (Li et al., 2015) version 1.1.1. Co-assembly was performed using the 'meta-large' preset for large and complex communities, and MEGAHIT was called as follows:

megahit –presets meta-large -r input --min-contig-len 1000 -o output -t 40

To recover the coding sequences of a significantly enriched PHB depolymerase (identified using the hydrolase database above), the representative PHB depolymerase gene sequence was aligned to the 118 520 co-assembled contigs using tblastn with an e-value cutoff of 10^{-5}, a minimum alignment length of 100 bp, and a minimum percent identity of 50%. An alignment to NCBI's RefSeq genomic database was carried out with the same parameters in an effort to include gene sequences from previously described organisms. The relatedness of the 46 PHB depolymerase gene sequences from this study and gene sequences from the top 10 most similar genera from RefSeq was inferred by constructing a maximum-likelihood (ML) tree with IQ-TREE (Nguyen et al., 2015) version 1.6.1. Sequences were aligned using the M-Coffee mode of T-Coffee (Notredame et al., 2000) that combines results from eight different aligners and the tree was generated with 1 000 ultrafast bootstraps (Minh et al., 2013) using the best-fit model (TPM3u+F+R3) as determined by ModelFinder (Kalyaanamoorthy et al., 2017). The phylogenetic tree was annotated with FigTree version 1.4.3 (http://tree.bio.ed.ac.uk/software/figtree/). Sequence similarity between the 46 PHB

depolymerase gene sequences was determined using trimAl (Capella-Gutiérrez et al., 2009) version 1.4.15.

Recovery and analysis of SRM genomes

To characterize individual SRM within the PHA biofilm community, metagenome-assembled genomes (MAGs) were recovered using a previously described method (Parks et al., 2017). Briefly, the processed reads were mapped to the co-assembled PHA metagenomic contigs (produced using MEGAHIT above) with BWA (Li and Durbin, 2010) version 0.7.15-r1142 using the BWA-MEM algorithm with default parameters. Genomes were recovered with MetaBAT (Kang et al., 2015) version 2.12.1 using default MetaBat2 settings and a minimum contig size of 2 000 bp. The resulting bins were merged, filtered, and refined using CheckM (Parks et al., 2015) version 1.0.11 and RefineM version 0.0.23, as described previously (Parks et al., 2017). Of the 46 bins produced, six MAGs were retained for further exploration based on criteria adopted by Parks *et al.* (Parks et al., 2017): an estimated quality of ≥ 50 (completeness – 5x contamination), scaffolds resulting in an N50 ≥ 10 kb, containing < 100 kb ambiguous bases, and consisting of < 1 000 contigs and < 500 scaffolds. Of those six MAGs, the three belonging to SRM as inferred with the 'tree_qa' function in CheckM were explored further.

The three SRM MAGs were analyzed with the Pathosystems Resource Integration Center's (PATRIC) (Wattam et al., 2017) comprehensive genome analysis service. The PATRIC database contains over 190 000 bacterial genomes and has been increasingly used in environmental studies (Harke et al., 2015; Skennerton et al., 2016; Ortiz-Álvarez et al., 2018).The automated PATRIC service includes annotation with RASTtk (Brettin et al., 2015), prediction of nearest neighbors with Mash/MinHash (Ondov et al., 2016), clustering of

homologous proteins with OrthoMCL (Enright et al., 2002), alignment of conserved clusters with MUSCLE (Edgar, 2004), trimming with Gblocks (Talavera and Castresana, 2007), and concatenation followed by inference of a ML tree with RAxML (Stamatakis, 2014). All complete *Desulfovibrionaceae*, *Desulfobacteraceae*, and *Desulfobulbaceae* genomes in the PATRIC database (n= 43, 21, and 11, respectively) were included in the analysis. The resulting tree was annotated using FigTree version 1.4.3. Subsequently, these three MAGs were compared to all publicly available *Desulfovibrionaceae*, *Desulfobacteraceae*, and *Desulfobulbaceae* genomes in GenBank (n= 122, 107, and 65, respectively) by average nucleotide identity (ANI) using fastANI (Jain et al., 2018), using > 95% ANI as the intra-species threshold and < 83% as an inter-species threshold. Additionally, PATRIC's 'Protein Family Sorter' tool was used to identify sulfate-reducing proteins within the three SRM MAGs. To identify any polymer degradation protein sequences within the MAGs, pCDS were generated using Prodigal (Hyatt et al., 2010) version 2.6.3 and were aligned against the custom hydrolase database (described above) using the same search parameters.

Dissimilatory sulfur reduction potential

Predicted coding sequences (pCDS) from each of the 12 metagenomes were aligned against three databases representing the three steps of the dissimilatory sulfate reduction pathway. The database for the first step of the pathway (reduction of sulfate to adenylyl sulfate [APS]) included all sulfate adenylyltransferase (SAT/MET3) protein sequences in the UniProtKB protein database. The database for the second step of the pathway (reduction of APS to sulfite) included all APS reductase (AprBA) protein sequences in the UniProtKB protein database. To address redundancy within both databases, CD-HIT (Clarke and Gorley, 2015)

version 4.7 was used to cluster protein sequences with default settings. This resulted in 612 and 239 protein sequences for the SAT/MET3 and AprBA databases, respectively. These two custom-made databases are also publicly available (turnerlab.tamucc.edu/research/databases). For the third step of the pathway (reduction of sulfite to sulfide), metagenomes were aligned against a published database of DsrAB (Müller et al., 2014) protein sequences. Alignments were performed using BLAST+ (Camacho et al., 2009) version 2.6.0 (blastp) with an e-value cutoff of 10^{-5}, a minimum alignment length of 30 amino acids, and a minimum percent identity of 50%. Positive alignments were normalized to the total pCDS, and the abundance of SAT/MET3, AprBA, and DsrAB sequences were compared between all samples (n=11; PET2 failed normality testing).

Statistical analyses

Unless stated otherwise, R (R Core Team, 2017) version 3.4.0 was used for statistical analysis of data. The combination of Shapiro-Wilk tests and quantile-quantile plots were used to test data for normality. One-way ANOVAs were generated using the R package multcomp, using a Tukey post-hoc test with Westfall values.

Data availability

All sequence reads were made available through the project accession ERP017130 at the European Nucleotide Archive. The six MAGs were deposited as (Madre1, 2, 3, 4, 5, and 6) at GenBank under the accession numbers QZKZ00000000, QZLA00000000, QZLB00000000, QZLC0000000, QZLD00000000, and QZLE00000000, respectively.

Results & Discussion.

Microbial community composition

Overall trends in the seawater, ceramic, PET, and PHA associated community compositions were visualized using the taxonomic rank of order based on the normalized proportion of OTUs assigned to each of the 12 samples (three seawater, three ceramic, three PET, and three PHA; Figure 1). The comparison of weighted UniFrac values revealed a significant difference between all three biofilm communities (ceramic, PET, and PHA) and the seawater community (PERMANOVA; p-value=<0.05). Additionally, a significant difference was found between the PHA biofilm communities and both the ceramic and PET biofilm communities (PERMANOVA; p-value=<0.05). By contrast, there was no significant difference between the PET and ceramic biofilm communities. Hierarchical clustering based on a Bray-Curtis resemblance matrix of OTU taxonomic assignments determined that the PET and ceramic biofilm communities were more closely related to the PHA biofilm community than to the seawater community (PERMANOVA; p-value=<0.05).

The comparison between surface-associated and free-living lifestyles has been a long-studied question in microbial ecology and thereby, considerable literature is available to inform the study of surface-associated bacterial communities (Biddanda and Pomeroy, 1988; Karner and Herndl, 1992; DeLong et al., 1993; Crump et al., 1999; Hollibaugh et al., 2000; Kellogg and Deming, 2014). Based on this literature, it was hypothesized that all surface-associated communities (i.e. ceramic, plastic, and bioplastic) would be distinct in comparison to free-living communities, and the results of this study supported that hypothesis. The more salient question was the distinction between different surfaces, and this study revealed that PET was not colonized by a distinct community in comparison to the ceramic biofilm control. This finding is

supported by a recent study demonstrating that pelagic microbial communities associated with PET were indistinguishable from those associated with a glass biofilm control (Oberbeckmann et al., 2016). Similarly, it was previously demonstrated that inert surfaces such as glass, ceramic, and coral skeleton have little influence on marine microbial community composition (Witt et al., 2011). The lack of distinction between PET and ceramic could also be due to the remote location of the study site seeing that previous reports of plastic degradation have occurred in highly polluted habitats that would select for and enrich plastic degraders (Nanda et al., 2010; Singh and Gupta, 2014; Yoshida et al., 2016).

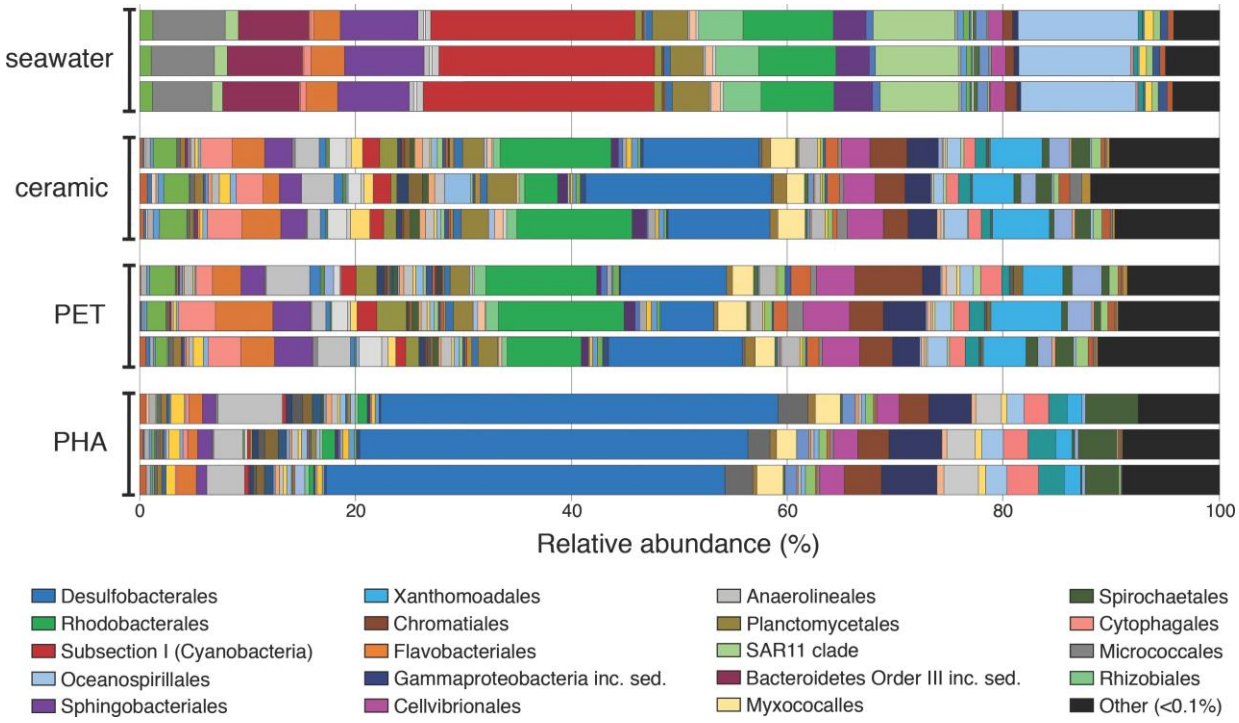

Figure 3. Bar plot showing the relative abundance of microbial orders. Abundances were normalized to the total number of sequences, and orders that constituted less than 0.1% of the community were grouped under other. The 20 most abundant orders across all samples displayed in the legend.

At the phylum level, OTUs belonging to Proteobacteria were the most abundant among all four community types, representing 42, 55, 59, and 72% of all OTUs in seawater, ceramic, PET, and PHA, respectively (Table 2). Cyanobacteria was the second most abundant phylum in the seawater community (22%), making up a larger proportion of the community compared to the PET and ceramic biofilm communities (~6% for each), and even more so compared to the PHA biofilm community (0.7%). The presence of Chloroflexi (4%), Spirochaetes (4%), and Firmicutes (2%) amongst the most abundant phyla was unique to the PHA biofilm communities. A detailed report of taxonomic rank based on normalized proportion is provided in Table 2.

The OTUs assigned to orders Subsection I of Cyanobacteria, Oceanospirillales, SAR11, and Sphingobacteriales were among the top five most abundant in the seawater community only, making up 20, 11, 8 and 7% of the total OTUs in seawater, respectively. The orders Desulfobacterales, Rhodobacterales, Xanthomondales, and Cellvibrionales were all among the top five most abundant orders in both the PET and ceramic biofilm communities. The abundance of Proteobacteria (72% of all OTUs) within the PHA biofilm community reflected the dominance of the order Desulfobacterales, an order of SRM that represented 37% of all OTUs and more than half of all Proteobacteria. Similar to the trends with phyla, the abundant orders within the PHA biofilm community were unique, with the orders of Gammaproteobacteria *incertae sedis*, Anaerolineales, and Spirochaetales being in the top five most abundantly assigned OTUs in the PHA biofilm communities.

Two genera of Cyanobacteria (*Synechococcus* and *Prochlorococcus*) represented almost 20% of all OTUs within the seawater community but made up a very small proportion (<1%) of all three biofilm communities. Members of uncultured genera from *Desulfobacteraceae*, *Rhodobacteracae*, and *Flammeovirgaceae* were among the five most abundant genera in the PET

and ceramic biofilm communities, representing almost 20% of all OTUs. Three genera within *Desulfobacteraceae* and an uncultured genus of *Desulfobulbaceae* combined to represent 20% of all OTUs within the PHA biofilm, reinforcing the dominance of SRM in that community (Table 2).

Table 2. The top five members from each taxonomic rank based on normalized proportion per sample. Means (n=3) plus or minus the standard error of mean are reported for each of the taxonomic assignments.

Seawater	**Ceramic**	**PET**	**PHA**
Phylum			
Proteobacteria (42.3% ± 0.56)	Proteobacteria (54.6% ± 1.77)	Proteobacteria (58.8% ± 1.84)	Proteobacteria (72.9% ± 1.33)
Cyanobacteria (22.2% ± 0.71)	Bacteroidetes (11.2% ± 0.08)	Bacteroidetes (12.3% ± 1.45)	Bacteroidetes (5.7% ± 0.04)
Bacteroidetes (17.7% ± 0.39)	Cyanobacteria (6.4% ± 0.62)	Cyanobacteria (6.2% ± 0.69)	Chloroflexi (4.2% ± 0.79)
Actinobacteria (8.9% ± 0.41)	Planctomycetes (4.7% ± 0.09)	Planctomycetes (3.7% ± 0.07)	Spirochaetes (3.8% ± 0.44)
Planctomycetes (4.0% ± 0.10)	Verrucomicrobia (3.2% ± 0.53)	Chloroflexi (3.7% ± 0.83)	Firmicutes (1.8% ± 0.11)
Order			
Subsection I (Cyanob.) (20.1% ± 0.71)	Desulfobacterales (12.4% ± 2.40)	Rhodobacterales (9.6% ± 1.42)	Desulfobacterales (36.5% ± 0.30)
Oceanospirillales (10.7% ± 0.22)	Rhodobacterales (8.0% ± 2.49)	Desulfobacterales (9.0% ± 2.18)	γ-proteo. *I. sedis* (4.6% ± 0.35)
SAR11 clade (7.5% ± 0.11)	Xanthomonadales (4.6% ± 0.41)	Xanthomonadales (4.7% ± 0.90)	Anaerolineales (4.0% ± 0.98)
Rhodobacterales (7.4% ± 0.49)	Cellvibrionales (3.0% ± 0.21)	Chromatiales (4.1% ± 1.04)	Spirochaetales (3.8% ± 0.53)
Sphingobacteriales (7.1% ± 0.22)	Cytophagales (2.9% ± 0.22)	Cellvibrionales (3.6 ± 0.26)	Chromatiales (3.0% ± 0.21)
Genus			
Synechococcus (14.1% ± 0.52)	uncult. Desulfobacteraceae (4.9% ± 1.13)	uncult. Desulfobacteraceae (3.6% ± 0.88)	uncult. Desulfobacteraceae (8.2% ± 0.14)
Litoricola (6.3% ± 0.13)	uncult. Rhodobacteraceae (3.0% ± 0.92)	uncult. Rhodobacteraceae (3.0% ± 0.68)	*Desulfobacter* (6.2% ± 0.82)
Prochlorococcus (5.3% ± 0.17)	Desulfobacteraceae Sva0081 (2.4% ± 0.35)	uncult. Anaerolineaceae (2.45 ± 0.72)	*Desulfospira* (3.0% ± 0.22)
uncult. Saprospiraca (4.6% ± 0.19)	uncult. γ-proteo. *I. sedis* (1.95% ± 0.20)	Candidatus Thiobios (2.1% ± 0.47	uncult. Desulfobulbaceae (3.0% ± 0.51)
Ambiguous SAR11 (4.7% ± 0.10)	uncult. Flammeovirgaceae (1.94% ± 0.25)	uncult. Flammeovirgaceae (1.90% ± 0.28)	*Spirochaeta* (2.3% ± 0.24)

Abbreviations: PET, polyethylene terephthalate; PHA, polyhydroxyalkanoate; uncult., uncultured; Cyanob., Cyanobacteria.

Whereas PET was not colonized by a distinct microbial community, the introduction of PHA promoted a significant and distinct response. In particular, SRM were the dominant members of the PHA-associated assemblage (see Figure 3). Typically, the three most common SRM families (*Desulfobacteraceae, Desulfobulbacaea*, and *Desulfovibrionacaea*) account for between 5-20% of the total bacterial community in estuarine sediments (Bowen et al., 2012; Cheung et al., 2018). In this study, these three families made up a similar fraction of the plastic and ceramic-associated benthic communities (9% and 12%, respectively) but they accounted for over 39% of the PHA-associated benthic community.

Naturally-occurring PHAs are carbon and energy storage polymers that are accumulated as intracellular granules that aid survival during periods of nutrient limitation and environmental stress (Dawes and Senior, 1973; Obruca et al., 2018). The ability to produce and degrade PHA is thought to be widespread (Reddy et al., 2003) but its prevalence among SRM and its importance in carbon and sulfur cycling has not been thoroughly characterized. A previous study has reported PHA accumulation in *Desulfococcus multivorans*, *Desulfobotulus sapovorans*, *Desulfonema magnum,* and *Desulfobacterium autotrophicum* (Hai et al., 2004). Importantly, two culture-dependent studies have shown that addition of PHA to incubation bottles was correlated with sulfide production in anoxic lake sediments (Mas-Castellà et al., 1995; Urmeneta et al., 1995). Taken together, the accumulation of PHA in SRM, the PHA stimulation of sulfide production, and the PHA-selection of SRM (this study) indicate that PHA is an important carbon source for sulfate reduction. However, it remains unknown if the sulfate-reducers in our study can directly degrade PHA or if they rely on primary fermenters to first degrade the polymer into simple organic substrates.

Enrichment of alpha/beta-hydrolases and the relatedness of PHB depolymerases

The comparison of normalized sequence abundance data revealed a significant enrichment of depolymerase and esterase gene sequences within the PHA biofilm communities versus the seawater, ceramic, and PET biofilm communities (ANOVA; p-value=<0.05; Figure 4). The increase in depolymerases was nearly 20-fold, while the increase in esterases was approximately 2.5-fold. The significant increase in depolymerases was largely attributed to a polyhydroxybutyrate (PHB) depolymerase that constituted 60% of all hydrolases in the PHA biofilm communities but less than 0.4% of all hydrolases in other community types (Figure 4). Conversely, no hydrolases were enriched in the PET biofilm community versus either the ceramic biofilm or seawater communities. Hierarchical clustering based on a Bray-Curtis resemblance matrix of hydrolase relative abundance confirmed that PHA biofilm enzyme pools were significantly different from all other community types (SIMPROF; p-value=<0.05). Seawater enzyme pools were also unique, while the PET and ceramic biofilms were indistinguishable (Figure 5).

To characterize the enriched PHB depolymerases within the PHA biofilm communities, the three PHA metagenomes were co-assembled, resulting in 118,520 contigs totaling 245 Mbp. The N50 of the co-assembly was 2,119 bp, and the lengths of the smallest and longest contigs were 1,000 and 107,130 bp, respectively. The average contig length was 2,251 bp. The PHB depolymerase gene sequence was detected in 46 contigs. The average sequence identity between the 46 PHB depolymerase gene sequences was 54.0% with a range of 7.8 to 98.9%, and the ML tree illustrated the diversity of those 46 genes along with PHB depolymerase gene sequences from 10 known PHB degraders (Figure 6).

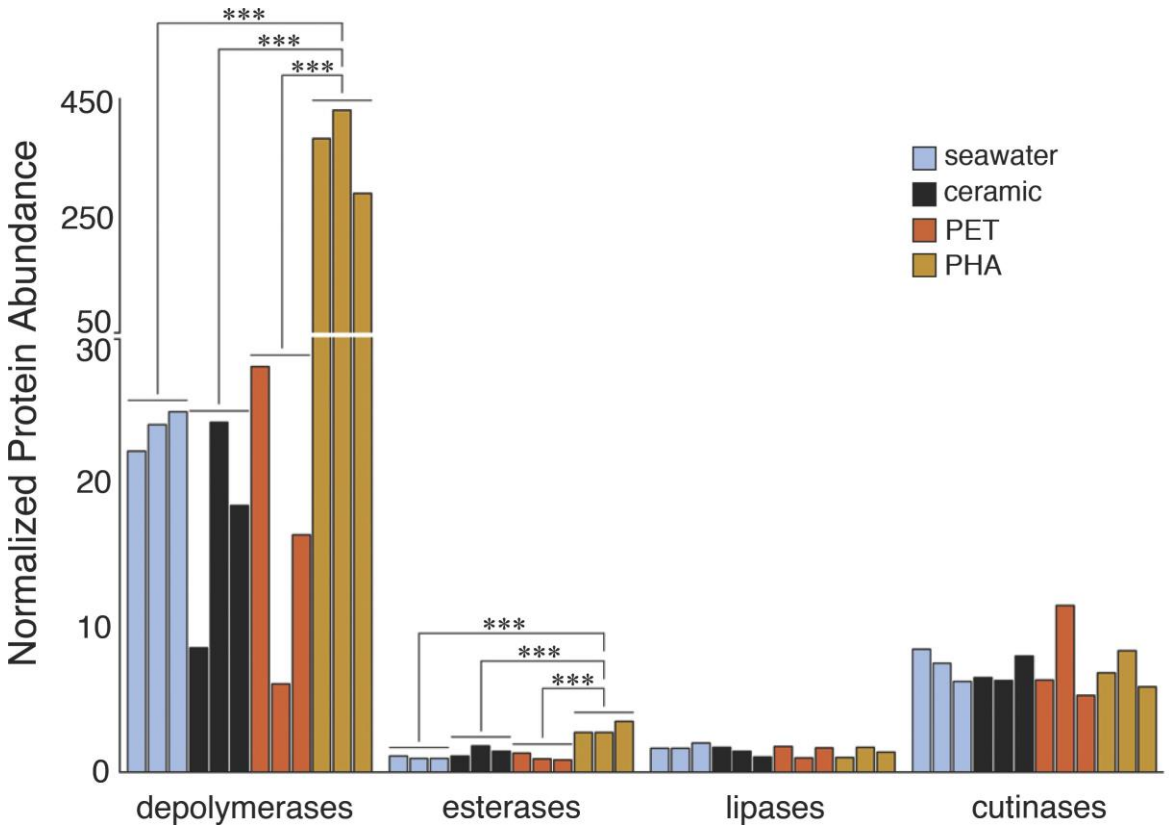

Figure 4. Bar plot showing the relative abundance of depolymerases, esterases, lipases, and cutinases. Gene sequences were normalized to the total pCDS in each sample, with individual samples plotted and grouped together based on community association (seawater, ceramic, PET, and PHA). Significance was determined using ANOVA (*** p-value=< 0.001, n=3).

A key reaction in PHA degradation is its depolymerization. In this study, a nearly 20-fold increase in the abundance of depolymerases indicated that PHA stimulated the growth of PHA-degrading bacteria. Further, the large diversity of the 46 depolymerases, recovered from the metagenome assembled genomes, suggested these enzymes were distributed across a mixed microbial consortium. Although we did not measure enzyme activity, the increased abundance and diversity of these depolymerases supports the hypothesis that PHA biofilms were sites of enhanced enzyme activity. Additional support for this hypothesis will be made available in a

parallel and forthcoming 15-month study wherein weight loss and scanning electron microscopy were used to quantify PHA degradation at the same study site (Figure 7).

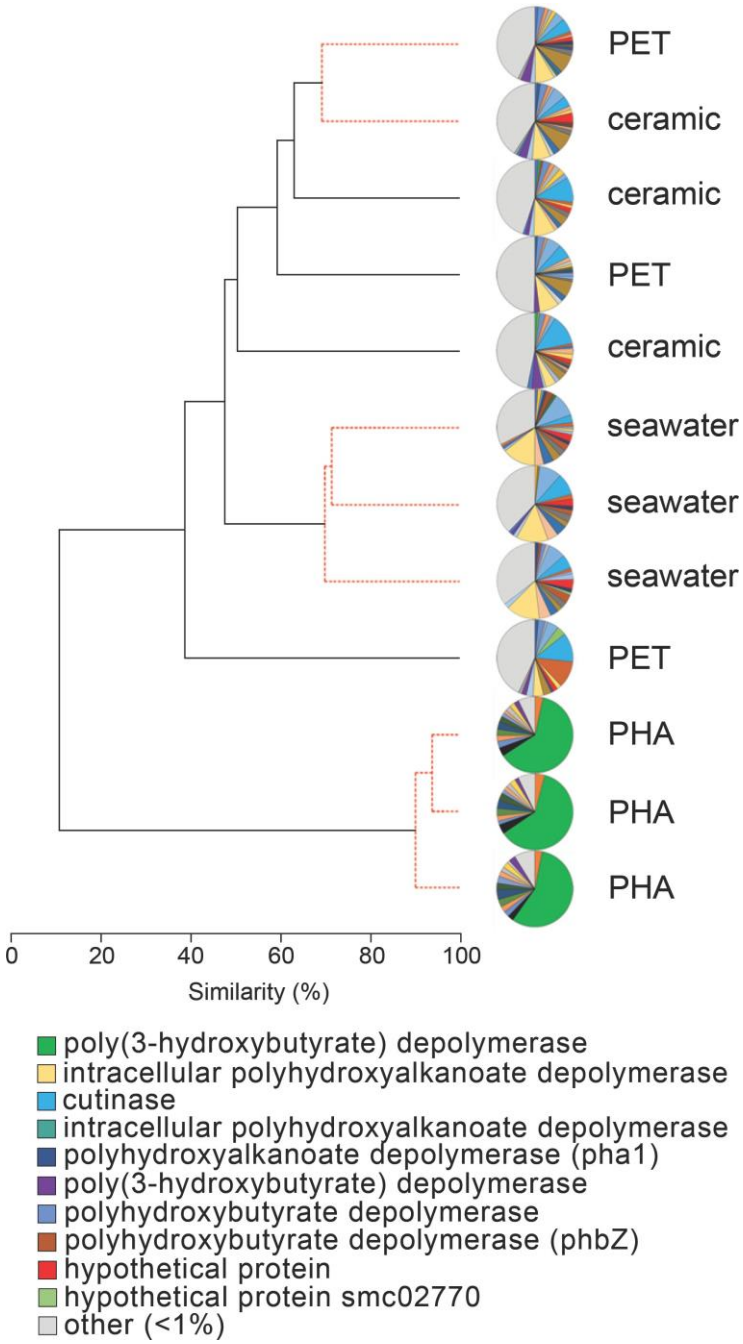

Figure 5. The relatedness of biofilm communities based on a normalized comparison of hydrolase gene pools. The PHB depolymerase, abundant in the PHA communities, is shown in green. Hierarchal clustering was performed based on a Bray-Curtis resemblance matrix. Solid black lines indicate hydrolase gene pools significantly different from one another, while dotted red lines indicate enzyme pools that are not significantly different (SIMPROF analysis; p=<0.05). The 10 most abundant enzymes across all samples displayed in the legend.

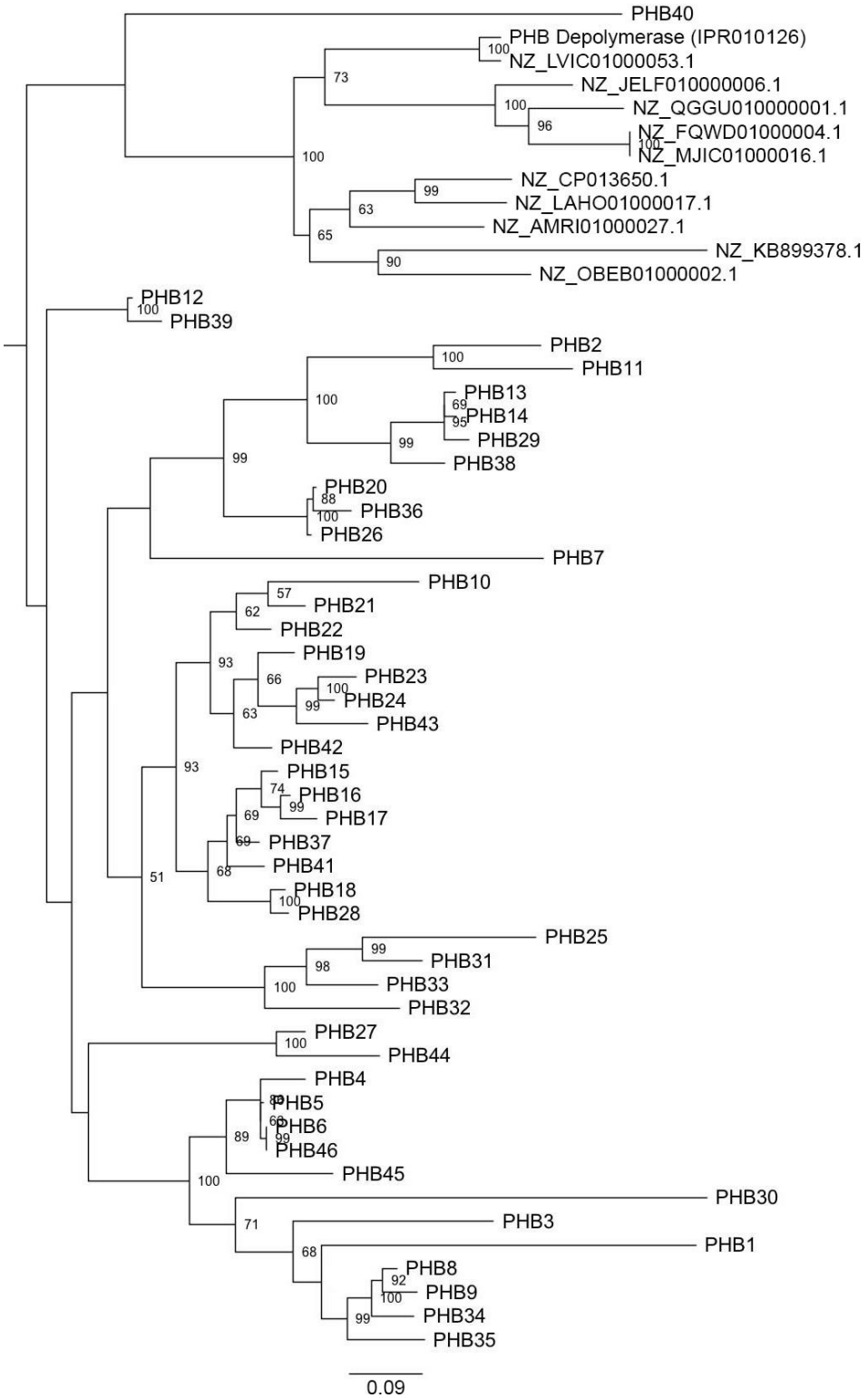

Figure 6. Maximum-likelihood tree showing the diversity of the 46 enriched PHB depolymerase gene sequences. Node labels show the bootstrap support values. Branch lengths represent the average number of substitutions per site. The tree was rooted to the original PHB depolymerase sequence.

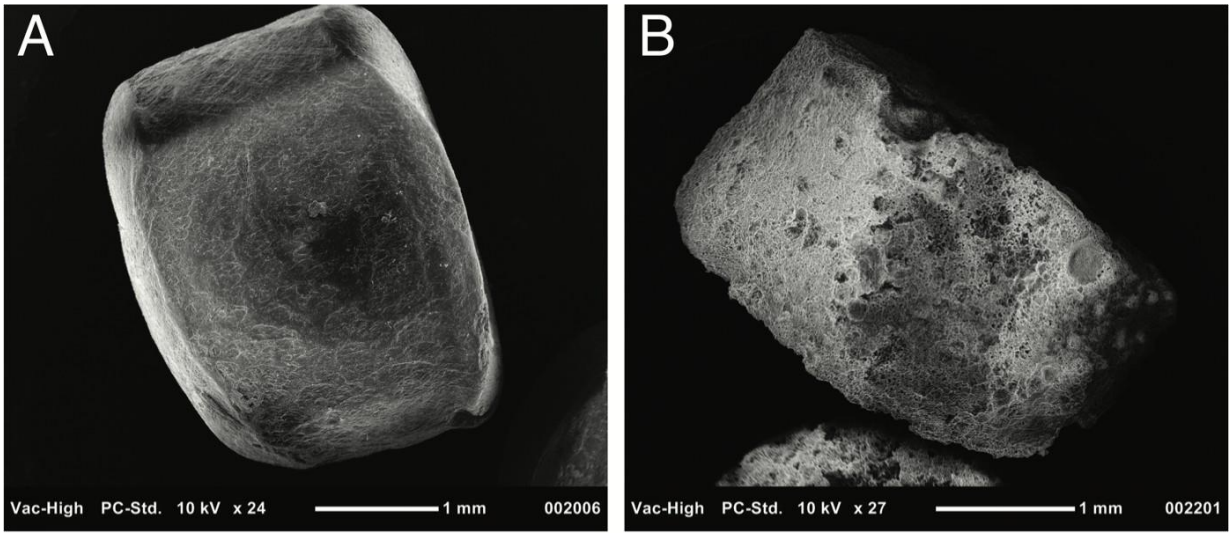

Figure 7. Scanning electron microscopy image of PHA pellets used to visualize signs of biodegradation. Panel A displays a pellet that was not exposed to benthic microbial communities, while Panel B shows a pellet exposed for 230 days.

Recovery and analysis of SRM genomes

Six high-quality MAGs were recovered from the co-assembled PHA biofilm metagenomes. Initial MAG identification was inferred with CheckM: Madre1 was placed in the genus *Desulfovibrio*, Madre2 in the *Desulfobacteraceae* family, Madre3 in the *Desulfobulbaceae* family, Madre4 in the *Spirochaetaceae* family, and Madre5 and Madre6 within the Gammaproteobacteria order (Table 3). The three SRM MAGs (Madre1, 2, and 3) averaged 391 contigs, a N50 value of 18,335 bp, and a maximum contig length of 76,914 bp. The genome sizes ranged from 3,852,664 to 5,613,049 bp (Madre1 and Madre2, respectively), while the number of genes ranged from 3,829 to 5,179 (Madre1 and Madre2, respectively), and the GC content ranged from 46.9 to 59.8% (Madre3 and Madre1, respectively).

Table 3. Six high-quality MAGs were recovered from the three PHA co-assembled metagenomes. MAGs with a quality score (% completeness – 5 x % contamination) of greater than 50 were considered high quality.

MAG	Completeness (%)	Contamination (%)	Quality	Genome size (Mbp)	Contigs	GC%	Taxonomy
Madre1	92.60	1.80	83.60	3.85	434	59.8	*Desulfovibrio*
Madre2	97.40	2.26	86.10	5.61	410	50.5	*Desulfobacteraceae*
Madre3	98.13	2.20	87.13	4.40	330	46.9	*Desulfobulbaceae*
Madre4	54.63	0.00	54.63	1.50	389	50.0	*Spirochaetaceae*
Madre5	76.65	2.26	65.35	2.77	339	39.7	γ-proteobacteria
Madre6	72.41	1.72	63.81	2.77	201	41.1	γ-proteobacteria

The identities of the three PHA-associated SRM genomes were further explored by building a genome-scale phylogenetic tree that included 43 *Desulfovibrionaceae*, 21 *Desulfobacteraceae*, and 11 *Desulfobulbaceae* reference genomes (Figure 8). The phylogeny confirmed the initial CheckM-based placement of the three MAGs and further refined their closest relatives. Madre1 was related to the type strain *Desulfovibrio gigas* DSM 1382 (ATCC 19364) (Le Gall, 1963; Morais-Silva et al., 2014). Madre2 was related to the uncultured *Desulfobacula toluolica* Tol2, an aromatic carbon-degrading SRM isolated from a seawater pond in Massachusetts (Wöhlbrand et al., 2013). Madre3 was related to the uncultured *Desulfofustis* sp. PB-SRB1 that was recovered from the "pink berry" consortia of the Sippewissett salt marsh (Wilbanks et al., 2014). However, a species could not be assigned to Madre 1, 2, or 3 given that each showed less than 83% ANI with the 122 *Desulfovibrionaceae*, 107 *Desulfobacteraceae*, and 65 *Desulfobulbaceae* reference genomes available in Genbank. The full tree, without collapsed branches, was included in the supplemental material (Appendix 1).

Analysis of the three SRM MAGs revealed the presence of SAT/MET3 (Madre1, 2, and 3), AprBA (Madre2, and 3) and DsrAB (Madre1, 2, and 3) protein sequences. Additionally, the

alignment of their pCDS to the custom hydrolase database revealed the presence of two distinct PHA depolymerase sequences in both Madre1 and Madre3.

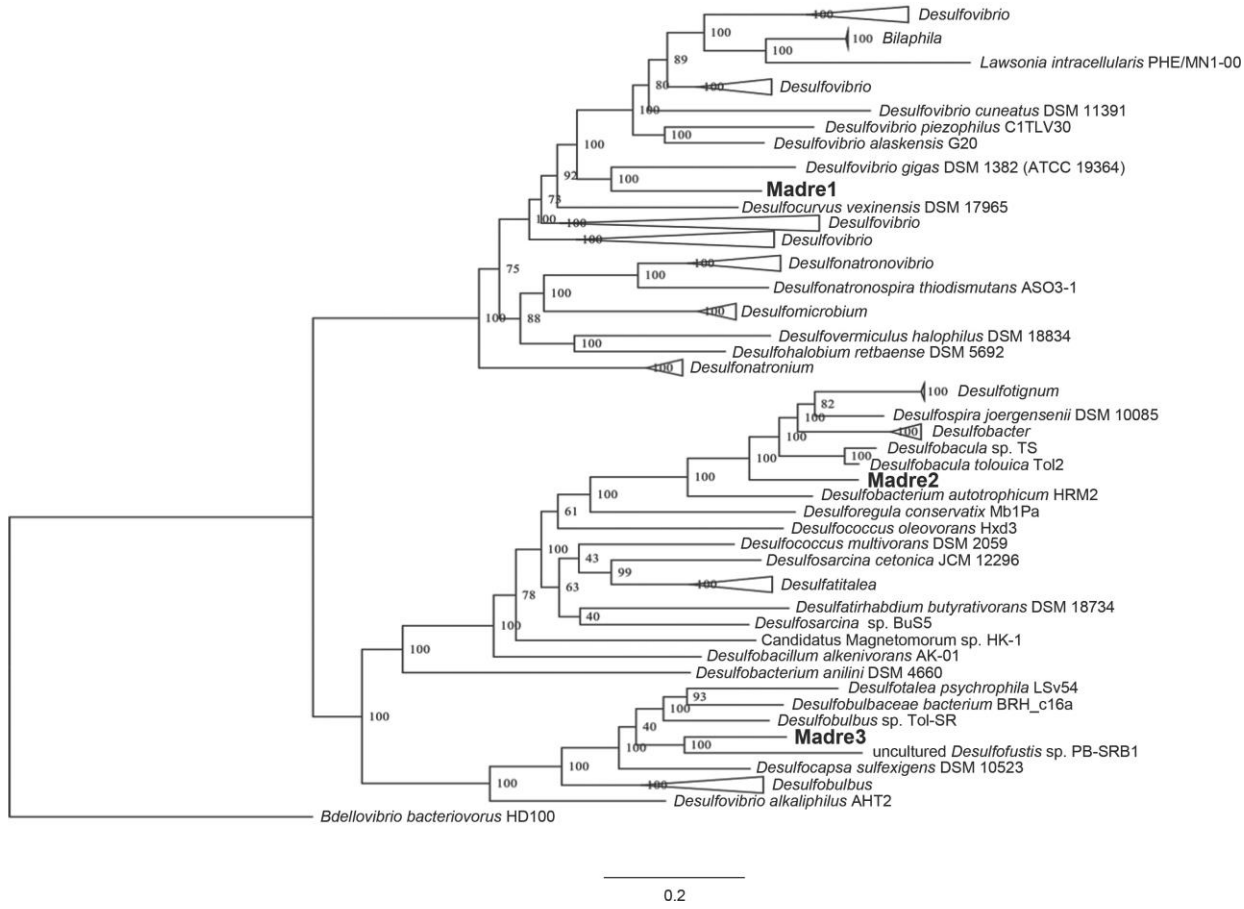

Figure 8. Genome-scale maximum-likelihood tree showing the relatedness of the three PHA biofilm SRB (Madre1, Madre2, and Madre3) to members of the *Desulfovibrionaceae*, *Desulfobacteraceae*, and *Desulfobulbaceae*. The Madre SRB were highlighted in bold font. Node labels show the bootstrap support values. Branch lengths represent the average number of substitutions per site. The tree was rooted to a more distantly related Deltaproteobacteria that is not a known SRB (*Bdellovibrio bacteriovorans* HD1000).

Dissimilatory sulfur reduction potential

The enrichment of dissimilatory sulfur reduction protein sequences within the PHA biofilm communities was assessed through the alignment of metagenomic pCDS against

databases of sulfate adenylyltransferases (SAT/MET3), adenylyl sulfate (APS) reductases (AprBA), and sulfite reductases (DsrAB). The comparison of normalized sequence abundance revealed no significant differences in SAT/MET3 protein abundances. A significant enrichment in AprBA and DsrAB was detected in the PHA biofilm communities (ANOVA; p-value=<0.05; Figure 9).

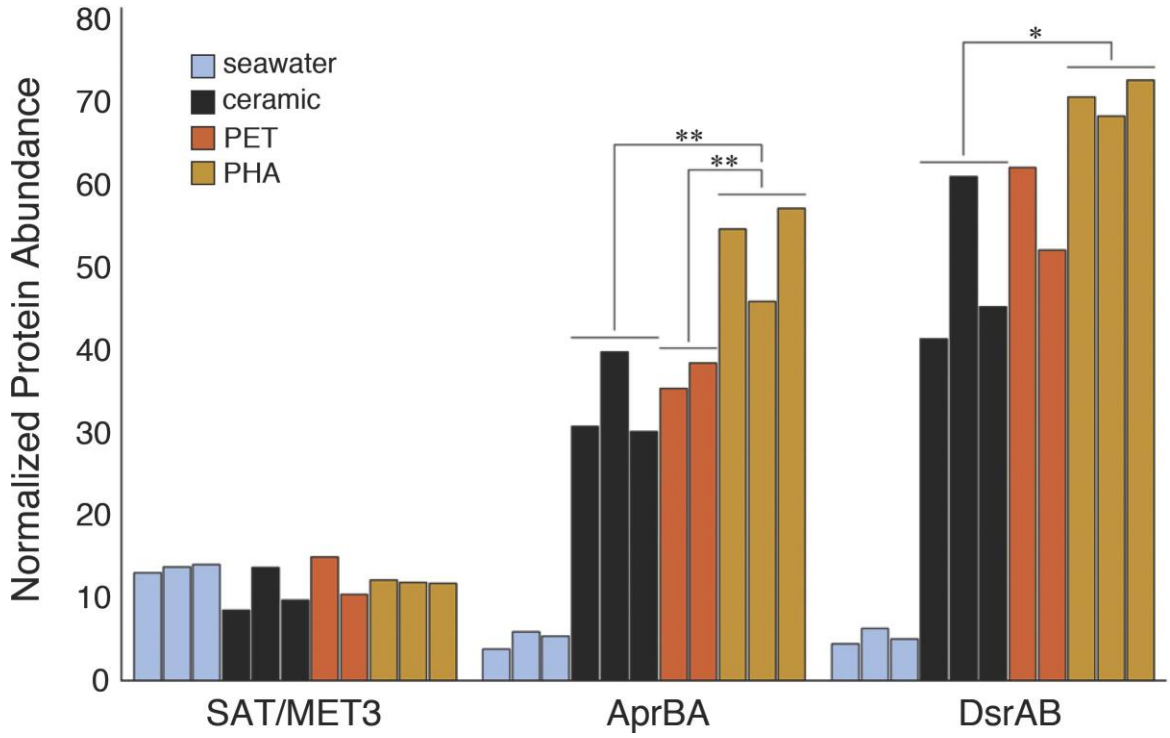

Figure 9. Bar plot showing the relative abundance of sulfate adenylyltransferase (SAT/MET3), APS reductase (AprAB), and dissimilatory sulfite reductase (DsrAB) protein sequences. Protein sequences were normalized to the total number of pCDS in each sample, with individual samples plotted and grouped together based on community association (seawater, ceramic, PET, and PHA). Significance was determined using ANOVA (** p-value=<0.01, * p-value=<0.05, n=2-3).

Previous studies have shown, using adenylyl sulfate reductases (*aprBA*) and dissimilatory sulphite reductases (*dsrAB*) as functional markers, that sulfate reduction is more diverse and widespread that previously thought (Müller et al., 2014; Anantharaman et al., 2018; Hausmann et al., 2018). Further, the detection of *apr* and *dsr* genes in new phyla, made possible through the

construction of genomes from metagenomes has expanded the known diversity of sulfate-reducing microorganisms (Anantharaman et al., 2018; Hausmann et al., 2018). Here, we demonstrated that bioplastic communities were significantly enriched with both sulfate and sulfite reductases. We also reconstructed genomes from metagenomes to discover new *Desulfovibrio*, *Desulfobacula*, and *Desulfofustis* species (Madre 1, 2, and 3, respectively). While it remains unknown if SRM possessing depolymerases (i.e. Madre1 and Madre 3) can directly degrade PHA, an ongoing study will shed light on their growth requirements. Despite this open question, the increased abundance of sulfate-reducing enzymes and the discovery of three uncultured sulfate-reducing species lends additional support to the hypothesis that sulfate reduction in marine sediments is stimulated by the addition of PHA.

Environmental implications & conclusions

In a scenario where bioplastic use and pollution are more common, what remains unclear is the larger effect of the PHA-selection for SRM. Sulfate-reducing bacteria play a critical role in biogeochemical cycling as sulfate-reduction is responsible for ~50% of organic carbon mineralization in marine sediments (Jørgensen, 1982), and the stimulation of SRM has been shown to suppress the growth of methanogenic archaea through the diversion of carbon flow from methane to carbon dioxide (Gauci et al., 2004). For example, the stimulation of SRM in coastal rice fields, through the application of sulfate-containing amendments, was shown to inhibit methane production (Lindau et al., 1994; Denier van der Gon et al., 2001). It is thus possible that bioplastic pollution and its stimulation of SRM could have unintended consequences that affect the balance between sulfate reduction and methanogenesis. More

generally, it is also possible that bioplastic loading could alter the natural syntrophic cycling of PHA in marine sediments.

In conclusion, this study demonstrated that the introduction of plastic had no measurable effect on the benthic microbial community. By contrast, the introduction of bioplastic selected for a distinct microbial community that was enriched for hydrolases and dominated by SRM. Recovered genomes, representing the three most common families of SRM, contained depolymerases as well as *aprBA* and *dsrAB* reductases. Findings indicate that SRM play an important role in PHA degradation in coastal marine sediments. Given that sulfate reduction is a key process in the oceanic sulfur cycle, we recommend that future scientific investigation, government legislation, and best-management practices related to plastic pollution consider the effects of plastic as well as bio-based alternatives on benthic biogeochemical activities.

Acknowledgements.

This study would not have been possible without the support of our friends and colleagues. Specifically, we thank Thomas Merrick for his assistance with data analysis, Robert "Bobby" Duke and the entire Center for Coastal Studies staff for assistance in the field, and Nicole C. Elledge for her assistance with large-scale ANI comparisons. This study was funded by the Texas General Land Office's Coastal Management Plan (GLO-CMP), the Texas Research and Development Fund (TRDF), Texas Sea Grant (TSG), and the National Sciences and Engineering Research Council of Canada (NSERC). The majority of computational data analysis was performed on TAMU-CC's high-performance computing cluster, which is funded in part by the National Science Foundation's CNS MRI Grant (No. 1429518).

CHAPTER 2:

MICROBIAL SUCCESSION DURING THE BIODEGRADATION OF BIOPLASTIC IN COASTAL MARINE SEDIMENT

This chapter under review as Pinnell LJ., Conkle, JL., and Turner JW. (2019). Microbial succession during the biodegradation of bioplastic in coastal marine sediment. *Environ. Sci. Technol.* (under review)

Abstract.

Marine environments are sinks for petroleum-based plastic waste. Bioplastics are a promising alternative as numerous studies have demonstrated their biodegradation in marine environments. However, rates of biodegradation vary and the succession of microorganisms responsible for the biodegradation remain largely unknown. This study determined the biodegradation rate of polyhydroxyalkanoate (PHA) pellets in marine sediment and characterized the temporal variability of PHA biofilms. For comparative purposes, polyethylene terephthalate (PET) and ceramic were included as biofilm controls and the free-living microorganisms in the overlying water column were included as a non-biofilm control. The PHA experienced a 51% mass loss after 424 days and a generalized additive mixed model predicted that 100% mass loss would require 909 days. The PHA was colonized by a distinct microbial community while the PET and ceramic biofilms were largely indistinguishable. In particular, PHA was progressively colonized by sulfate-reducing microorganisms (SRM), such as *Desulfobacteraceae*, *Desulfovibrionaceae* and *Desulfarculaceae*, that accounted for 25-40% of the most abundant taxa. Seeing that SRM are largely responsible for the mineralization of organic matter in anoxic marine sediments, the loading of PHA may affect carbon and sulfur biogeochemistry, provided sedimentary inputs are large.

Introduction.

Beginning with the mass production of plastic in the 1940s, the Plastic Age has transformed modern society (Thompson et al., 2009a). Today, plastic pollution is widely regarded as an environmental crisis. It was estimated that 5.5 billion metric tons of plastic waste has entered landfills and natural environments (Geyer et al., 2017). The oceans in particular are sinks for plastic debris and it was estimated that between 4.8 and 12.7 million metric tons of plastic debris entered the oceans in 2010 alone (Jambeck et al., 2015).

One proposal for combatting the crisis of plastic pollution is the increased use of bioplastic alternatives. More than 60 countries have approved plastic bans or levies for the purpose of reducing single-use plastics as well as promoting the manufacture and use of bioplastic alternatives (E.U., 2018; U.N.E.P., 2018). As a result of these legislative actions and increased public awareness, the global production of bioplastics has increased and is forecasted to grow substantially in the near future. For example, the production capacity of polyhydroxyalkanoate (PHA) was predicted to increase tenfold between 2013 and 2020 (Aeschelmann and Carus, 2015). A clear understanding of the microorganisms involved in its biodegradation is therefore a critical need.

PHAs are a diverse group of natural biodegradable polyesters. They are linear polyesters composed of ester bonds between the carboxyl group of one monomer and the hydroxyl group of neighboring monomers (Verlinden et al., 2007), and more than 100 distinct monomers have been identified (Li et al., 2016b). Numerous genera of microorganisms synthesize PHA as intracellular carbon and energy storage compounds during periods of excess carbon coupled with nutrient limitation (Ishizaki et al., 2001). Manufactured PHA is typically the product of microbial synthesis under fermentation conditions (Lee, 1996) and it is increasingly regarded as a

promising alternative to petroleum-based plastics given its high biodegradation potential (Nehra et al., 2017). Further, innovative physical blends and chemical modifications are predicted to expand PHA's functionality (Li et al., 2016b).

Microorganisms capable of biodegrading PHA are abundant, phylogenetically diverse, and widely distributed (Emadian et al., 2017). Most have been isolated from soil or compost but they have been found in virtually all biomes. In the marine environment, members of diverse genera (e.g. *Bacillaceae, Enterobacteriaceae, Comamonadaceae, Alteromonadaceae, Pseudoalteromonadaceae* and *Alcaligenaceae*) are capable of biodegrading PHA (Mukai et al., 1993; Mergaert et al., 1995; Kita et al., 1997; Leathers et al., 2000; Volova et al., 2010). In a recent synthesis of published PHA biodegradation data, the average rate of biodegradation in the marine environment was estimated to be 0.04-0.09 $mg \cdot day^{-1} \cdot cm^{-2}$ (Dilkes-Hoffman et al., 2019), and at least one study reported enhanced biodegradation in sediment versus the overlaying water column (Mayer, 1990).

The biodegradation of PHA under anaerobic conditions is an important process for efficient waste management in waste treatment plants and landfills as well as natural sediments (Abou-Zeid et al., 2001). Sulfate-reducing microorganisms (SRM) contribute to PHA biodegradation under anaerobic laboratory conditions (Çetin, 2009) while in situ microcosm studies have shown that SRM contribute to PHA biodegradation in anoxic lake sediments (Mas-Castellà et al., 1995; Urmeneta et al., 1995). Additionally, we recently demonstrated that PHA loading stimulates the growth of SRM in marine sediments (Pinnell and Turner, 2019). What remains unclear is the structure and temporal variability of the microbial community associated with its biodegradation.

This study utilized small subunit ribosomal RNA (SSU rRNA) sequencing to monitor microbial succession during the biodegradation of PHA in coastal marine sediment over a 424-day period. Importantly, polyethylene terephthalate (PET) and ceramic were included as biofilm controls, and the free-living microbial community in the overlying water was included as a non-biofilm control. We hypothesized that the microbial communities colonizing PHA would be distinct in comparison to the biofilm and non-biofilm controls. Further, we hypothesized that microbial succession would favor sulfate-reducers.

Materials & Methods.

Site description

The Laguna Madre, a bar-built coastal lagoon, is the largest estuarine system along the Texas coast of the United States. The lagoon is divided into two subunits, the Upper Laguna Madre (ULM) and the Lower Laguna Madre (LLM). The microcosms described below were deployed in the ULM adjacent to an island located at 27°32'39.0"N and 97°17'07.7"W (Figure 10).

Experimental design

Microcosms were designed as described previously (Pinnell and Turner, 2019). Briefly, 3.0 g of PET pellets (M&G Chemicals, Ettelbruck, Luxembourg), 3.0 g of PHA pellets (Doctors Foster and Smith, Rhinelander, WI, USA) and 6.0 g of ceramic pellets (Lyman Products, Middletown, CT, USA) were deployed in custom-made capsules at the sediment-water interface. A total of 180 capsules (n=60 ceramic, n=60 PET, n=60 PHA) were deployed on October 24, 2016. Before deployment, the aggregate mass of the pellets in each capsule was determined to

the nearest 1.0 µg using a Sartorius Cubis Microbalance (Sartorius AG, Göttingen, Germany). Quadruplicates of each sample type were collected at approximately 4-week intervals for a total of 424 days (final collection date December 15, 2017). Additionally, triplicate 1 L seawater samples from the sediment-water interface were collected. All samples were stored on ice, transported to the laboratory and processed within two hours of sample collection. Environmental parameters (i.e. temperature, salinity, DO, and pH) were measured using a 6920 V2-2 Multi-Parameter Water Quality Sonde (YSI, Yellow Springs, OH, USA; Table 4) at the deployment date and each of the 15 collection timepoints.

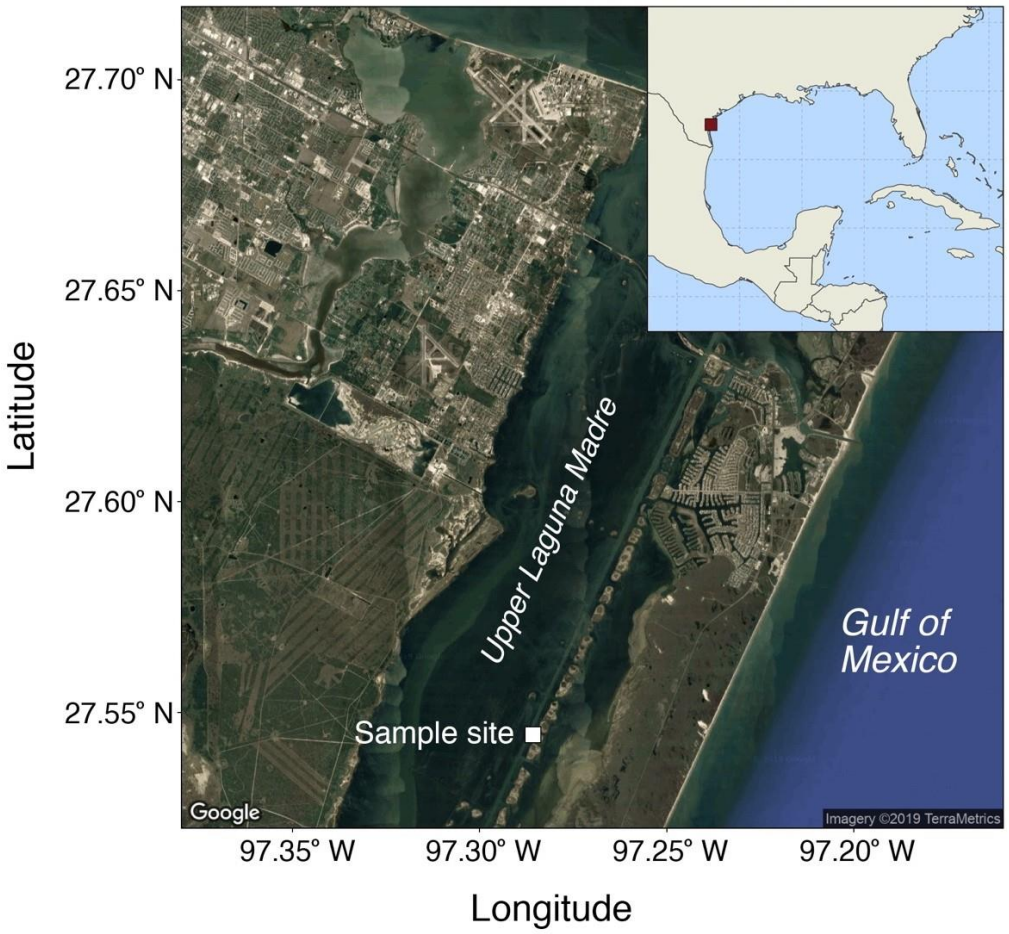

Figure 10. Map showing the Upper Laguna Madre (ULM) along the northwestern Gulf of Mexico (Texas, USA). A square marks the study site, which was adjacent to a dredge material island that is used by Texas A&M University - Corpus Christi as a field station.

Table 4. Environmental parameters measured at the sample site at the deployment and each subsequent collection date.

Event	Date	Exp. (days)	pH	DO (mg/L)	DO (% sat.)	W.T. (°C)	Salinity	Conduct. (µmhos/cm)
Deployment	18-Oct-16	0	8.50	6.78	101.1	25.32	35.95	54,089
Collection 1	15-Nov-16	28	8.20	7.16	100.3	22.63	33.05	50,359
Collection 2	13-Dec-16	56	8.28	9.68	126.4	18.37	34.28	52,005
Collection 3	12-Jan-17	86	8.03	7.73	103.2	19.92	33.13	50,434
Collection 4	06-Feb-17	111	7.85	7.85	99.1	16.44	34.73	52,635
Collection 5	07-Mar-17	140	7.92	7.42	111.1	24.98	37.70	56,633
Collection 6	06-Apr-17	170	8.25	7.53	107.9	21.98	38.75	58,006
Collection 7	02-May-17	196	8.31	8.00	119.8	27.11	33.93	51,677
Collection 8	30-May-17	224	8.29	8.69	137.5	27.63	39.48	59,144
Collection 9	29-Jun-17	254	8.55	9.50	159.1	31.02	39.98	59,954
Collection 10	25-Jul-17	280	8.46	8.99	156.8	29.91	50.54	73,516
Collection 11	21-Aug-17	307	8.37	6.24	110.9	32.03	48.24	70,723
Collection 12	20-Sep-17	337	8.14	7.52	126.5	30.50	42.38	63,084
Collection 13	25-Oct-17	372	8.12	6.25	88.7	22.55	35.33	53,402
Collection 14	27-Nov-17	405	8.15	6.64	94.6	21.24	40.15	59,848
Collection 15	15-Dec-17	424	8.00	7.40	95.1	11.67	36.10	54,722

Abbreviations: Exp., Exposure; sat., saturation; DO, dissolved oxygen; W.T., water temperature; Conduct., Conductivity

DNA isolation

Genomic DNA was isolated from three of the four replicates (i.e. in triplicate) for each sample type (PET, PHA, ceramic, and seawater). Pellets were washed three times with 25 mL of 0.22 µm filter-sterilized, site-specific seawater to remove any organisms that were not part of the biofilm. Seawater was pre-filtered (315 µm Nitex mesh) and the free-living microorganisms were collected by vacuum filtration on a 0.22 µm polycarbonate filter (MilliporeSigma, Burlington, MA, USA). DNA was isolated from the pellets and filters using a modified version of a high-salt and sodium dodecyl sulfate-based method (Zhou et al., 1996) as described

previously (Pinnell and Turner, 2019). DNA was quantified ($ng_X L^{-1}$) and assayed for quality (A_{260}/A_{280} and A_{260}/A_{230}) using a BioPhotometer D30 (Eppendorf, Hamburg, Germany). DNA concentrations were verified using a Qubit Fluorometer (Thermo Fisher Scientific, Waltham, MA, USA) and stored in the dark at -20 °C prior to sequencing.

Biodegradation rate

The pellet-associated biofilms were removed during the DNA isolation procedure (above). Following biofilm removal, the pellets were rinsed twice with 50 mL of ultrapure water (Milli-Q; MilliporeSigma, Burlington, MA, USA) and incubated in 50 mL of ultrapure water for 12-15 hours at room temperature. The ultrapure water was decanted and the pellets were again rinsed twice with 50 mL of ultrapure water. Pellets were transferred to glass Petri dishes, dried for 24 hours at 60 °C and their aggregate mass was determined to 1.0 μg using a Sartorius Cubis Microbalance. The percent mass loss (X, %) was calculated as a ratio of the final mass (X_2) to the initial mass (X_1) multiplied by 100 with the following equation:

$$X = \frac{X_{\$}}{X_{\%}} \times 100$$

Virgin pellets that were not exposed to marine sediment were processed identically as controls. To estimate how long it would take for the pellets to completely biodegrade, a generalized additive mixed model was fitted to the data using R version 3.5.2 and the package 'mgcv'. Due to heteroscedasticty in the data, an exponential variance function was added to the model using the R package 'nlme'. The best fit model was chosen based on corrected Akaike Information Criterion (AICc).

Visualization of biofilms and biodegradation

The fourth replicate, stored in the dark at -80 °C, was used for visualizing biofilms and biodegradation with scanning electron microscopy (SEM). Pellets were thawed, freeze-dried, mounted to stubs using double-stick tape and imaged using a Jeol JCM-6000 Neoscope SEM (JEOL Inc., Peabody, MA, USA). Virgin pellets and virgin pellets subjected to the DNA isolation procedure (above) were used as controls.

16S rRNA PCR amplification and sequencing

The V4 region of the 16S rRNA gene was amplified with an iTaq DNA Polymerase Kit (Bio-Rad, Hercules, CA, USA) using the improved 515f (5´ – GTG YCA GCM GCC GCG GTA A – 3´) and 806r (5´ – GGA CTA CNV GGG TWT CTA AT – 3´) primers (Walters et al., 2016) and 40 ng of DNA as template. Amplification conditions were 95 ℃ for 3 minutes followed by 35 cycles of 30 seconds at 95 ℃, 30 seconds at 50 ℃, and 72 ℃ for one minute. Final elongation occurred at 72 ℃ for 5 minutes. Amplification was confirmed visually using gel electrophoresis. Excess primers and unincorporated nucleotides were removed using a EXOSAP-IT Express PCR Cleanup Kit (Thermo Fisher Scientific, Waltham, MA, USA). The cleaned amplicons were pooled in equal proportions based on their molecular weight and DNA concentrations. Pooled amplicons were purified using calibrated Ampure XP beads (Beckman Coulter, Indianapolis, Indiana, USA) and the resulting pooled library was sequenced on an Illumina MiSeq instrument using paired-end chemistry (2 x 250 bp) at Molecular Research LP (Shallowater, TX, USA).

Community structure

Raw sequence reads were processed using a combination of QIIME v1.9 and QIIME2 version 2018.11 (Caporaso et al., 2010). Barcodes were extracted from the paired-end reads using the 'extract_barcodes.py' tool in QIIME v1.9. Reads were then imported into QIIME2 where they were demultiplexed and denoised with DADA2 (Callahan et al., 2016) to generate amplicon sequence variants (ASVs). DADA2 was also used to filter the reads for quality, remove chimeric sequences, and merge overlapping paired-end reads. Trim lengths of 242 and 233 bp were used on the forward and reverse reads, respectively. A phylogenetic tree was then generated using the 'q2-phylogeny' pipeline with default settings, which was used to calculate phylogeny-based diversity metrics. Taxonomy was assigned using a Naïve Bayes classifier trained on the SILVA release 132 99% OTUs database (Quast et al., 2013), where sequences had been trimmed to include only the 250 bases from the V4 region bound by the 515F/806R primer pair. Reads that mapped to chloroplast and mitochondrial sequences were filtered from the sequence variants table using the 'filter_taxa' function. Faith's phylogenetic distance (FPD), a metric of alpha-diversity incorporating taxonomic richness (Faith, 1992), was calculated for all samples using the 'qiime diversity alpha-phylogenetic' function. Data was then imported into phyloseq (McMurdie and Holmes, 2013) using the "import_biom" and 'import_qiime_sample_data' functions and merged into a phyloseq object. Samples with less than 6,048 reads were discarded and remaining samples (n=45 PHA, n=40 PET, n=36 ceramic, and n=40 seawater) were proportionally transformed to a normalized read count of 6,048. Beta-diversity was analyzed using weighted UniFrac (Lozupone et al., 2011) distances calculated in phyloseq. From these distances, a principal coordinates analysis (PCoA) was calculated and plotted, and a permutational multivariate analysis of variance (PERMANOVA) was used to test for significant differences

between communities using the 'vegan' (Oksanen et al., 2019) and 'pairwiseAdonis' (Arbizu, 2017) packages in R version 3.5.2 (R Core Team, 2017). To ensure differences in microbial communities were not due to unequal dispersion of variability among groups, permutational analyses of dispersion (PERMDISP) were conducted for all significant PERMANOVA outcomes with the 'vegan' package in R.

Microbial succession

To facilitate the observation of temporal patterns, substrate-associated communities were divided into five stages: 1) 28, 56, and 86 days, 2) 111, 140, and 170 days, 3) 196, 224, and 254 days, 4) 280, 307, and 337 days, and 5) 372, 405, and 424 days. These five stages were approximately equal in sample size and approximated the seasonal periods of the study (i.e. fall 2016, winter 2016, spring 2017, summer 2017, and fall 2017). Three tests were then used to examine temporal patterns: FPD comparison, weighted UniFrac comparison, and relative abundance comparison. For the latter, relative abundances from the nine most abundant microbial classes and families were compared between each of the five stages to observe changes in community structure over time. Additionally, PERMANOVAs and PERMDISPs were conducted (as described above) to test for significant differences between communities.

SRM abundance

To compare abundances of SRM within each community, ASVs mapped to known SRM (67 genera representing 17 families, 11 orders, and 5 phyla; Table 5) were filtered using phyloseq's 'subset_taxa' function. The relative abundances of SRM were then calculated for each substrate type and compared at each timepoint.

Table 5. List of known sulfur reducing microorganisms (SRM) used to investigate the sulfur reducing potential of each community.

Phylum	Order	Family	Genus
Proteobacteria	Desulfobacterales	3 families	all 33 genera
Proteobacteria	Desulfovibrionales	4 families	6 genera*
Proteobacteria	Desulfoarculales	*Desulfoarculaceae*	all 5 genera
Proteobacteria	Syntrophobacterales	*Syntrophobacteraceae*	all 8 genera
Proteobacteria	Syntrophobacterales	*Syntrophaceae*	*Desulfobacca*
Proteobacteria	Syntrophobacterales	*Syntrophaceae*	*Desulfomonile*
Proteobacteria	unclassified	unclassified	*Desulfocaldus*
Firmicutes	Clostridiales	*Peptococcaceae*	*Desulfosporosinus*
Firmicutes	Clostridiales	*Peptococcaceae*	*Desulfotomaculum*
Firmicutes	Selenomonadales	*Sporomusaceae*	*Desulfosporomusa*
Firmicutes	Thermoanaerobacterales	*Thermodesulfobiaceae*	*Thermodesulfobium*
Thermodesulfobacteria	Thermodesulfobacteriales	*Thermodesulfobacteriaceae*	all 5 genera
Crenarchaeota	Thermoproteales	*Thermoproteaceae*	*Caldivirga*
Crenarchaeota	Thermoproteales	*Thermoproteaceae*	*Thermocladium*
Euryarchaeota	Archaeoglobales	Archaeoglobaceae	*Archaeoglobus*

* does not include *Lawsonia* and *Bilophilia*, which are not known SRM

Statistical analyses

Unless specified otherwise, R version 3.5.2 (R Core Team, 2017) was used for statistical analysis of data. One-way ANOVAs were generated with the R package ‘multcomp’ (Hothorn et al., 2008) using a Tukey post-hoc test with Westfall values.

Data availability

All sequence reads were made available through the BioProject PRJNA551219 at the NCBI’s Sequence Read Archive.

Results & Discussion.

Biodegradation rates

To determine the rate of PHA biodegradation, the mass loss was calculated as a ratio of the final mass to the initial mass. Following 424 days, the mass of PHA pellets decreased by an

average of 1,512 mg, representing a loss of 51% (Figure 11). Generalized additive mixed models were fitted to the PHA mass loss data using all combinations of environmental variables collected during this study (i.e. temperature, salinity, DO, and pH; Table S1) but the rate of biodegradation was not correlated with environmental variability. The best fit model based on AICc scores used only the length of exposure to account for the loss in mass. The adjusted r-squared value for this model was 0.97 and it predicted that 100% mass loss would occur after 909 days or approximately 2.5 years. This lifetime estimate is in agreement with rates reported in a recent meta-study of PHA biodegradation: 1.5-3.5 years for bottles (Dilkes-Hoffman et al., 2019). The linear shape of the mass loss curve is also in agreement with previous studies of PHA biodegradation in marine environments (Volova et al., 2010; Dilkes-Hoffman et al., 2019).

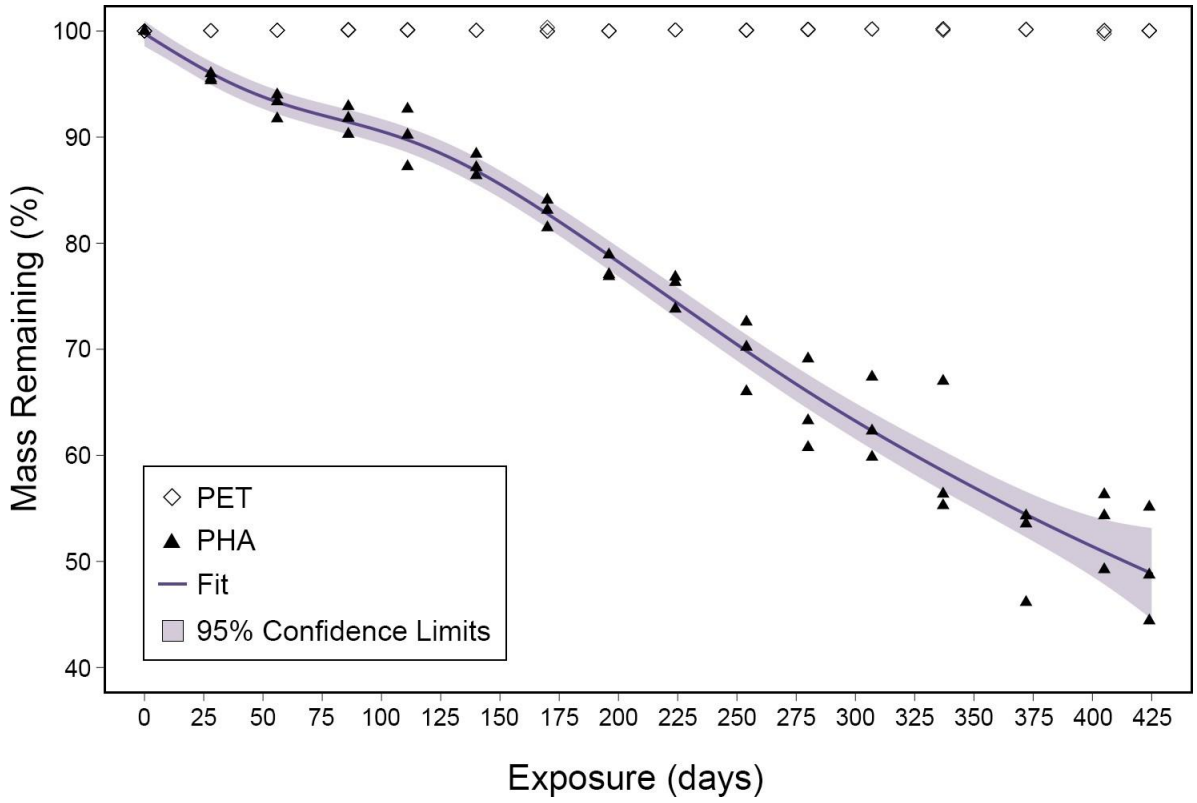

Figure 11. Mass loss ratios plotted for both PHA and PET over the 424-day exposure. The fit of the generalized additive mixed model is displayed as a purple line and the 95% confidence limits are shown as light purple shading.

Previous studies have reported the discovery of microorganisms that metabolize plastic (Orr et al., 2004; Gajendiran et al., 2016; Yoshida et al., 2016) but mass loss measurements showed no evidence of PET biodegradation in this study (Figure 11). Microbes capable of biodegrading plastic may be restricted to highly polluted habitats that select for the growth or evolution of plastic-biodegraders. For example, polyethylene-biodegrading strains of *Rhodococcus ruber* and *Aspergillus clavatus* were isolated from soils with a history of polyethylene contamination (Orr et al., 2004; Gajendiran et al., 2016), a PET-biodegrading strain of *Ideonella sakaiensis* was isolated from a bottle-recycling facility (Yoshida et al., 2016), and a PET-biodegrading consortia was recently isolated from petroleum contaminated soil (León-Zayas et al., 2019). By contrast, this study was conducted on a remote dredge material island that is surrounded by a sparsely populated and largely undeveloped coastline (Parsons et al., 1984).

Visualization of biofilms and biodegradation

To visualize microbial colonization and biodegradation, SEM was used to image pellets with and without biofilms. Images revealed that microorganisms formed biofilms on both PHA (Figure 12, panels A-C) and PET (Figure 12, panels D-F). Previous studies have shown that microorganisms form biofilms on pelagic plastic debris after two weeks (Lobelle and Cunliffe, 2011) and diverse microbial communities have been observed after six weeks (Oberbeckmann et al., 2014).

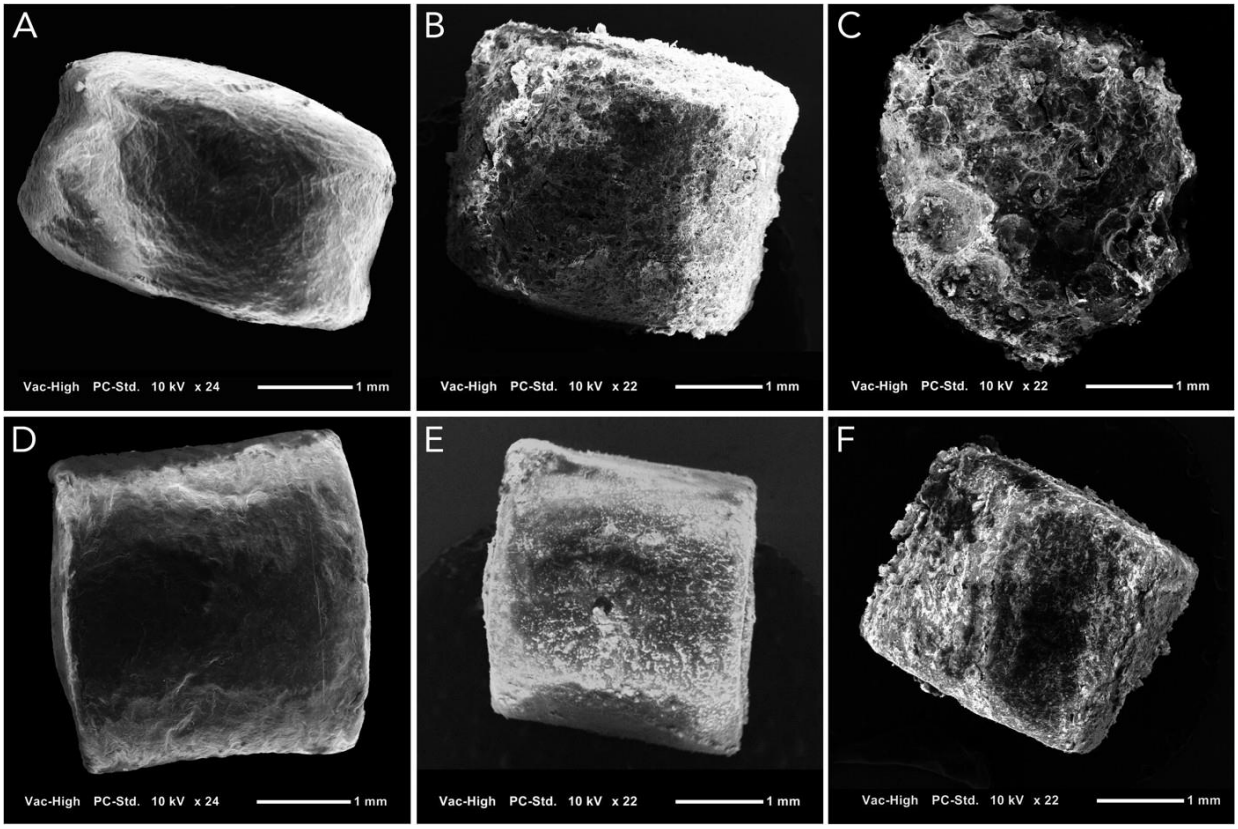

Figure 12. Scanning electron images of PHA and PET pellets with biofilms at approximately 20X magnification. The top panels show PHA pellets while the bottom shows PET pellets. Images demonstrate a time series: 0 (A and D), 196 (B and E), and 424 (C and F) days exposure.

Imaging of pellets without biofilms revealed that the PHA pellets experienced significant size reduction and extensive pitting over time (Figure 13, panel A-C). This clear visual size reduction confirms the above mass loss calculation (51% after 424 days; Figure 1). In comparison, PET experienced no size reduction or pitting at any point during the 424 exposure (Figure 13, panels D-F).

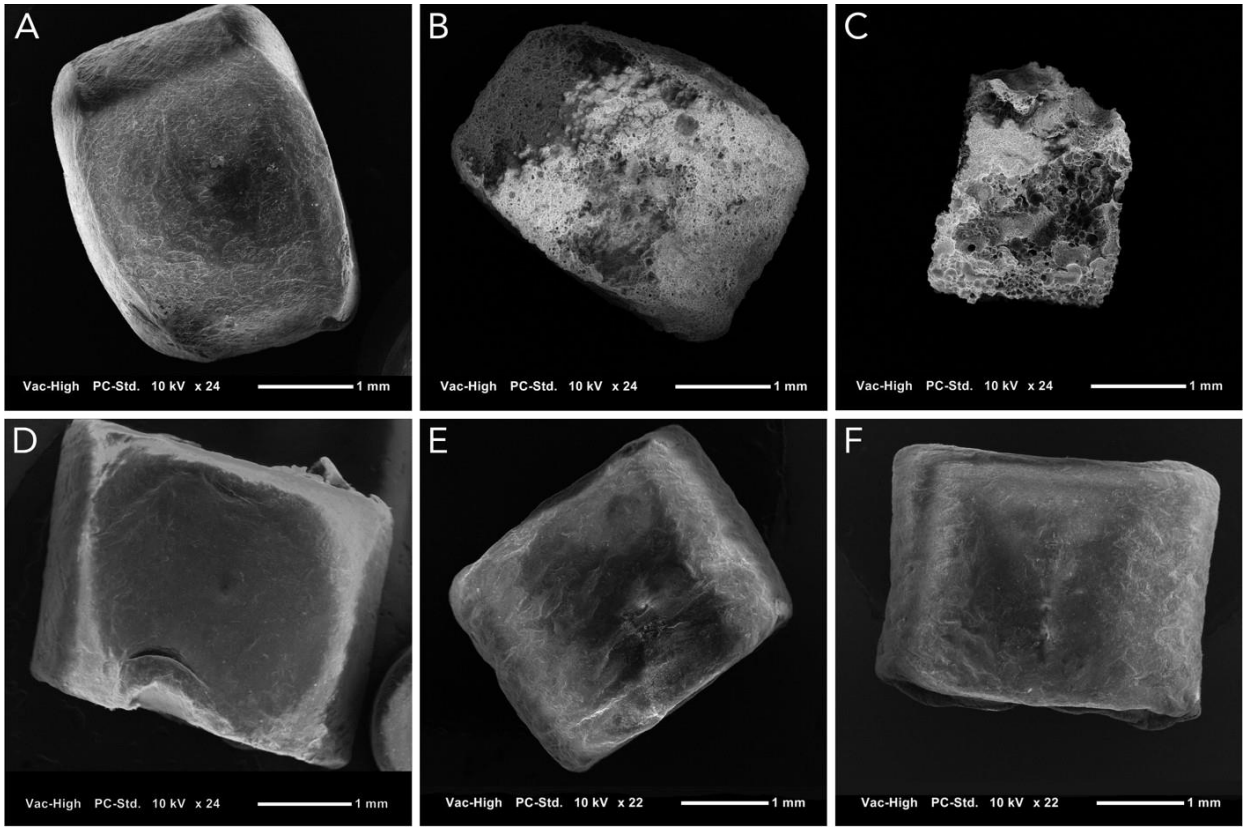

Figure 13. Scanning electron images of PHA and PET pellets without biofilm at approximately 20X magnification. The top panels show PHA pellets while the bottom shows PET pellets. Images demonstrate a time series: 0 (A and D), 196 (B and E), and 424 (C and F) days exposure.

Microbial community structure

The effect of sample type (PET, PHA, ceramic, and seawater) on community structure was analyzed by PCoA, and PERMANOVA and PERMDISP were used to test for significant differences between all communities. The PCoA analysis illustrated that 1) the communities associated with substrates (i.e. biofilms) were clearly different from the free-living communities in the overlying seawater, 2) the communities fouling ceramic and PET were indistinguishable, and 3) the communities fouling PHA were distinct in comparison to the communities fouling PET and ceramic (Figure 14). Taxonomic differences between substrate-associated and free-living communities is a well-established dichotomy in microbial ecology (DeLong et al., 1993;

Murrell et al., 1999; Hollibaugh et al., 2000; Kellogg and Deming, 2014). The apparent lack of distinction between ceramic and PET indicates that PET was not colonized by a unique community and this result supports previous studies that utilized a biofilm control (Oberbeckmann et al., 2016; Pinnell and Turner, 2019). The PERMANOVA analysis indicated that all four community types (pairwise test between all community types: adjusted $p<0.05$) were significantly different but the PERMDISP (pairwise test between all samples: $p>0.05$) indicated that the significance between communities may be the result of the unequal dispersion of variability among samples.

Relative abundances from each sample were calculated to identify dominant community members across all time points in each sample type. At the class level, ASVs assigned to Deltaproteobacteria were the most abundant among all three biofilm communities but made a much larger proportion of the PHA biofilms (39%) versus PET (25%) and ceramic (25%). Contrastingly, Alphaproteobacteria was the most abundant class in seawater communities (47%) and among the top five most abundant classes in PET and ceramic biofilms (8.3% and 7.0%, respectively) but not in PHA biofilms. While Bacteroidia was among the top five in all four communities, it made up a considerably larger proportion in PET, ceramic, and seawater communities (~15%) than in PHA biofilms (6%). Members of Alphaproteobacteria and Bacteroidia are typical marine surface colonizers and would be expected among the most common organisms within biofilm communities in marine environments (Salta et al., 2013; Dang and Lovell, 2016). Their decreased abundance within PHA biofilms lends further support to previous work demonstrating that PHA recruited a specific assemblage of microbial colonizers atypical of inert surfaces (Pinnell and Turner, 2019). A detailed report of taxonomic classes based on relative abundance is provided in Table 5.

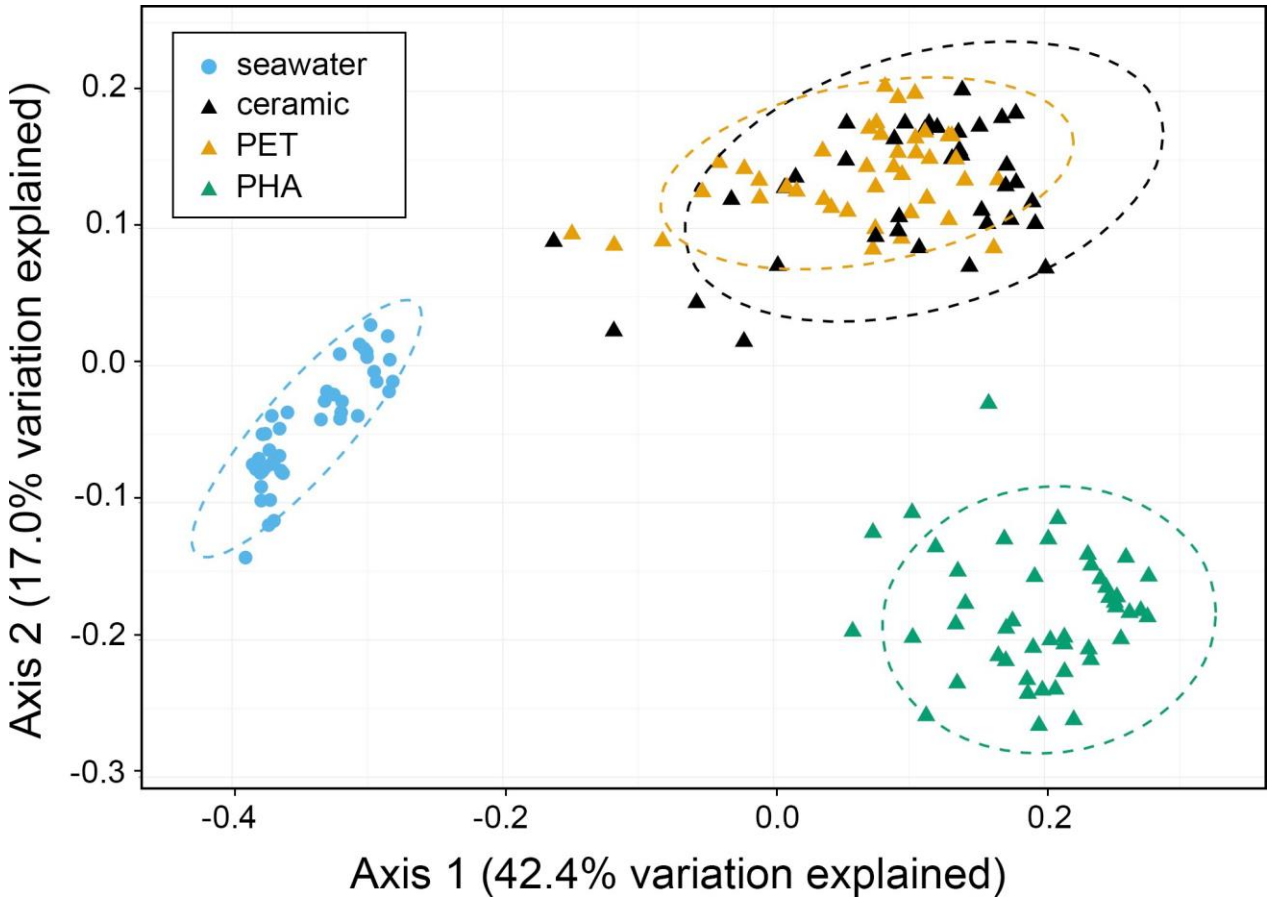

Figure 14. Principal coordinates analysis (PCoA) of weighted Unifrac distances illustrating the variation in microbial community structure. The PCoA demonstrates the clustering of 16S rRNA gene sequences from seawater (n=45), ceramic (n=40), PET (n=40), and PHA (n=45). Dashed lines represent the 95% confidence ellipses for each community type.

Table 6. Top 10 members from each taxonomic family based on normalized relative abundance. Means (n=2-3 seawater, ceramic, PET; n=3 PHA) plus or minus one standard deviation are reported for each taxonomy.

PHA

Date; Exp.*	November 15; 28 days	December 13; 56 days	January 12; 86 days	February 6; 111 days	March 7; 140 days
	Sedimenticolaceae (40.35% ± 9.15)	*Sedimenticolaceae* (28.61% ± 5.74)	*Sedimenticolaceae* (19.86% ± 4.81)	*Sedimenticolaceae* (13.56% ± 7.30)	*Desulfobacteraceae* (20.73% ± 1.98)
	Desulfobacteraceae (16.45% ± 3.49)	*Desulfobacteraceae* (16.35% ± 5.22)	*Desulfobacteraceae* (10.99% ± 8.62)	*Desulfobacteraceae* (13.05% ± 0.74)	*Spirochaetaceae* (8.63% ± 9.11)
	Desulfobulbaceae (5.61% ± 0.52)	*Desulfobulbaceae* (8.45% ± 3.19)	*Desulfobulbaceae* (10.83% ± 3.62)	*Desulfobulbaceae* (11.90% ± 2.24)	*Anaerolineaceae* (6.72% ± 1.38)
	Desulfovibrionaceae (4.47% ± 1.19)	*Anaerolineaceae* (6.08% ± 2.31)	*Bacteroidetes BD2-2* (5.76% ±)	*Spirochaetaceae* (9.39% ± 2.11)	Cand. Moranbacteria (6.45% ± 11.17)
	Spirochaetaceae (4.07% ± 1.04)	*Spirochaetaceae* (4.39% ± 0.78)	*Anaerolineaceae* (4.94% ± 0.25)	*Anaerolineaceae* (4.88% ± 1.04)	*Desulfobulbaceae* (5.76% ± 3.64)
	Anaerolineaceae (2.95% ± 1.13)	*Bacteroidetes BD2-2* (3.22% ± 1.66)	*Spirochaetaceae* (4.28% ± 0.25)	*Bacteroidetes BD2-2* (3.84% ± 0.53)	*Sedimenticolaceae* (5.01% ± 0.87)
	Bacteroidetes BD2-2 (2.01% ± 0.94)	*Desulfovibrionaceae* (2.66% ± 1.65)	*Flavobacteriaceae* (3.45% ± 0.25)	*GW2011_AR13* (3.54% ± 6.13)	*Desulfovibrionaceae* (4.80% ± 1.36)
	Salinivirgaceae (1.72% ± 0.76)	uncult. Anaerolineae (1.31% ± 0.58)	*Desulfovibrionaceae* (3.34% ± 0.25)	*Desulfovibrionaceae* (2.42% ± 2.33)	*Bacteroidetes BD2-2* (2.09% ± 0.94)
	Leptospiraceae (1.21% ± 1.16)	*Calditrichaceae* (1.26% ± 0.53)	*Acanthopleuribacteraceae* (2.96% ± 0.25)	*Flavobacteriaceae* (2.25% ± 0.67)	uncult. Rhodospirillales (2.03% ± 1.48)
	Flavobacteriaceae (1.09% ± 1.01)	*Leptospiraceae* (1.22% ± 1.06)	*UASB-TL25* (2.53% ± 0.25)	uncult. Anaerolineae (2.03% ± 0.35)	*Calditrichaceae* (2.00% ± 2.01)
Date; Exp.*	**April 6; 170 days**	**May 7; 196 days**	**May 30; 224 days**	**June 29; 254 days**	**July 25; 280 days**
	Desulfobacteraceae (21.77% ± 5.70)	*Desulfobacteraceae* (27.04% ± 0.91)	*Desulfobacteraceae* (31.36% ± 1.48)	*Desulfobacteraceae* (27.79% ± 2.85)	*Desulfobacteraceae* (19.98% ± 1.15)
	Desulfobulbaceae (8.27% ± 2.53)	*Sedimenticolaceae* (8.30% ± 1.92)	*Sedimenticolaceae* (4.65% ± 0.72)	*Desulfovibrionaceae* (5.84% ± 1.23)	Cand. Pacebacteria (6.12% ± 7.73)
	Sedimenticolaceae (7.92% ± 5.13)	*Desulfobulbaceae* (5.92% ± 0.44)	*Desulfobulbaceae* (4.51% ± 2.22)	*Sedimenticolaceae* (4.01% ± 3.18)	*Desulfarculaceae* (5.74% ± 3.76)
	Anaerolineaceae (6.49% ± 0.45)	*Anaerolineaceae* (5.80% ± 1.14)	*Desulfovibrionaceae* (4.50% ± 2.01)	*Anaerolineaceae* (3.93% ± 1.60)	*Desulfovibrionaceae* (3.52% ± 2.69)
	Desulfovibrionaceae (3.82% ± 0.89)	*Desulfovibrionaceae* (4.87% ± 0.80)	*Calditrichaceae* (3.51% ± 0.73)	*Desulfobulbaceae* (3.78% ± 0.84)	*Calditrichaceae* (2.56% ± 1.11)
	Spirochaetaceae (3.80% ± 1.15)	*Spirochaetaceae* (4.18% ± 0.55)	*Anaerolineaceae* (3.26% ± 2.39)	*Lentimicrobiaceae* (2.41% ± 1.51)	*Anaerolineaceae* (2.52% ± 0.76)
	Calditrichaceae (2.70% ± 2.06)	*Calditrichaceae* (2.42% ± 0.33)	*Spirochaetaceae* (3.19% ± 0.95)	*Spirochaetaceae* (2.36% ± 0.92)	*Bacteroidetes BD2-2* (2.46% ± 1.18)
	Bacteroidetes BD2-2 (2.66% ± 1.02)	*Acanthopleuribacteraceae* (2.19% ± 0.09)	*Bacteroidetes BD2-2* (2.08% ± 0.63)	*Calditrichaceae* (2.22% ± 0.36)	*Spirochaetaceae* (2.36% ± 1.09)
	uncult. Aegiribacteria (1.72% ± 1.76)	*Bacteroidetes BD2-2* (2.00% ± 0.55)	*Acanthopleuribacteraceae* (1.96% ± 0.45)	*Acanthopleuribacteraceae* (2.14% ± 1.64)	*Acanthopleuribacteraceae* (1.66% ± 0.58)
	uncult. Anaerolineae (1.68% ± 0.26)	*UASB-TL25* (1.75% ± 0.81)	*Thermoanaerobaculaceae* (1.39% ± 0.13)	uncult. Cand. Pacebacteria (1.72% ± 1.22)	*Desulfobulbaceae* (1.62% ± 0.60)
Date; Exp.*	**August 21; 307 days**	**September 20; 337 days**	**October 18; 373 days**	**November 27; 405 days**	**December 15; 424 days**
	Desulfobacteraceae (21.60% ± 3.15)	*Desulfobacteraceae* (18.86% ± 3.91)	*Desulfobacteraceae* (16.14% ± 0.10)	*Desulfobacteraceae* (16.88% ± 0.80)	*Desulfobacteraceae* (18.52% ± 1.58)
	Desulfovibrionaceae (9.28% ± 7.92)	*Desulfarculaceae* (11.15% ± 5.72)	*Desulfovibrionaceae* (12.76% ± 11.68)	*Desulfovibrionaceae* (13.51% ± 11.40)	*Desulfovibrionaceae* (13.48% ± 10.11)
	Anaerolineaceae (4.09% ± 2.07)	*Desulfovibrionaceae* (10.08% ± 4.48)	*Desulfarculaceae* (7.31% ± 7.00)	*Desulfarculaceae* (7.32% ± 2.26)	*Desulfarculaceae* (6.39% ± 3.02)
	Desulfarculaceae (3.94% ± 1.31)	*Anaerolineaceae* (3.20% ± 1.11)	*Sedimenticolaceae* (3.84% ± 5.58)	*Calditrichaceae* (2.37% ± 0.35)	*Anaerolineaceae* (3.05% ± 2.23)
	Spirochaetaceae (2.59% ± 0.74)	*Bacteroidetes BD2-2* (1.80% ± 0.26)	*Calditrichaceae* (2.26% ± 1.40)	*Anaerolineaceae* (2.22% ± 1.10)	*Spirochaetaceae* (1.87% ± 1.00)
	Calditrichaceae (1.83% ± 0.87)	*Spirochaetaceae* (1.62% ± 0.74)	*Spirochaetaceae* (2.09% ± 0.81)	*Bacteroidetes BD2-2* (1.94% ± 0.55)	*Bacteroidetes BD2-2* (1.85% ± 0.52)
	uncult. Thermoplasmatales (1.39% ± 0.22)	*Calditrichaceae* (1.18% ± 0.10)	*Anaerolineaceae* (2.04% ± 0.31)	*Spirochaetaceae* (1.82% ± 0.94)	*AKAU3564 sed. grp.* (1.69% ± 1.06)
	Bacteroidetes BD2-2 (1.25% ± 0.40)	*Thermoanaerobaculaceae* (1.18% ± 0.17)	*Bacteroidetes BD2-2* (1.41% ± 0.49)	*AKAU3564 sed. grp.* (1.50% ± 0.29)	uncult. Thermoplasmatales (1.63% ± 0.86)
	Acanthopleuribacteraceae (1.17% ± 0.82)	uncult. Thermoplasmatales (1.11% ± 0.30)	uncult. Thermoplasmatales (1.08% ± 0.28)	*Sedimenticolaceae* (1.20% ± 0.83)	*Sedimenticolaceae* (1.38% ± 0.65)
	uncult. Cand. Pacebacteria (1.03% ± 0.35)	*Acanthopleuribacteraceae* (1.01% ± 0.26)	*Rhodobacteraceae* (1.04% ± 0.32)	uncult. Omnitrophia (0.90% ± 0.61)	*Syntrophaceae* (1.04% ± 0.49)

PET

Date; Exp.*	November 15; 28 days	December 13; 56 days	January 12; 86 days	February 6; 111 days	March 7; 140 days
	uncultured LCP-89 (9.27% ± 12.46)	*Desulfobacteraceae* (10.80% ± 10.68)	*Desulfobacteraceae* (15.73% ± 5.28)	*Desulfobacteraceae* (9.28% ± 8.76)	*Desulfobacteraceae* (9.85% ± 2.77)
	Desulfuromonadaceae (8.08% ± 7.27)	*Rhodobacteraceae* (5.83% ± 3.70)	*Bacteroidetes BD2-2* (5.88% ± 0.06)	*Rhodobacteraceae* (8.25% ± 5.44)	*Desulfobulbaceae* (7.11% ± 8.92)
	Desulfobacteraceae (7.97% ± 0.32)	*Sedimenticolaceae* (3.56% ± 3.95)	*Rhodobacteraceae* (5.29% ± 0.91)	*Microtrichaceae* (6.79% ± 0.70)	*Rhodobacteraceae* (5.24% ± 2.87)
	Bacteroidetes BD2-2 (5.32% ± 1.55)	*Bacteroidetes BD2-2* (3.45% ± 2.93)	*Chromatiaceae* (3.03% ± 1.22)	*Saprospiraceae* (4.70% ± 4.09)	*Bacteroidetes BD2-2* (4.63% ± 1.95)
	Bacteroidales *SB-5* (4.19% ± 0.16)	*Saprospiraceae* (2.99% ± 3.86)	uncult. γ-protebacterium (2.82% ± 0.85)	*Bacteroidetes BD2-2* (2.26% ± 3.20)	*Vibrionaceae* (4.34% ± 9.21)
	Desulfobulbaceae (3.86% ± 0.82)	*Calditrichaceae* (2.43% ± 1.58)	*Desulfobulbaceae* (2.80% ± 0.19)	*Cyclobacteriaceae* (1.89% ± 1.61)	*Lentimicrobiaceae* (2.48% ± 1.31)
	Anaerolineaceae (3.79% ± 1.16)	Bacteroidales *SB-5* (2.27% ± 3.21)	uncult. Actinomarinales (2.61% ± 1.10)	*Sedimenticolaceae* (1.72% ± 0.86)	*Chromatiaceae* (2.47% ± 0.84)
	Sedimenticolaceae (2.77% ± 2.77)	*Anaerolineaceae* (2.04% ± 1.13)	uncult. *Bacteroidetes* (2.53% ± 0.94)	*Desulfobulbaceae* (1.59% ± 0.10)	*Cyclobacteriaceae* (2.32% ± 0.05)
	Spirochaetaceae (2.33% ± 0.80)	*Cyclobacteriaceae* (1.90% ± 0.37)	*Cyclobacteriaceae* (2.30% ± 0.71)	*Halieaceae* (1.39% ± 0.64)	*Sedimenticolaceae* (2.12% ± 0.83)
	Myxococcales *MidBa8* (1.80% ± 2.54)	*Pirellulaceae* (1.86% ± 1.09)	*Halieaceae* (2.12% ± 1.19)	*Pirellulaceae* (1.33% ± 0.78)	*Prolixibacteraceae* (2.12% ± 0.62)
Date; Exp.*	**April 6; 170 days**	**May 7; 196 days**	**May 30; 224 days**	**June 29; 254 days**	**July 25; 280 days**
	Desulfobacteraceae (18.41% ± 3.87)	*Desulfobacteraceae* (18.11% ± 2.09)	*Desulfobacteraceae* (15.08% ± 5.10)	*Desulfobacteraceae* (22.63% ± 2.16)	*Desulfobacteraceae* (18.98% ± 5.27)
	Bacteroidetes BD2-2 (6.25% ± 0.25)	*Saprospiraceae* (4.91% ± 0.49)	*Rhodobacteraceae* (6.40% ± 1.55)	*Bacteroidetes BD2-2* (5.48% ± 1.00)	*Bacteroidetes BD2-2* (4.82% ± 0.71)
	Rhodobacteraceae (3.62% ± 0.49)	*Rhodobacteraceae* (4.28% ± 0.49)	*Saprospiraceae* (4.50% ± 0.95)	*Rhodobacteraceae* (3.55% ± 0.74)	*Rhodobacteraceae* (4.11% ± 1.88)
	Calditrichaceae (3.31% ± 1.85)	*Bacteroidetes BD2-2* (4.08% ± 0.49)	*Bacteroidetes BD2-2* (3.56% ± 1.00)	*Anaerolineaceae* (2.97% ± 1.23)	*Spirochaetaceae* (3.65% ± 0.20)
	Prolixibacteraceae (2.83% ± 2.22)	*Anaerolineaceae* (3.51% ± 0.49)	*Calditrichaceae* (2.53% ± 0.47)	*Calditrichaceae* (2.94% ± 1.83)	*Anaerolineaceae* (3.52% ± 1.12)
	Desulfobulbaceae (2.47% ± 0.80)	*Calditrichaceae* (2.27% ± 0.49)	uncult. Actinomarinales (2.43% ± 0.65)	uncult. Actinomarinales (2.52% ± 1.05)	*Chromatiaceae* (2.53% ± 2.16)
	uncult. Actinomarinales (2.33% ± 0.66)	*Chromatiaceae* (2.23% ± 0.49)	*Anaerolineaceae* (2.32% ± 0.59)	*Spirochaetaceae* (2.42% ± 2.14)	*Calditrichaceae* (2.47% ± 1.08)
	Cyclobacteriaceae (2.33% ± 0.42)	*Cyclobacteriaceae* (2.16% ± 0.49)	*Desulfobulbaceae* (2.29% ± 0.41)	*Cyclobacteriaceae* (2.27% ± 0.52)	uncult. Actinomarinales (2.40% ± 0.01)
	Lentimicrobiaceae (2.06% ± 0.28)	uncult. Actinomarinales (2.08% ± 0.49)	*Chromatiaceae* (2.24% ± 0.34)	*Desulfobulbaceae* (2.23% ± 1.67)	*Saprospiraceae* (2.37% ± 0.19)
	Chromatiaceae (2.02% ± 1.90)	*Woeseiaceae* (1.98% ± 0.49)	*Cyclobacteriaceae* (1.91% ± 0.96)	*Chromatiaceae* (1.84% ± 0.29)	*Desulfobulbaceae* (2.27% ± 0.24)
Date; Exp.*	**August 21; 307 days**	**September 20; 337 days**	**October 18; 373 days**	**November 27; 405 days**	**December 15; 424 days**
	Desulfobacteraceae (15.94% ± 4.09)	*Desulfobulbaceae* (14.51% ± 5.72)	*Desulfobacteraceae* (19.73% ± 11.20)	*Desulfobacteraceae* (19.14% ± 2.20)	*Desulfobacteraceae* (19.19% ± 0.35)
	Bacteroidetes BD2-2 (6.98% ± 0.76)	*Desulfobacteraceae* (14.04% ± 3.44)	*Bacteroidetes BD2-2* (5.88% ± 2.86)	*Anaerolineaceae* (5.63% ± 0.35)	*Anaerolineaceae* (5.09% ± 0.71)
	Calditrichaceae (4.37% ± 1.89)	*Anaerolineaceae* (5.68% ± 1.68)	*Anaerolineaceae* (4.29% ± 1.06)	*Desulfobulbaceae* (3.66% ± 0.90)	*Desulfobulbaceae* (4.11% ± 2.03)
	Anaerolineaceae (4.05% ± 0.90)	*Bacteroidetes BD2-2* (4.22% ± 1.35)	*Rhodobacteraceae* (2.67% ± 1.06)	*Rhodobacteraceae* (3.46% ± 0.16)	*Bacteroidetes BD2-2* (4.03% ± 0.60)
	uncult. Actinomarinales (3.18% ± 0.26)	*Rhodobacteraceae* (4.10% ± 2.02)	*Spirochaetaceae* (2.59% ± 0.65)	*Bacteroidetes BD2-2* (3.09% ± 1.03)	*Spirochaetaceae* (3.52% ± 1.64)
	Chromatiaceae (3.08% ± 0.99)	*Saprospiraceae* (3.32% ± 0.82)	*Desulfobulbaceae* (2.34% ± 2.19)	*Calditrichaceae* (2.70% ± 0.19)	*Rhodobacteraceae* (2.54% ± 0.69)
	Rhodobacteraceae (3.03% ± 0.87)	*Cyclobacteriaceae* (3.17% ± 0.30)	*Cyclobacteriaceae* (2.25% ± 1.88)	*Spirochaetaceae* (2.62% ± 0.38)	*Chromatiaceae* (2.47% ± 0.65)
	Lentimicrobiaceae (2.78% ± 1.25)	*Calditrichaceae* (2.06% ± 0.69)	*Calditrichaceae* (2.06% ± 0.29)	*Pirellulaceae* (2.19% ± 1.15)	*Calditrichaceae* (2.43% ± 072)
	Melioribacteraceae (2.28% ± 1.65)	*Chromatiaceae* (2.00% ± 0.40)	*Chromatiaceae* (2.04% ± 2.50)	*Saprospiraceae* (1.87% ± 0.20)	*Halieaceae* (1.90% ± 0.78)
	Spirochaetaceae (2.00% ± 1.58)	*Sandaracinaceae* (1.84% ± 0.04)	*Desulfarculaceae* (2.04% ± 0.03)	*Chromatiaceae* (1.83% ± 0.46)	uncult. Actinomarinales (1.87% ± 0.99)

ceramic

Date; Exp.*	November 15; 28 days[#]	December 13; 56 days	January 12; 86 days	February 6; 111 days	March 7; 140 days[#]
		Desulfobacteraceae (11.13% ± 6.96)	*Desulfobacteraceae* (12.05% ± 6.96)	*Desulfobacteraceae* (18.74% ± 5.00)	
		Rhodobacteraceae (6.81% ± 4.57)	*Rhodobacteraceae* (7.28% ± 4.57)	*Anaerolineaceae* (4.65% ± 3.48)	
		Desulfobulbaceae (6.45% ± 6.48)	*Pirellulaceae* (3.41% ± 4.57)	*Pirellulaceae* (4.02% ± 3.07)	
		Saprospiraceae (3.92% ± 3.49)	*Anaerolineaceae* (2.46% ± 4.57)	*Rhodobacteraceae* (3.01% ± 2.34)	
		Anaerolineaceae (3.26% ± 2.05)	*Chromatiaceae* (2.40% ± 4.57)	*Calditrichaceae* (2.98% ± 1.15)	
		Bacteroidetes BD2-2 (2.57% ± 1.82)	*Streptococcaceae* (2.12% ± 4.57)	*Bacteroidetes BD2-2* (2.75% ± 1.21)	
		uncult. Actinomarinales (2.27% ± 0.82)	γ-proteobacteria *inc. sed.* (2.08% ± 4.57)	*Desulfobulbaceae* (2.29% ± 0.89)	
		Pirellulaceae (2.24% ± 0.94)	*Saprospiraceae* (2.06% ± 4.57)	*Saprospiraceae* (2.04% ± 1.37)	
		Sedimenticolaceae (1.51% ± 1.35)	*Desulfobulbaceae* (1.80% ± 4.57)	uncult. Actinomarinales (1.84% ± 0.86)	
		Microtrichaceae (1.45% ± 2.06)	*Cyclobacteriaceae* (1.74% ± 4.57)	*Spirochaetaceae* (1.77% ± 0.65)	
Date; Exp.*	**April 6; 170 days**	**May 7; 196 days**	**May 30; 224 days**	**June 29; 254 days**	**July 25; 280 days**
	Desulfobacteraceae (14.76% ± 5.40)	*Desulfobacteraceae* (18.00% ± 2.50)	*Desulfobacteraceae* (17.72% ± 6.35)	*Desulfobacteraceae* (20.33% ± 4.15)	*Desulfobacteraceae* (25.14% ± 3.07)
	Rhodobacteraceae (4.87% ± 4.38)	*Anaerolineaceae* (4.55% ± 1.61)	*Anaerolineaceae* (5.07% ± 0.70)	*Bacteroidetes BD2-2* (6.88% ± 0.75)	*Anaerolineaceae* (7.64% ± 2.56)
	Anaerolineaceae (4.62% ± 3.93)	*Rhodobacteraceae* (3.89% ± 1.22)	*Calditrichaceae* (4.33% ± 1.07)	*Anaerolineaceae* (5.69% ± 0.38)	*Calditrichaceae* (4.15% ± 0.05)
	Saprospiraceae (4.23% ± 2.22)	*Bacteroidetes BD2-2* (3.62% ± 0.63)	*Pirellulaceae* (4.27% ± 0.88)	*Spirochaetaceae* (3.37% ± 0.54)	*Bacteroidetes BD2-2* (4.13% ± 2.28)
	Pirellulaceae (4.04% ± 0.74)	*Saprospiraceae* (3.62% ± 1.73)	*Bacteroidetes BD2-2* (3.47% ± 0.89)	*Prolixibacteraceae* (3.43% ± 1.39)	*Spirochaetaceae* (3.44% ± 0.01)
	Calditrichaceae (3.48% ± 1.87)	*Calditrichaceae* (2.86% ± 1.04)	*Rhodobacteraceae* (3.42% ± 2.32)	*Desulfobulbaceae* (2.77% ± 1.34)	*Rhodobacteraceae* (3.24% ± 3.89)
	Bacteroidetes BD2-2 (2.83% ± 2.28)	*Pirellulaceae* (2.86% ± 0.49)	*Saprospiraceae* (2.75% ± 1.45)	*Chromatiaceae* (2.74% ± 0.20)	*Pirellulaceae* (2.31% ± 0.42)
	Cyclobacteriaceae (1.94% ± 0.43)	*uncult. Actinomarinales* (2.43% ± 0.19)	*Desulfobulbaceae* (2.53% ± 1.38)	*Saprospiraceae* (2.70% ± 0.65)	*uncult. Actinomarinales* (2.24% ± 0.72)
	Desulfobulbaceae (1.82% ± 0.70)	*Cyclobacteriaceae* (1.89% ± 0.70)	*Prolixibacteraceae* (2.38% ± 1.28)	*uncult. Actinomarinales* (2.69% ± 0.65)	*Prolixibacteraceae* (2.23% ± 1.45)
	Lentimicrobiaceae (1.68% ± 1.29)	*Chromatiaceae* (1.87% ± 0.57)	*Chromatiaceae* (1.78% ± 0.65)	*Calditrichaceae* (2.47% ± 0.14)	*Desulfobulbaceae* (1.92% ± 1.20)
Date; Exp.*	**August 21; 307 days**	**September 20; 337 days**	**October 18; 373 days**	**November 27; 405 days**	**December 15; 424 days**
	Desulfobacteraceae (21.89% ± 2.52)	Desulfobacteraceae (23.87% ± 0.93)	Desulfobacteraceae (17.91% ± 3.77)	Desulfobacteraceae (21.52% ± 2.82)	Desulfobacteraceae (14.15% ± 4.88)
	Anaerolineaceae (8.69% ± 3.45)	Anaerolineaceae (10.39% ± 2.07)	Anaerolineaceae (6.81% ± 1.47)	Anaerolineaceae (5.90% ± 3.40)	Anaerolineaceae (5.65% ± 1.60)
	Calditrichaceae (4.35% ± 1.61)	Pirellulaceae (3.80% ± 1.59)	Bacteroidetes BD2-2 (6.15% ± 2.86)	Calditrichaceae (4.04% ± 1.53)	Bacteroidetes BD2-2 (5.23% ± 0.67)
	Pirellulaceae (4.30% ± 0.19)	Calditrichaceae (3.07% ± 0.35)	Pirellulaceae (3.83% ± 1.96)	Bacteroidetes BD2-2 (3.77% ± 0.76)	Desulfobulbaceae (3.28% ± 1.76)
	Spirochaetaceae (2.93% ± 0.32)	Bacteroidetes BD2-2 (2.71% ± 0.23)	Desulfobulbaceae (3.72% ± 0.56)	Saprospiraceae (3.64% ± 4.79)	Calditrichaceae (2.95% ± 0.71)
	Bacteroidetes BD2-2 (2.75% ± 0.80)	Desulfobulbaceae (2.02% ± 0.55)	Spirochaetaceae (3.32% ± 1.46)	Pirellulaceae (2.53% ± 0.35)	Pirellulaceae (2.81% ± 0.93)
	Desulfobulbaceae (2.66% ± 0.24)	Chromatiaceae (1.90% ± 0.10)	Calditrichaceae (2.91% ± 1.19)	Rhodobacteraceae (2.35% ± 3.23)	Halieaceae (2.53% ± 0.74)
	Chromatiaceae (2.16% ± 0.49)	Rhodobacteraceae (1.84% ± 0.75)	Rhodobacteraceae (2.68% ± 0.78)	Spirochaetaceae (2.35% ± 1.10)	Cyclobacteriaceae (2.42% ± 0.23)
	Rhodobacteraceae (1.97% ± 0.38)	Spirochaetaceae (1.70% ± 0.30)	Desulfarculaceae (2.18% ± 0.60)	Desulfarculaceae (2.33% ± 0.87)	Spirochaetaceae (2.32% ± 0.41)
	Lentimicrobiaceae (1.83% ± 0.82)	uncult. Actinomarinales (1.66% ± 0.73)	Saprospiraceae (1.75% ± 1.23)	Desulfobulbaceae (2.21% ± 0.60)	Lentimicrobiaceae (2.27% ± 1.08)

Abbreviations: Exp., Exposure Length; uncult., uncultured; Cand., Candidatus; *mar. grp.*, *marine group*; *inc. sed., incertae* sedis; *sed. grp., sediment group*

* exposure length only relevant to substrate-based communities (ceramic, PET, PHA)

[#] no data for this date and exposure length

Microbial succession

Temporal changes in biofilm community structure were first analyzed by comparing the relative abundances of the top nine microbial classes (e.g. Deltaproteobacteria, Gammaproteobacteria, Bacteroidia, Anarolineae, Alphaproteobacteria, Spirochaetia, Calditrichia, Woesearchaeia, and Phycisphaerae). Data showed that all three substrates experienced an increase in Deltaproteobacteria and a decrease in Gammaproteobacteria (Figure 15). Trends were more divided between remaining classes: Bacteroidia decreased in PHA and PET biofilms, Anarolineae increased in PET and ceramic biofilms, Spirochaetia decreased in PHA biofilms, Calditrichia increased in ceramic biofilms, and Phycisphaerae increased in PHA biofilms (ANOVA; p-value=<0.05; Figure 15).

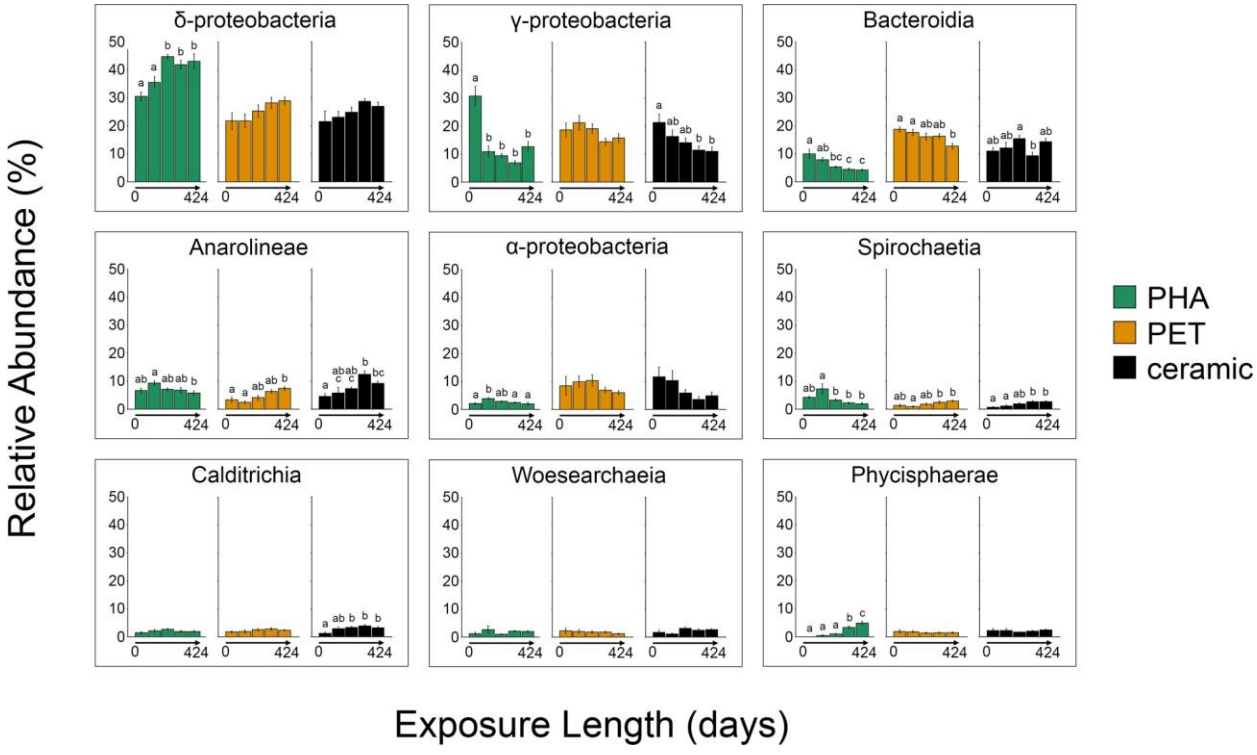

Figure 15. Barplot showing the relative abundances of the top nine taxonomic classes across the three substrate types (PHA, PET, and ceramic) at each temporal stage. Error bars display the standard error of the mean. Significant differences in abundance between temporal stages are illustrated by different letters (ANOVA, p-value<0.05, n=7-9).

In marine environments, the *Rhodobacteraceae, Alteromonaceae,* and *Flavobacteriaceae* are common surface colonizers (Salta et al., 2013; Dang and Lovell, 2016), and their prominence was observed here in the PET and ceramic biofilms throughout all five temporal stages (Table 5; Figure 15). They were less prominent across time within PHA biofilms where an increased abundance of Deltaproteobacteria was coupled with a decreased abundance of *Rhodobacteraceae* and *Flavobacteriaceae* (Table 5; Figure 15), demonstrating that despite the temporal changes, the PHA-associated community structure remained atypical of marine biofilms throughout the course of this study.

Temporal changes in biofilm community structure were further analyzed by comparing diversity indices. A comparison of FPD (i.e. alpha-diversity) was used to test temporal differences within sample types. Both PHA and PET biofilm alpha-diversity increased significantly over time (ANOVA; p-value=<0.05, Figure 16), although PHA biofilm diversity increased more rapidly, reaching a significantly higher FDP at stage 4, while PET biofilm diversity was not significantly higher until stage 5. This increase in diversity over time confirms previous reports that mature biofilms are typically more diverse (Jackson et al., 2001; Chung et al., 2010). The more rapid increase in PHA biofilm diversity may reflect the formation of ecological niches due to its biodegradation. For instance, the extensive pitting observed in the PHA pellets (see Figure 12) may have created anoxic microenvironments that selected for the growth of anaerobes.

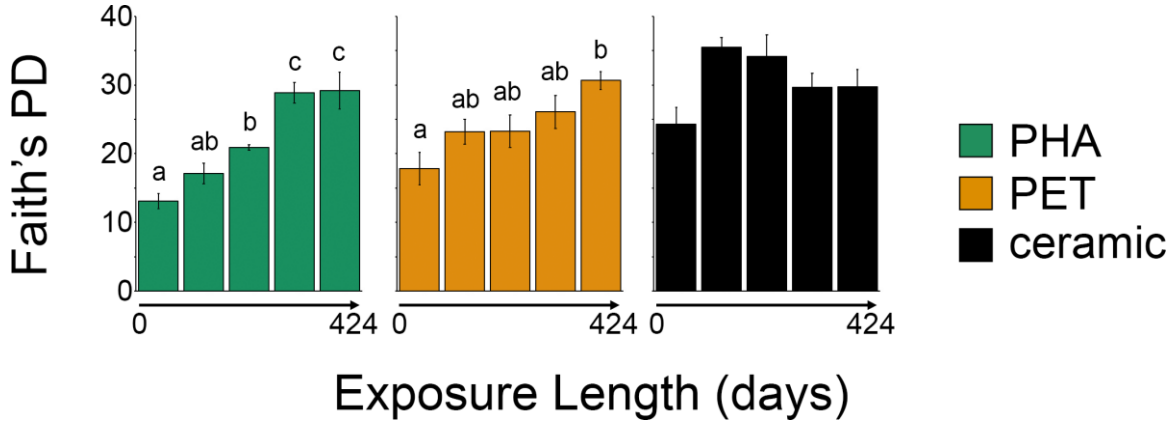

Figure 16. Barplot showing Faith's phylogenetic distance for each substrate type (PHA, PET, and ceramic) at each temporal stage. Error bars display the standard error of the mean. Significant differences in alpha-diversity between temporal stages are illustrated by different letters (ANOVA, p-value<0.05, n=7-9).

A comparison of weighted UniFrac values (i.e. beta-diversity) was used to test temporal differences between sample types. PHA biofilm beta-diversity was significantly different than PET and ceramic biofilm beta-diversity during all 5 stages (PERMANOVA; adj. p-value<0.05), although the PERMDISP test at stage 3 was significant (pairwise test: adj. p-value<0.05). By contrast, PET and ceramic beta-diversity were not significantly different during stages 1, 2, 3, and 5. At the fourth stage, each of the three substrate types were significantly different (PERMANOVA; pairwise test between all community types: adj. p-value<0.05) and the PERMDISP test was not significant. Thus, this comparison of beta-diversity mirrored the results of the above PCoA analysis with one exception: this temporal analysis makes clear that PET and ceramic diversity was significantly different during stage 4 (280-337 days) when the water temperature and salinity were at a maximum (see Table 4). This significant difference could be the result of temperature or salinity as De Tender et al. showed that both parameters influence

the microbial colonization of plastics (De Tender et al., 2015) and Oberbeckmann et al. showed that higher salinities support plastic-specific microbial assemblages (Oberbeckmann et al., 2018).

SRM Abundance

To further explore changes in Deltaproteobacteria abundance and diversity, known SRM (Table 6) were filtered from the total microbial community and relative abundances were calculated and compared at each of the 15 timepoints. Data showed that the relative abundance of SRM was significantly higher in PHA biofilms, compared to PET and ceramic, at 12 of the 15 sampling dates (ANOVA; p-value=<0.05; Figure 17). SRM were visually more abundant during the three non-significant timepoints (86, 280, and 405 days) but large data variation within those three dates diminished statistical power. The composition of SRM families also differed: *Desulfobacteraceae*, *Desulfobulbaceae*, and *Desulfovibrionaceae* were abundant in PHA biofilms while *Desulfobacteraceae* and *Desulfobulbaceae* were abundant in PET and ceramic biofilms. SRM typically comprise between 5-25% of the total bacterial community in estuarine sediments (Purdy et al., 2002; Bowen et al., 2012; Cheung et al., 2018). In this study, SRM abundance in the PHA biofilms ranged from 25-40% while abundance in the PET and ceramic biofilms ranged from 10-25% (Figure 17).

The significant increase in the relative abundance of Deltaproteobacteria in the PHA biofilm was primarily the result of increases in three SRM families. *Desulfobacteraceae* increased during stages 2 and 3 (days 111-224; Figure 17; Table 6) and remained the most abundant family throughout. A subsequent decrease in the relative abundance of *Desulfobacteraceae*, during stage 4, gave rise to other SRM families (days 280-337; Figure 17; Table 6). In particular, *Desulfovibrionaceae* and *Desulfarculaceae* increased significantly,

becoming the second and third most abundant families (~13% and ~7% relative abundance, respectively; Table 6). This increased relative abundance indicates that PHA biofilm maturation favored sulfate reducers. While *Desulfobacteraceae* abundance increased slightly within PET and ceramic biofilms during stages 2 and 3 (days 111-224; Supplemental Table 6; Figure 17), it was not followed by a stage 4 decrease accompanied by increases in *Desulfovibrionaceae* and *Desulfarculaceae*.

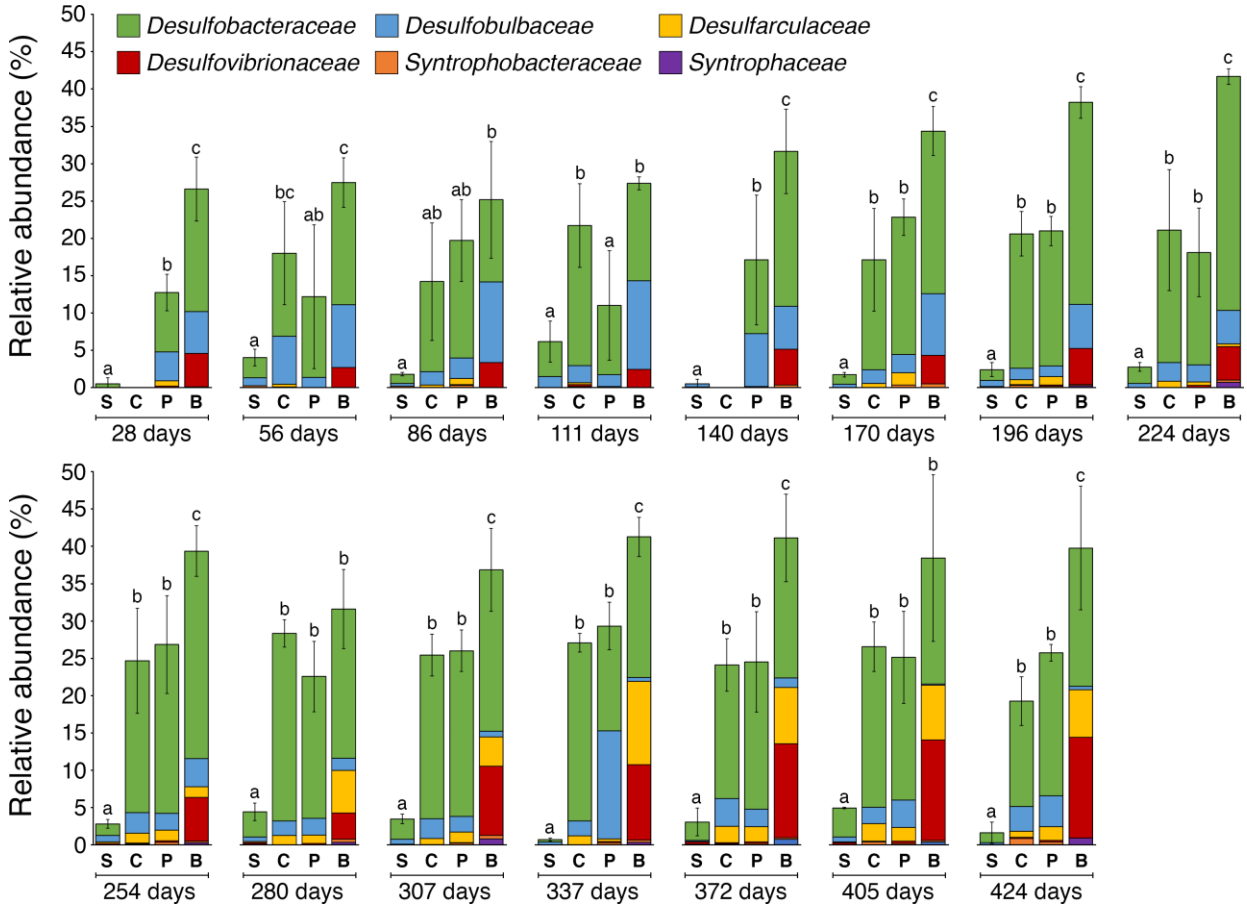

Figure 17. Barplot showing the relative abundance of the SRM families within each microbial community (S, seawater; C, ceramic; P, PET; B, PHA). Error bars display the standard deviation of total combined SRM abundance within each community. Significant differences between total SRM abundance are illustrated by different letters (ANOVA, p-value<0.05, n=2-3).

The rise of *Desulfarculaceae* after 224 days warrants further consideration. The *Desulfarculaceae* represent a distant lineage within the Deltaproteobacteria capable of oxidizing

long-chain fatty acids similar in structure to PHA (Sun et al., 2010). *Desulfarculaceae* are also underrepresented in the literature, with only three described genera and eight representative genomes in NCBI. Isolates from *Desulfarculaceae* are strictly anaerobic (Kuever, 2014) and capable of degrading a variety of complex carbon sources including pyruvate (Davidova et al., 2016), benzoate (An and Picardal, 2014), sorbate (Schnell et al., 1991), and 3-hydroxybutyrate (Schnell et al., 1991), the latter of which is the building block of common PHAs. It follows that members of *Desulfarulaceae* could be utilizing PHA as a carbon source and their enrichment during the later stages of the experiment may have been facilitated by substrate pitting and the creation of anoxic microenvironments.

Environmental Implications

The global market for bioplastics is forecasted to increase by 20% over the next five years, and the production of PHA is expected to grow by 400% in the same time frame (Chinthapalli et al., 2019). It is therefore imperative to understand how PHA loading impacts natural environments. In marine environments, where sinking facilitates sedimentary biodegradation, the impact of PHA on benthic microbial communities remains an open question. The results of this study confirmed that PHA biodegrades slowly, on the order of two to three years, in marine sediments. Further, PHA was shown to stimulate SRM, which catalyze the mineralization of organic matter in anaerobic sediments (Jørgensen et al., 2019). Future work will inquire 1) how PHA loading impacts the balance between sulfate-reducing and methane-producing microbial populations and 2) how PHA loading potentially alters the sediment buffer capacity against sulfide release.

Acknowledgements.

This study would not have been possible without the support of our friends and colleagues. Specifically, we thank Robert “Bobby” Duke and the entire Center for Coastal Studies staff for assistance in the field. This study was funded by the Texas General Land Office’s Coastal Management Plan (GLO-CMP), the Texas Research and Development Fund (TRDF), Texas Sea Grant (TSG), and the National Sciences and Engineering Research Council of Canada (NSERC). The majority of computational data analysis was performed on TAMU-CC’s high-performance computing cluster, which is funded in part by the National Science Foundation’s CNS MRI Grant (No. 1429518).

CHAPTER 3:

ISOLATION AND GENOMIC CHARACTERIZATION OF THREE MEMBERS FROM A MARINE CONSORTIUM THAT DEGRADES POLYHYDROXYALKANOATE

Abstract.

Plastic is the most prominent type of anthropogenic debris found in marine environments, and one proposed solution for the reduction of plastic loading is the increased production and use of bioplastic alternatives. As a result, the production of polyhydroxyalkanoate (PHA) is expected to quadruple over the next five years. As PHA is denser than seawater and the majority of plastic debris is transported to coastal marine sediments, the increased deposition of PHA into benthic environments is likely. Within coastal sediments, microorganisms play important roles in ecosystem processes such as dissimilatory sulfate reduction (DSR), which is the dominant terminal step in the mineralization of organic matter. Previous research has demonstrated that benthic microbial communities exposed to PHA have an increased capacity for both sulfate reduction and PHA degradation, but the individual organisms capable of DSR and PHA degradation remain unknown. This study utilized selective enrichment and whole-genome sequencing to characterize individual members of a consortium degrading PHA at the sediment-water interface of a coastal lagoon. Findings demonstrate that species from the *Bacillus cereus* group are capable of undertaking the entire DSR pathway and also utilizing PHA as their sole carbon source for growth. These isolates represent the first described members of *Bacillus* capable of reducing sulfate, expanding the phylogenetic diversity of SRM. Further, in coastal sediments, where sulfate reduction is prominent and the majority of PHA deposition will occur, these organisms represent a previously unknown reservoir of both sulfate reduction and PHA degradation genes.

Introduction.

Plastic debris enters the marine environment at an astounding rate, with up to 14.0 million tons of plastic waste entering the ocean in 2010 alone (Jambeck et al., 2015). As a result, plastic has been added to the list of global threats to the ocean (Amaral-Zettler Linda et al., 2015). One proposed solution for the reduction of plastic loading is the increased production and use of bioplastic alternatives, including both bio-based plastics and biodegradable plastics. In particular, bio-based plastics that are also biodegradable such as polyhydroxyalkanoates (PHAs) are considered strong candidates for replacing petroleum-based plastics given their structural similarities and high biodegradation potential (Nehra et al., 2017).

The basic structure of PHAs consist of linear polyesters made up of ester bonds between neighboring monomers (Verlinden et al., 2007). A wide variety of distinct PHAs have been described (Li et al., 2016b), but the most abundant and best characterized is poly-(3-hydroxybutyrate) (PHB), a compound synthesized by numerous microorganisms as intracellular storage granules during periods of nutrient limitation (Ishizaki et al., 2001). Due to the promising characteristics of these bioplastics, the industrial production of PHA is expected to quadruple between 2018 and 2023 (Chinthapalli et al., 2019).

The ability to biodegrade PHAs is widely distributed amongst a phylogenetically diverse group of microorganisms (Emadian et al., 2017). In the marine environment, members from diverse lineages are capable of biodegrading PHA (Mergaert et al., 1993; Mukai et al., 1993; Kita et al., 1997; Leathers et al., 2000; Volova et al., 2010). A recent review of published PHA degradation data estimated that the average rate of degradation was 0.04 - 0.09 $mg \times day^{-1} \times cm^{-2}$ in marine environments (Dilkes-Hoffman et al., 2019). In comparison, we recently demonstrated

that PHA pellets were rapidly degraded at a rate of approximately 3.6 $mg_X day^{-1}$ in coastal marine sediment (Pinnell et al., 2019).

In anoxic sediments, it has been reported that sulfate-reducing microorganisms (SRM) contribute to the degradation of PHA (Mas-Castellà et al., 1995), and degradation by SRM has also been shown under anaerobic laboratory settings (Çetin, 2009). The impact of PHA loading on sulfate reduction is of particular importance in anoxic marine sediments, as sulfate reduction is the dominant terminal step in the remineralization of organic matter (Jørgensen, 1977). We have shown previously that PHA loading stimulates the growth of SRM in marine sediments (Pinnell et al., 2019) and enriches the overall community's DSR potential (Pinnell and Turner, 2019), but the individuals responsible for PHA degradation and DSR have yet to be isolated in culture.

This study utilized selective isolation and whole-genome sequencing to characterize three members of a consortium that degrades PHA in coastal marine sediments. The isolation and whole-genome sequencing of these individuals provides a high-resolution analysis of their degradation potential not possible through amplicon-based community surveys. To this end, we designed an enrichment experiment to isolate PHA biofilm community members capable of PHA degradation and sulfate reduction. We hypothesized that some members of the PHA biofilm capable of using PHA as a sole carbon source would also be capable of DSR.

Materials & Methods.

Sample deployment and collection

5.0 g of PHA pellets (Doctors Foster & Smith, Rhinelander, WI, USA) were deployed in microcosms at the sediment-water interface of the Upper Laguna Madre (ULM), Texas as

described previously (Pinnell and Turner, 2019). The ULM is a subunit of the larger Laguna Madre, which is a bar-built coastal lagoon and the largest estuarine system along the Texas coast (Tunnell, 2002). The microcosms described above were deployed adjacent to a dredge material island within the ULM that is located at 27°32'39.0"N and 97°17'07.7"W. A total of three microcosms were deployed on September 20, 2018. The first microcosm was collected after 153 days of exposure (February 20, 2019), and the second was collected after 181 days exposure (March 20, 2019). All samples were stored in site-specific water at ambient temperature, transported to the lab and processed within two hours of sample collection.

Selective isolation of PHA biofilm members

Two variations of an isolation procedure that utilized both sulfate-reducing broth (SRB) and a minimal-salts medium containing poly-(3-hydroxybutyrate) as the sole carbon source (MSM-PHB) were used to promote the growth and isolation of SRM capable of utilizing PHB as a sole carbon source. MSM-PHB media has been previously used to selectively isolate PHA degrading microorganisms (Salim et al., 2012; Vigneswari et al., 2015). PHA pellets collected at the first collection date (153 days exposure) were initially cultured in SRB under anaerobic conditions at 30 °C with 200 rpm shaking for 48 hours. Anaerobic conditions were established through the use of Oxyrase for broth (Oxyrase Inc., Mansfield, Ohio), which is a proprietary sterile blend of enzymes that renders media and container headspace anaerobic. After 48 hours, cultures were transferred to MSM-PHB broth and anaerobic conditions were established by bubbling the media with N_2 gas for ten minutes, followed by bubbling of the headspace for an additional five minutes. The cultures in the MSM-PHB broth were then incubated under anaerobic conditions at 30 °C with shaking at 200 rpm for seven days. Individual isolates were

separated by plating on SRB overlay plates for 48 hours at 30 °C, as described previously (Mabrouk and Sabry, 2001). Oxyrase was used to maintain anaerobic conditions in the SRB overlay plates. This procedure produced six separate isolates (SRB1LM – SRB6LM), of which two were chosen (SRB1LM and SRB3LM) for whole-genome sequencing based on differing morphologies.

PHA pellets collected at the second collection data (181 days exposure) were initially cultured in MSM-PHB broth under anaerobic conditions at 37 °C with 150 rpm shaking for seven days. Cultures were then plated on SRB (+ thiosulfate) overlay plates and incubated at 37 °C for 72 hours. Anaerobic conditions for the MSM-PHB and SRB were established in the same methods described above. This procedure resulted in three separate isolates (SRB7LM – SRB9LM), of which one was chosen (SRB7LM) for whole-genome sequencing based on morphology.

DNA isolation

Genomic DNA was isolated from overnight cultures of the three selected isolates (SRB1LM, SRB3LM, and SRB7LM) using the DNeasy UltraClean Microbial Kit (Qiagen, Hilden, Germany) according to the manufacturer's instructions. The DNA was quantified and assayed for quality (A_{260}/A_{280}) using a BioPhotometer D30 (Eppendorf, Hamburg, Germany) and stored at -20 °C.

Whole-genome sequencing and assembly

Genomic library preparation and sequencing was carried out by Molecular Research LP (Shallowater, TX, USA). Libraries were prepared using a Nextera DNA Flex Library Preparation

Kit (Illumina, San Diego, CA) and 50 ng of genomic DNA. Final library concentration was measured using the Qubit dsDNA HS Assay Kit (Life Technologies, Carlsbad, CA) and the average library size was determined using an Agilent 2100 Bioanalyzer (Agilent Technologies, Santa Clara, CA). Before sequencing, 700 bp size selection was performed using a BluePippin DNA size selection system (Sage Science, Beverly, MA). DNA was sequenced using an Illumina NovaSeq instrument using paired-end chemistry (2 x 150 bp). The DNA concentration (ng μL^{-1}) and average size (bp) of the sequencing libraries and the number of sequence reads produced are reported in Table 7. Overlapping paired reads were merged using FLASH version 1.2.11 (Magoc and Salzberg, 2011). Merged reads were trimmed of adapter sequences and low-quality bases with TrimGalore! version 0.4.4 (https://github.com/FelixKrueger/TrimGalore), which is a wrapper script for Cutadapt (Martin, 2011) and FastQC (Andrews, 2010). The optimal k-mer size for each assembly was determined manually by evaluating assembly metrics for each k-mer ranging from 11 to 111, and the draft genomes were assembled *de novo* with Velvet version 1.2.10 (Zerbino and Birney, 2008). The assembled genomes were initially annotated and analyzed with the web-based RAST annotation service and SEED Viewer (Aziz et al., 2008; Overbeek et al., 2014), and the final annotations were completed with the National Center for Biotechnology Information's (NCBI) Prokaryotic Genome Annotation Pipeline (PGAP) (Klimke et al., 2009).

Table 7. Library preparation and basic sequencing metrics.

Isolate	**Final library DNA concentration (ng/μL)**	**Average library size (bp)**	**No. reads**
SRB1LM	10.70	679	5,905,778
SRB3LM	8.24	644	5,431,640
SRB7LM	4.54	625	7,748,150

Phylogenetics

The genomes from the three isolates were compared to all publicly available bacterial genomes in Genbank (n = 209,807) by average nucleotide identity (ANI) with fastANI (Jain et al., 2018), using > 95% ANI as the intra-species threshold and < 83% ANI as the inter-species threshold. Based on the ANI results, the relatedness of SRB1LM and SRB3LM to all chromosome-level (n = 71) and reference (n = 4) genomes within the *Bacillus cereus* group in GenBank was inferred by constructing a ML tree using a set of homologs present in all 77 genomes. Similarly, based on the ANI results, the relatedness between SRB7LM and all genomes in GenBank within the genus *Exiguobacterium* (n = 83) was also inferred through the construction of a ML tree using a set of homologs present in all 84 genomes. To construct the ML trees, all genomes were annotated with prokka version 1.14.0 (Seemann, 2014) and homologous genes were clustered using get_homologs (Contreras-Moreira and Vinuesa, 2013) with the OrthoMCL algorithm (Li et al., 2003). Program options dictated that 1) the search was carried out using the default *E*-value cutoff of 10^{-5}, 2) the search clustered all homologs present in every genome while excluding paralogs, and 3) the search was guided with a closed reference genome (*B. cereus* ATCC 14579 and *E. sibiricum* 255-15 for SRB1LM/SRB3LM and SRB7LM, respectively). Full versions of each tree without collapsed branches, are found in Appendix 2 and Appendix 3.

PHA degradation potential and growth with PHB as sole carbon source

Predicted coding sequences (pCDS) from each of the three annotated genomes were aligned against the four super-families of extracellular PHA depolymerase protein sequences within the PHA Depolymerase Engineering Database (PHA-DED). The PHA-DED contains 587

PHA depolymerases and was established as a tool for the systematic analysis of PHA depolymerases (Knoll et al., 2009). The four super-families of extracellular enzymes (n = 374) in the PHA-DED are medium-chain length depolymerases that degrade denatured extracellular PHA ($dPHA_{MCL}$), two types of short-chain length depolymerases that degrade denatured extracellular PHA ($dPHA_{SCL}$ type 1 catalytic domain and $dPHA_{SCL}$ type 2 catalytic domain), and short-chain length depolymerases that degrade native intracellular PHA ($nPHA_{SCL}$). Alignments were performed with BLAST+ version 2.6.0 (Camacho et al., 2009) and an e-value cutoff of 10^{-5}. Positive alignments were summed and the abundance of $dPHA_{MCL}$, $dPHA_{SCL}$ type 1, $dPHA_{SCL}$ type 2, and $nPHA_{SCL}$ sequences were compared between all three genomes with a heatmap generated using the R package ggplot2 (Wickham, 2016) .

To determine if their genetic potential for utilizing PHA was reflected physiologically, agar plates containing powered PHB as the sole carbon source were prepared as described previously (Mabrouk and Sabry, 2001). Briefly, overlay plates were prepared with a lower layer of MSM and an upper layer of 1.5% agar containing 0.1% w v^{-1} PHB. A sterile toothpick was used to inoculate cultures between the two layers of the plate. Isolates were grown under both aerobic and anaerobic conditions. Anaerobic conditions were achieved by bubbling both media layers with N_2 gas for ten minutes before solidifying. Anaerobic plates were incubated using an AnaeroPack system (Mitsubishi Gas Chemical Company, Tokyo, Japan), which maintains anaerobic conditions while sealed. All plates were incubated at 37 °C for five days, and resulting isolates were imaged using a Bio-Rad Gel Doc XR+ imaging system (Bio-Rad, Hercules, California).

Dissimilatory sulfate reduction potential

The pCDS from each of the three annotated genomes were aligned against three databases representing the three steps of the dissimilatory sulfate reduction pathway. For the first and second steps of the pathway (reduction of sulfate to adenylyl sulfate [APS] and the reduction of APS to sulfite), pCDS were aligned against previously published databases of sulfate adenylyltransferase (SAT/MET3) and APS reductase (AprBA) protein sequences, respectively (Pinnell and Turner, 2019). Similarly, pCDS were aligned against a previously published database of dissimilatory sulfite reductase (DsrAB) protein sequences (Müller et al., 2014) for the final step of the pathway. Alignments were performed with BLAST+ version 2.6.0 (Camacho et al., 2009) and an e-value cutoff of 10^{-5}. Positive alignments were summed and the abundance of SAT/MET3, AprBA, and DsrAB sequences were compared between all three genomes with a heatmap generated using the R package ggplot2.

Data availability

All sequence reads were made available through the BioProject Accession PRJNA564300 at NCBI. Additionally, the sequenced three genomes (SRB1LM, SRB3LM, and SRB7LM) were deposited at GenBank under the accession numbers VWVP00000000, VWVQ00000000, and VWVR00000000, respectively.

Results & Discussion.

Selective isolation of PHA biofilm members

A total of nine different isolates were cultured from the PHA biofilms collected at both collection dates (SRB1LM – SRB9LM). Of these eleven, three isolates were selected for further

analysis and whole genome sequencing based on differing morphologies. Two of the selected organisms (SRB1LM and SRB3LM) were isolated using the first described procedure (SRB broth followed by MSM-PHB plates), and the third (SRB7LM) was isolated using the second described procedure (MSM-PHB broth followed by SRB plates). All three were isolated under anaerobic conditions. Typically, the isolation of PHA degraders have been carried out under aerobic conditions, and as a result the majority of isolates are aerobes (Jendrossek and Handrick, 2002). As SRM are anaerobic (Muyzer and Stams, 2008), the lack of SRM associated with PHA degradation may be a result of the prominence of aerobic isolation.

Genome Sequencing

The three draft genomes averaged 59 contigs, an N50 value of 1,168,382 bp, and a maximum contig length of 2,758,154 bp. The genome sizes ranged from 2,890,966 to 6,545,436 bp (SRB7LM and SRB3LM, respectively), the number of genes ranged from 2,790 to 7,073 (SRB7LM and SRB3LM, respectively), and GC content ranged from 35.13 to 48.04% (SRB3LM and SRB7LM, respectively). Table 8 provides full assembly metrics for all three draft genomes. The considerably larger genome sizes of SRB1LM and SRB3LM suggests these isolates could be capable of surviving a range of growth conditions, as this capability has been roughly correlated with genome size (Land et al., 2015).

Table 8. Assembly metrics from the three isolates that underwent whole-genome sequencing.

	SRB1LM	**SRB3LM**	**SRB7LM**
No. contigs	43	123	10
Total length (bp)	5,590,746	6,545,436	2,890,966
Average GC content (%)	35.2	35.1	48.0
N50	745,621	478,895	2,758,154
No. pCDS	6263	7073	2970
No. RNAs	145	158	91

Phylogenetics

To determine the phylogeny of each isolate, their genomes were aligned to all bacterial genomes available in GenBank with fastANI, and their relatedness was inferred by constructing ML trees based on homologous proteins within all genomes. Both SRB1LM and SRB3LM had alignments over the intra-species threshold (> 95% ANI) with multiple genomes in the *Bacillus cereus* group (Table 9). Four of the top five highest ANI alignments with SRB1LM were with strains of *B. anthracis*, but *B. cereus* and *B. tropicus* were also among the top ten highest values. SRB3LM had ANI alignments over the intra-species threshold with strains of *B. cereus* and *B. thuringiensis* along with two unspecified species of *Bacillus*. Interestingly, while both SRB1LM and SRB3LM have ANI values over 95% with multiple strains of *B. cereus*, they were only 91% similar with each, suggesting they may be different species. Based on the genome-level ML tree, the nearest neighbors to SRB1LM and SRB3LM were *B. cereus* BC-AK and *B. thuringiensis* serovar huazhonggensis GBSC-4DB1 (Figure 18). Both nearest neighbors were isolated in China, and both species are typically associated with soil (Helgason et al., 2000). The *B. cereus* group consists of spore-forming organisms, and because of their high economic and medical importance, contains the highest number of closely related fully sequenced genomes (Rasko et al., 2005). Despite being well known and thoroughly characterized, the lack of distinct species

assignments within the *B. cereus* group is typical, as its phylogeny has proven difficult to classify (Liu et al., 2015).

Table 9. The top ten average nucleotide identity (ANI) values between each of the three isolates and every available genome in GenBank. SRB3LM was included with SRB1LM to demonstrate the ANI values between the two presumptive *Bacillus* isolates in this this study. ANI values over the intra-species threshold of 95% are in bold.

	SRB1LM	**SRB3LM**	**SRB7LM**
B. anthracis AFS057764	**98.18**		
B. anthracis AFS032297	**98.15**		
B. anthracis AFS044825	**98.15**		
B. cereus AFS021040	**98.13**		
B. anthracis AFS017361	**98.12**		
B. tropicus DE0443	**98.10**		
B. anthracis AFS012870	**98.08**		
B. anthracis AFS041580	**98.07**		
B. cereus AFS067103	**98.07**		
B. anthracis AFS018197	**98.06**		
SRB3LM	91.89		
B. sp B25(2016b)		**98.99**	
B. thuringiensis MS532a		**98.93**	
B. cereus MOD1_Bc23		**98.92**	
B. cereus VD014		**98.83**	
B. thuringiensis HM-311		**98.81**	
B. sp M13(2017)		**98.81**	
B. cereus B4080		**98.78**	
B. thuringiensis ser. huazhongensis BGSC 4DB1		**98.75**	
B. thuringiensis 78-2		**98.73**	
B. thuringiensis Bt185		**98.71**	
E. produndum PHM 11			**98.09**
E. sp. HVEsp1			**96.14**
E. sp. UBA4960			**95.43**
E. sp. NG55			**95.40**
E. sp. AT1b			**95.29**
E. sp. JLM-2			**95.15**
E. marinum DSM 16307			88.39
E. aurantiacum DSM 6208			81.28
E. chiriqhucha GIC31			81.20
E. sp. 8-11-1			81.11

Abbreviations: *B., Bacillus; E., Exiguobacteirum;* ser., serovar

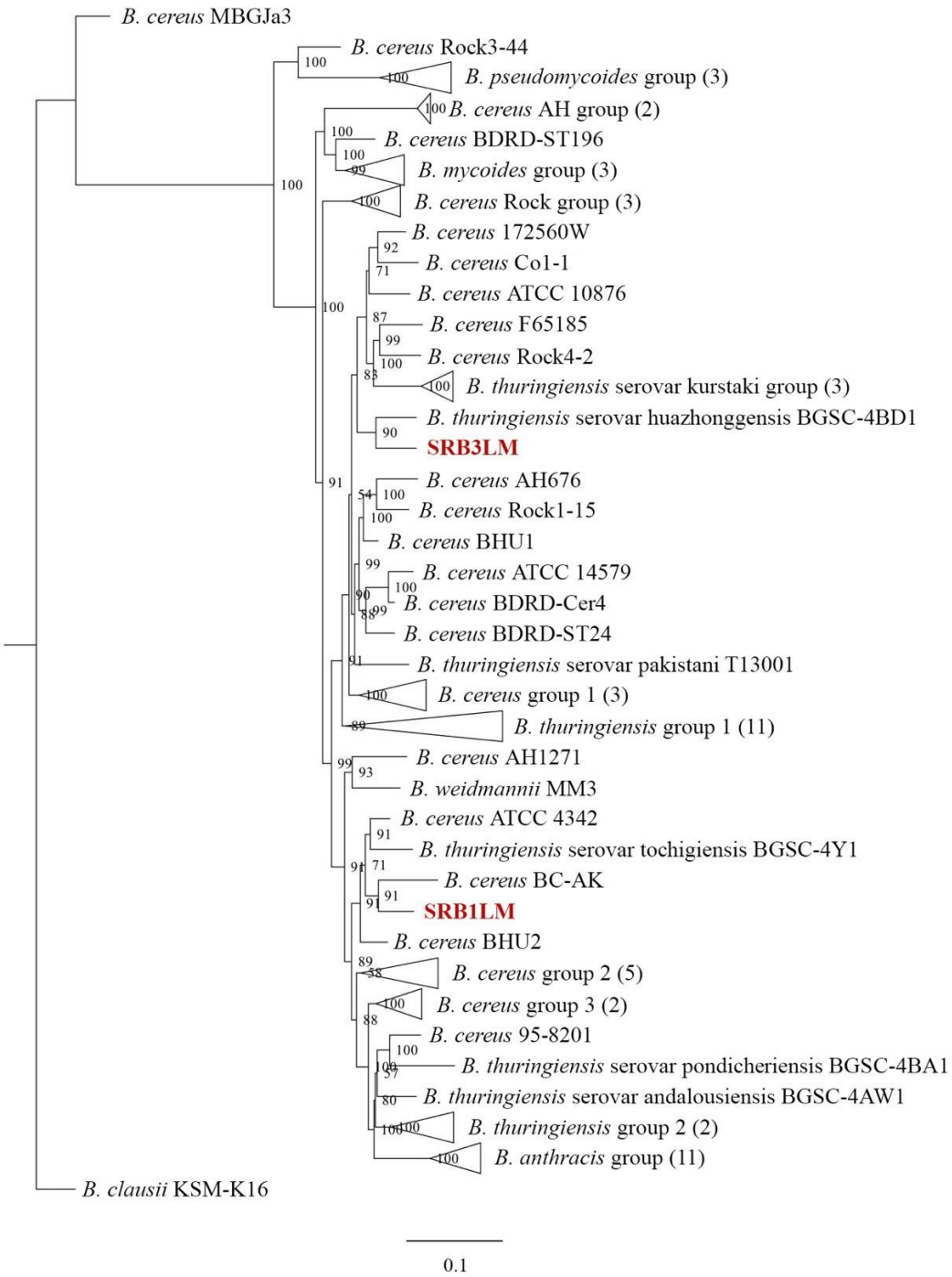

Figure 18. Genome-scale ML tree demonstrating the relatedness of SRB1LM and SRB3LM to every chromosome-level and reference assembly with the *B. cereus* group available in GenBank. The two isolates from this study were highlighted in red, bold typeface. Node labels show the bootstrap support values. Branch lengths represent the average number of substitutions per site. The tree was rooted to a more distantly related *Bacillus* that is not within the *B. cereus* group (*B. clausii* KSM-K16).

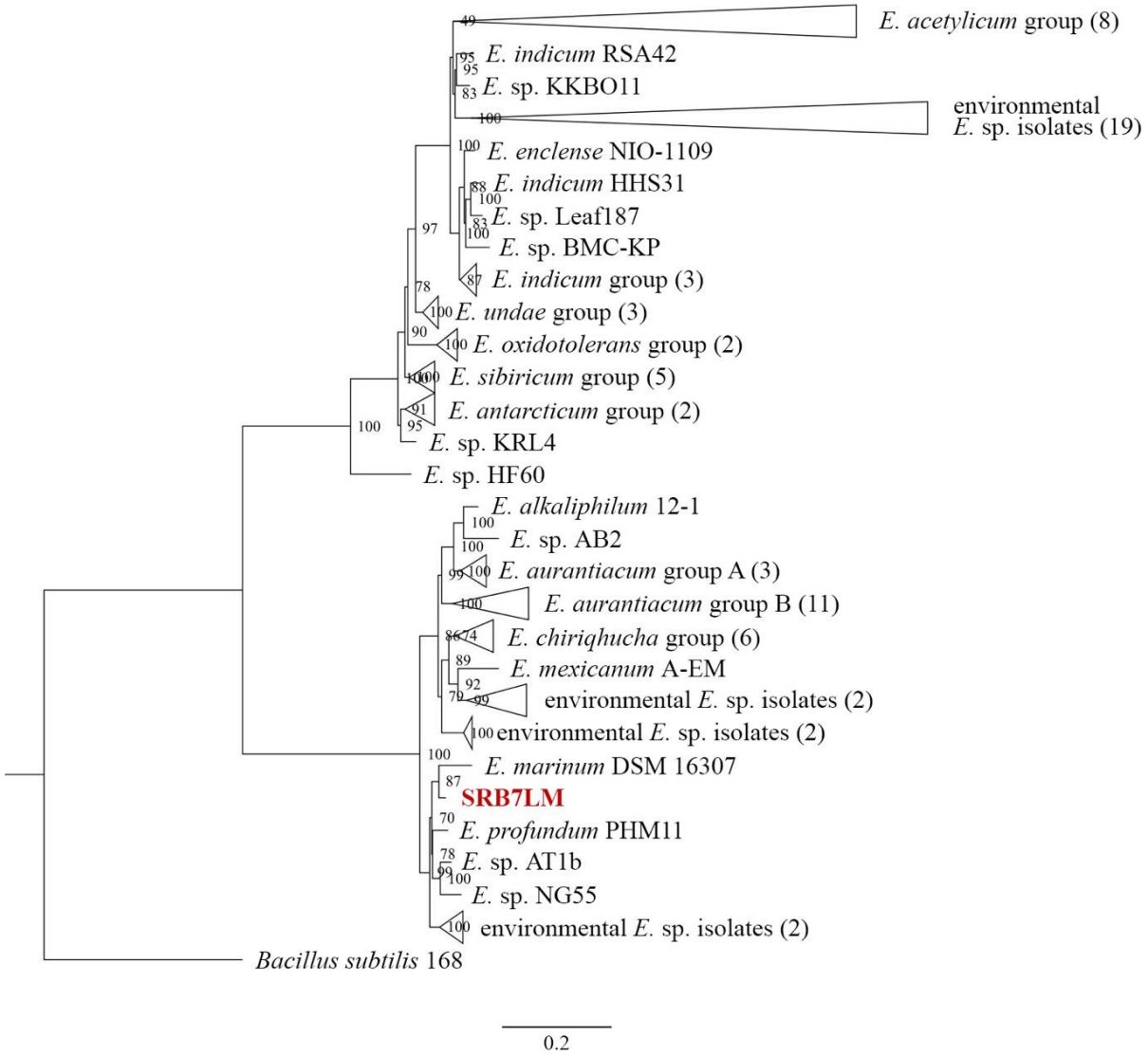

Figure 19. Genome-scale ML tree demonstrating the relatedness of SRB7LM to every available *Exiguobacterium* assembly in GenBank. The isolate from this study was highlighted in red, bold typeface. Node labels show the bootstrap support values. Branch lengths represent the average number of substitutions per site. The tree was rooted to a distantly related reference genome that is in a different genus but within the *Bacillaceae* family (*B. subtilis* 168).

The ANI alignments were more definitive for SRB7LM, with *Exiguobacterium profundum* being the only characterized species having an alignment over the intra-species threshold (Table 9). An additional five uncharacterized species of *Exiguobacterium* had

alignments over 95%, but all other alignments fell below the threshold. In the genome-level ML tree, SRB7LM was most closely related to *E. marinum* with *E. profundum* the next closest relative (Figure 19). Both *E. profundum* and *E. marinum* are halotolerant species and their GenBank representatives were isolated from soil and a tidal pool, respectively (Kim et al., 2005; Patel et al., 2018). As a whole, the *Exiguobacterium* genus contains 83 representative genomes in GenBank, and its members are facultative anaerobes isolated from a markedly diverse variety of environments ranging from glacial ice to hydrothermal vents (Vishnivetskaya et al., 2009). Interestingly, one strain (*E.* sp. YT2) isolated from the gut of mealworms has been proven capable of degrading polystyrene (Yang et al., 2015).

PHA degradation potential and growth with PHB as sole carbon source

To characterize each isolate's potential for PHA degradation, their genomes were aligned with the four super-families of extracellular PHA depolymerases within the PHA-DED database. SRB3LM contained the highest number of extracellular PHA depolymerases (n = 14), while SRB1LM contained 12, and SRB7LM only contained one (Figure 3). All three isolates contained more protein sequences from the $dPHA_{SCL}$ type 1 catalytic domain superfamily than each of the other three super-families, and none of the isolates contained protein sequences from the $nPHA_{SCL}$ superfamily. The two presumptive *Bacillus* isolates had a higher PHA degradation potential as they contained protein sequences from three of the four extracellular super-families. Additionally, SRB1LM and SRB3LM had the genetic capability to degrade both short-chain (SCL) and medium-chain length (MCL) PHAs, while SRB7LM contained only a SCL-PHA depolymerase protein sequence. The majority of described PHA depolymerases are SCL as the most commonly used PHAs are SCL (Reddy et al., 2003; Knoll et al., 2009), but MCL-PHAs

have greater structural diversity than SCL-PHAs and are therefore more readily tailor-made for specific applications (Rai et al., 2011). Microorganisms with the ability to degrade MCL-PHAs are believed to be far less widespread than those capable of degrading SCL-PHAs (Jendrossek and Handrick, 2002), and the capability of SRB1LM and SRB3LM to degrade both suggest they have a high potential for degrading a wider range of PHAs. While PHA-degrading *Bacillus* have not been as widely described, one strain of *B. pumilus* is capable degrading PHB (Volova et al., 2017) and another uncharacterized *Bacillus* species can degrade poly(3-hydroxybutyrate-co-3-hydroxyvalerate) (Shah et al., 2007).

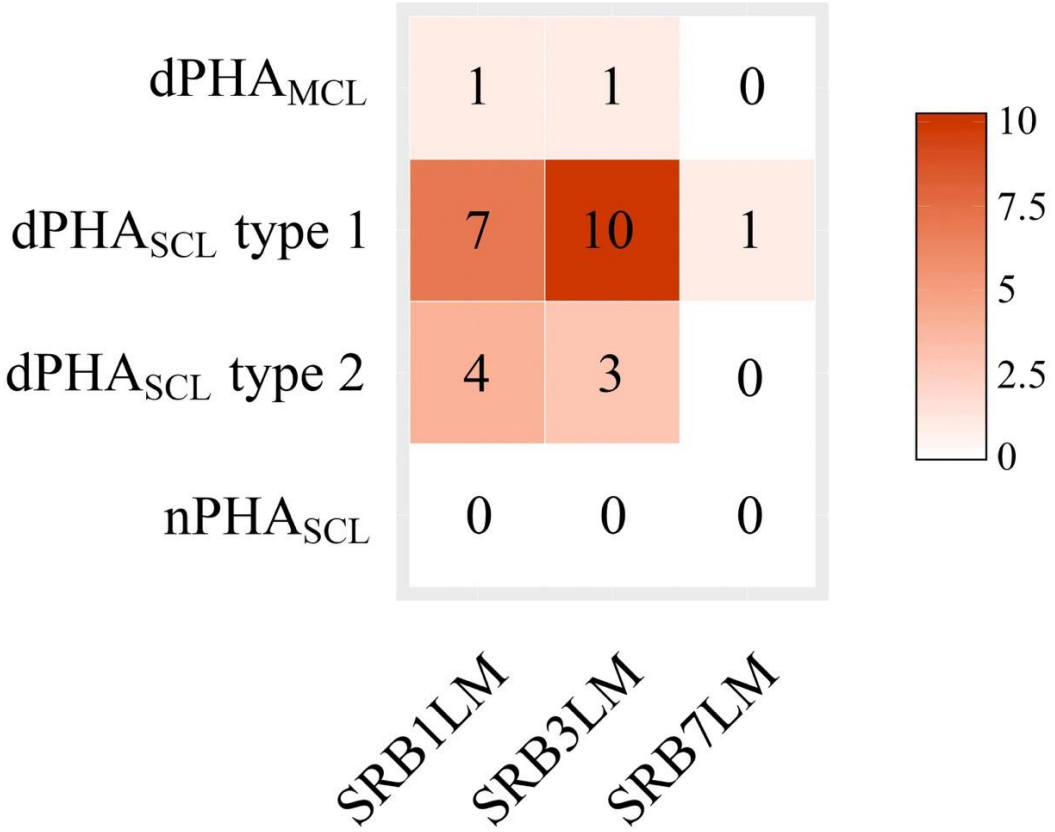

Figure 20. Heatmap of extracellular PHA depolymerase protein sequences. Coloring correlates with the abundance of positive alignments for each genome to the four super-families from the PHA-DED database, with absent sequences appearing white and abundant sequences appearing red.

To determine if their genetic capabilities were reflected physiologically, the isolates were grown on a media containing PHB as the sole carbon source. As presumptive facultative anaerobes, they were grown under both aerobic and anaerobic conditions. While SRB7LM did not grow under either condition with PHB as the sole carbon source, both SRB1LM and SRB3LM grew under aerobic conditions (Figure 4). The growth of SRB1LM and SRB3LM confirmed their genetic capability to utilize PHB as a sole carbon source. Their ability to do so aerobically supports previous findings of *Bacillus* species being able to degrade PHA under aerobic conditions (Shah et al., 2007; Volova et al., 2017). Under aerobic conditions the degradation of PHA results in carbon dioxide and water, while under anaerobic conditions it produces carbon dioxide and methane (Reddy et al., 2003). While less-studied, the anaerobic degradation of PHA can be facilitated by certain SRM (Mas-Castellà et al., 1995; Urmeneta et al., 1995).

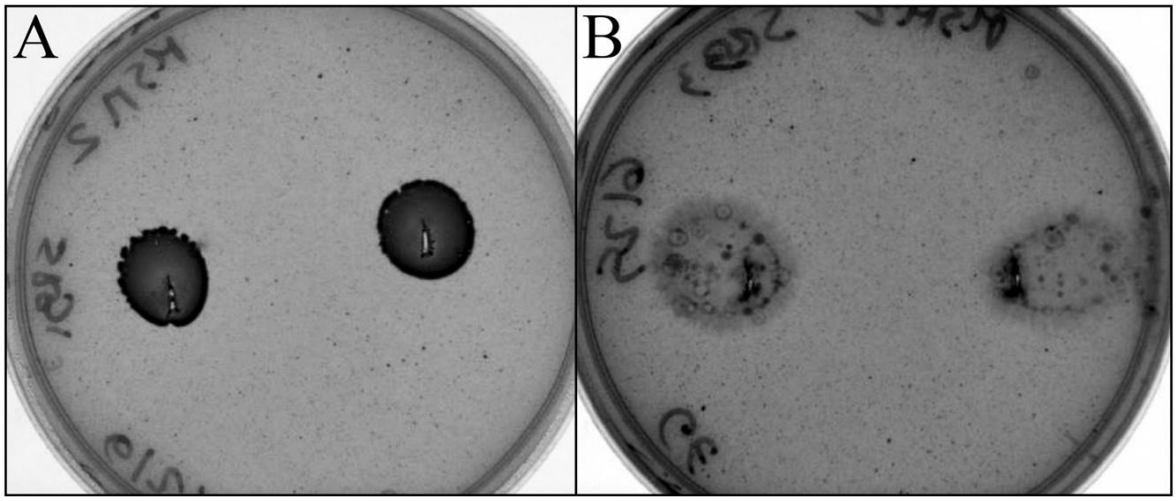

Figure 21. Images of MSM-PHB plates demonstrating growth of isolates capable of using PHB as their sole carbon source under aerobic and anaerobic conditions (top and bottom row, respectively). Panel A displays SRB1LM and panel B displays SRB3LM.

Dissimilatory sulfate reduction potential

To characterize each isolate's potential for dissimilatory sulfate reduction, their genomes were aligned with three databases containing protein sequences from each of the three steps of the pathway. All three isolates had multiple positive alignments with both SAT/MET3 and AprBA, and SRB1LM and SRB3LM also aligned to DsrAB, demonstrating that both presumptive *Bacillus* isolates were capable of completing the entire dissimilatory sulfate reduction pathway on their own (Figure 5).

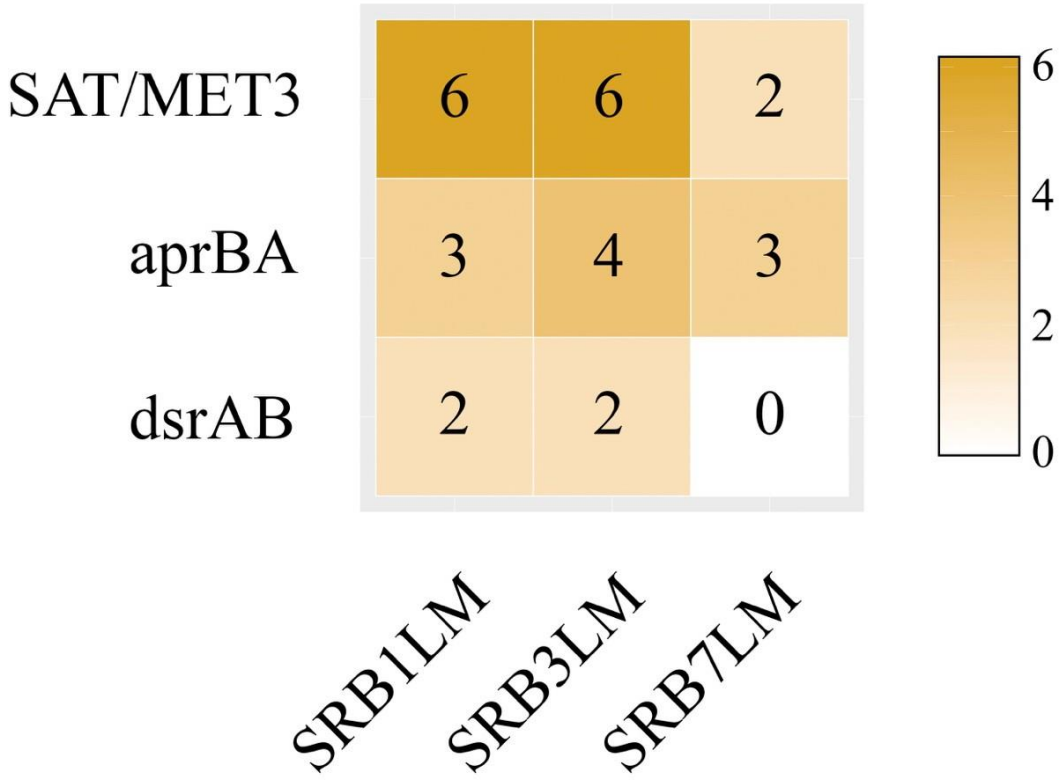

Figure 22. Heatmap of extracellular dissimilatory sulfate reduction pathway protein sequences. Coloring correlates with the abundance of positive alignments for each genome to protein sequences from each of three steps of the pathway, with absent sequences appearing white and abundant sequences appearing yellow.

While neither *Bacillus* nor *Exiguobactertium* are commonly considered SRMs, there is a known group of Firmicutes capable of reducing sulfur (Kjeldsen et al., 2007; Anantharaman et al., 2018) as well as a large number of unclassified environmental lineages within said Firmicutes group (Müller et al., 2014). Further, a spore-forming member of the order Bacillales has been described as a dissimilatory sulfur reducer (Sorokin et al., 2012). Previously, we have shown that SRM are enriched within PHA biofilms in marine sediments (Pinnell et al., 2019), but to our knowledge, SRB1LM and SRB3LM represent the first two cultured *Bacillus* isolates from a marine environment with the capability to both reduce sulfate and degrade PHA. In environments like coastal sediments, were sulfate reduction is the predominant terminal step in the remineralization of organic matter (Jørgensen, 1982), a microorganism with the ability to complete the dissimilatory sulfate reduction pathway and degrade a variety of PHAs may play an important role in benthic biogeochemical cycling.

Conclusions

As PHA production will increase in the near future, more PHA will sink to marine sediments where its degradation will be largely governed by anaerobic microorganisms. Previous research has shown that PHA degrades slowly in marine sediments and alters the microbial communities living there (Dilkes-Hoffman et al., 2019; Pinnell and Turner, 2019). Therefore, it is of great importance to understand how PHA loading affects microorganisms living in marine sediments. This study characterized individual members of a microbial consortium responsible for degrading PHA in marine sediments. Additionally, we also found that some members of the consortium were capable of both PHA degradation and sulfate reduction. To our knowledge, two of the isolates represent the first strains of *Bacillus* described as capable of reducing sulfate. The

predicted increase in PHA production will likely result in higher PHA deposition in coastal sediments, which coupled with favorable conditions for sulfate reduction, may result in growth conditions favoring the types of microorganisms characterized in this study, including species of *Bacillus*.

Acknowledgements.

This study would not have been possible without the support of our friends and colleagues. Specifically, we thank Robert "Bobby" Duke and the entire Center for Coastal Studies staff for assistance in the field. This study was funded by Texas Sea Grant (TSG), and the National Sciences and Engineering Research Council of Canada (NSERC). The majority of computational data analysis was performed on TAMU-CC's high-performance computing cluster, which is funded in part by the National Science Foundation's CNS MRI Grant (No. 1429518).

SUMMARY

Plastic is an incredible material; it is inexpensive, lightweight, durable, strong, corrosion-resistant, and cheap. Its mass production was celebrated as the dawning of a new age, and today plastic is used in an extensive range of applications. Our prolific use of plastic has resulted in a 500-fold increase in production since the 1950s (Thompson et al., 2009b). While the benefits of plastic were obvious, the disadvantages of its prolific use were not fully understood. In particular, the detriments associated with the loading of natural environments with plastic waste were not anticipated. For example, a recent study estimated 5.5 billion tons of plastic have ended up in natural environments (Geyer et al., 2017), which has negatively impacted the vast majority of marine organisms. Despite breaking into smaller pieces, plastic is believed to remain in the environment for centuries due to its recalcitrant nature. Bioplastic alternatives, notably biodegradable polymers, are considered a promising solution for easing plastic loading on natural environments.

Numerous studies have characterized the microbial communities colonizing floating plastic debris in marine environments (e.g. Lobelle and Cunliffe 2011, Zettler et al., 2013, Bryant et al., 2016). By contrast, few studies have characterized the microbial communities that colonize benthic plastic and bioplastic. To address this knowledge gap, the objectives of this research were fourfold: 1) determine if plastic or bioplastic recruited a specific assemblage of benthic microorganisms, 2) determine if the microbial assemblages were enriched for polymer degrading enzymes and quantify any evidence of degradation, 3) determine if the microbial assemblages were enriched for enzymes that facilitate dissimilatory sulfate reduction, and 4) characterize individual members of the assemblage involved plastic or bioplastic degradation. To complete

these objectives, we designed a benthic microcosm to circumvent the challenges of isolating pre-existing plastic debris from heterogeneous sediment samples. Importantly, the experimental design permitted the inclusion of a ceramic biofilm control and the ability to quantify degradation. This experimental design, coupled with culture-dependent methodologies as well as next-generation sequencing and high-performance computing, allowed us to achieve these objectives.

Results demonstrated that plastic (PET) associated communities were not unique versus a ceramic biofilm control, but bioplastic (PHA) did recruit a unique microbial assemblage. PHA-associated communities were dominated by SRM, a trend throughout the 424 days of biofilm development. Similarly, the PET biofilms were not enriched for hydrolases or sulfate reduction genes, but PHA assemblages were enriched for both, indicating a potential for polymer degradation as well as sulfate reduction. This degradation potential was confirmed by SEM imaging and mass loss experiments that showed extensive pitting and a 51% mass loss of PHA after 424 days of exposure. Additionally, we identified nine members of the PHA-degrading consortia: two species of *Bacillus* (SRB1LM and SRB3LM), two Gammaproteobacteria (Madre5 and Madre6), and one species each of *Exiguobacterium* (SRB7LM), *Spirochaetaceae* (Madre4), *Desulfovibrio* (Madre1), *Desulfobacteraceae* (Madre2), and *Desulfobulbaceae* (Madre 3). Madre1-6 were metagenome recovered genomes while SRB1, 3, and 7 were isolated and cultured in the laboratory. We screened Madre1-3 and the three cultured isolates for genes associated with PHA degradation and sulfate reduction. Five of the six (Madre1, Madre2, Madre3, SRB1LM, and SRB3LM) contained PHA depolymerase genes, but SRB1LM and SRB3LM contained the highest diversity and abundance of these genes. All six genomes contained the genes required to reduce sulfate and four (Madre2, Madre3, SRB1LM, SRB3LM)

contained genes for the entirety of the dissimilatory sulfate reduction pathway. Together, these results clearly show that SRM play an important role in the degradation of PHA in marine sediments. This study also resulted in the discovery, culture, and characterization of *B. cereus* strains capable of both PHA degradation and sulfate reduction, which effectively expands the known diversity of SRM.

The global market for bioplastics is forecasted to increase by 20% over the next five years, and the production of PHA is expected to grow by 400% in the same time frame (Chinthapalli et al., 2019). In turn, the increase use of PHA in a range of industries (e.g. cosmetics, packaging, and single-use items like bags, straw, and bottles) will translate into increased bioplastic waste. Knowing how microbes respond to bioplastic waste will be critical when considering bioplastics as a replacement for traditional petroleum-based plastics, especially when bioplastics are mass produced. The research presented here indicates that bioplastic loading in marine environments will stimulate the growth SRM, which play a dominant role in carbon cycling in marine sediments. The stimulation of SRM could alter the balance between sulfate-reducing and methane-producing microbial communities or alter sediment capacity to buffer against sulfide release. We recommend that researchers, legislators, and coastal managers investigate and consider the ecological consequences of bioplastic loading when developing plans for combating plastic pollution.

REFERENCES

Abou-Zeid, D.-M., Müller, R.-J., and Deckwer, W.-D. (2001). Degradation of natural and synthetic polyesters under anaerobic conditions. *J. Biotechnol.* 86**,** 113-126.

Acosta, T. (2019). Corpus Christi Polymers set to resume work on M&G plant in May. *Corpus Christi Caller-Times,* Feburary 21, 2019.

Aeschelmann, F., and Carus, M. (2015). Biobased building blocks and polymers in the world: capacities, production, and applications – status quo and trends towards 2020. *Ind. Biotechnol.* 11**,** 154-159.

Albuquerque, M.G.E., Eiroa, M., Torres, C., Nunes, B.R., and Reis, M.a.M. (2007). Strategies for the development of a side stream process for polyhydroxyalkanoate (PHA) production from sugar cane molasses. *J. Biotechnol.* 130**,** 411-421.

Amaral-Zettler Linda, A., Zettler Erik, R., Slikas, B., Boyd Gregory, D., Melvin Donald, W., Morrall Clare, E., Proskurowski, G., and Mincer Tracy, J. (2015). The biogeography of the plastisphere: implications for policy. *Front. Ecol. Environ.* 13**,** 541-546.

An, T.T., and Picardal, F.W. (2014). *Desulfocarbo indianensis* gen. nov., sp. nov., a benzoate-oxidizing, sulfate-reducing bacterium isolated from water extracted from a coal bed. *Int. J. Syst. Evol. Microbiol.* 64**,** 2907-2914.

Anantharaman, K., Hausmann, B., Jungbluth, S.P., Kantor, R.S., Lavy, A., Warren, L.A., Rappé, M.S., Pester, M., Loy, A., Thomas, B.C., and Banfield, J.F. (2018). Expanded diversity of microbial groups that shape the dissimilatory sulfur cycle. *ISME J.* 12**,** 1715-1728.

Anderson, A.J., and Dawes, E.A. (1990). Occurrence, metabolism, metabolic role, and industrial uses of bacterial polyhydroxyalkanoates. *Microbiol. Rev.* 54**,** 450.

Andrady, A.L. (2011). Microplastics in the marine environment. *Mar. Pollut. Bull.* 62**,** 1596-1605.

Andrews, S. (2010). FastQC: a quality control tool for high throughput sequence data. Babraham Bioinformatics Cambridge, United Kingdom.

Antipov, E.M., Dubinsky, V.A., Rebrov, A.V., Nekrasov, Y.P., Gordeev, S.A., and Ungar, G. (2006). Strain-induced mesophase and hard-elastic behaviour of biodegradable polyhydroxyalkanoates fibers. *Polymer* 47**,** 5678-5690.

Arbizu, P.M. (2017). pairwiseAdonis: Pairwise Multilevel Comparison using Adonis. https://github.com/pmartinezarbizu/pairwiseAdonis.

Azam, F., and Long, R.A. (2001). Oceanography: sea snow microcosms. *Nature* 414**,** 495-498.

Azam, F., Smith, D.C., Steward, G.F., and Hagström, Å. (1994). Bacteria-organic matter coupling and its significance for oceanic carbon cycling. *Microb. Ecol.* 28**,** 167-179.

Aziz, R.K., Bartels, D., Best, A.A., Dejongh, M., Disz, T., Edwards, R.A., Formsma, K., Gerdes, S., Glass, E.M., Kubal, M., Meyer, F., Olsen, G.J., Olson, R., Osterman, A.L., Overbeek, R.A., Mcneil, L.K., Paarmann, D., Paczian, T., Parrello, B., Pusch, G.D., Reich, C., Stevens, R., Vassieva, O., Vonstein, V., Wilke, A., and Zagnitko, O. (2008). The RAST Server: rapid annotations using subsystems technology. *BMC Genomics* 9**,** 75.

Baird, R.W., and Hooker, S.K. (2000). Ingestion of plastic and unusual prey by a juvenile harbour porpoise. *Mar. Pollut. Bull.* 40**,** 719-720.

Bakir, A., Rowland, S.J., and Thompson, R.C. (2014). Enhanced desorption of persistent organic pollutants from microplastics under simulated physiological conditions. *Environ. Pollut.* 185**,** 16-23.

Barnes, D.K., Galgani, F., Thompson, R.C., and Barlaz, M. (2009). Accumulation and fragmentation of plastic debris in global environments. *Philos. Trans. R. Soc. Lond. B Biol. Sci.* 364**,** 1985-1998.

Barnes, D.K.A. (2005). Remote islands reveal rapid rise of Southern Hemisphere sea debris. *The Scientific World Journal* 5**,** 915-921.

Beck, C.A., and Barros, N.B. (1991). The impact of debris on the Florida manatee. *Mar. Pollut. Bull.* 22**,** 508-510.

Bellas, J., Martínez-Armental, J., Martínez-Cámara, A., Besada, V., and Martínez-Gómez, C. (2016). Ingestion of microplastics by demersal fish from the Spanish Atlantic and Mediterranean coasts. *Mar. Pollut. Bull.* 109**,** 55-60.

Besseling, E., Foekema, E.M., Van Franeker, J.A., Leopold, M.F., Kühn, S., Bravo Rebolledo, E.L., Heße, E., Mielke, L., Ijzer, J., Kamminga, P., and Koelmans, A.A. (2015). Microplastic in a macro filter feeder: humpback whale *Megaptera novaeangliae*. *Mar. Pollut. Bull.* 95**,** 248-252.

Bharti, S., and Swetha, G. (2016). Need for bioplastics and role of biopolymer PHB: a short review. *J. Pet. Environ. Biotechnol.* 7**,** 2.

Biddanda, B.A., and Pomeroy, L.R. (1988). Microbial aggregation and degradation of phytoplankton-derived detritus in seawater. I. Microbial succession. *Mar. Ecol. Prog. Ser.* 42**,** 79-88.

Block, B. (2013). China reports 66-percent drop in plastic bag use. Worldwatch Institute, Washington, D.C., USA.

Boerger, C.M., Lattin, G.L., Moore, S.L., and Moore, C.J. (2010). Plastic ingestion by planktivorous fishes in the North Pacific central gyre. *Mar. Pollut. Bull.* 60**,** 2275-2278.

Bolger, A.M., Lohse, M., and Usadel, B. (2014). Trimmomatic: a flexible trimmer for Illumina sequence data. *Bioinformatics* 30**,** 2114-2120.

Boren, L.J., Morrissey, M., Muller, C.G., and Gemmell, N.J. (2006). Entanglement of New Zealand fur seals in man-made debris at Kaikoura, New Zealand. *Mar. Pollut. Bull.* 52**,** 442-446.

Bowen, J.L., Morrison, H.G., Hobbie, J.E., and Sogin, M.L. (2012). Salt marsh sediment diversity: a test of the variability of the rare biosphere among environmental replicates. *ISME J.* 6**,** 2014-2023.

Brettin, T., Davis, J.J., Disz, T., Edwards, R.A., Gerdes, S., Olsen, G.J., Olson, R., Overbeek, R., Parrello, B., Pusch, G.D., Shukla, M., Thomason, J.A., Stevens, R., Vonstein, V., Wattam, A.R., and Xia, F. (2015). RASTtk: A modular and extensible implementation of the RAST algorithm for building custom annotation pipelines and annotating batches of genomes. *Sci. Rep.* 5**,** 8365.

Browne, M.A., Dissanayake, A., Galloway, T.S., Lowe, D.M., and Thompson, R.C. (2008). Ingested microscopic plastic translocates to the circulatory system of the mussel, *Mytilus edulis* (L). *Environ. Sci. Technol.* 42**,** 5026-5031.

Browne, M.A., Galloway, T.S., and Thompson, R.C. (2010). Spatial patterns of plastic debris along estuarine shorelines. *Environ. Sci. Technol.* 44**,** 3404-3409.

Bryant, J.A., Clemente, T.M., Viviani, D.A., Fong, A.A., Thomas, K.A., Kemp, P., Karl, D.M., White, A.E., Delong, E.F., and Jansson, J.K. (2016). Diversity and activity of communities inhabiting plastic debris in the North Pacific gyre. *mSystems* 1**,** e00024-00016.

Callahan, B.J., Mcmurdie, P.J., Rosen, M.J., Han, A.W., Johnson, A.J., and Holmes, S.P. (2016). DADA2: High-resolution sample inference from Illumina amplicon data. *Nat. Methods* 13**,** 581-583.

Camacho, C., Coulouris, G., Avagyan, V., Ma, N., Papadopoulos, J., Bealer, K., and Madden, T.L. (2009). BLAST+: architecture and applications. *BMC Bioinformatics* 10**,** 421.

Capella-Gutiérrez, S., Silla-Martínez, J.M., and Gabaldón, T. (2009). trimAl: a tool for automated alignment trimming in large-scale phylogenetic analyses. *Bioinformatics* 25**,** 1972-1973.

Caporaso, J.G., Kuczynski, J., Stombaugh, J., Bittinger, K., Bushman, F.D., Costello, E.K., Fierer, N., Pena, A.G., Goodrich, J.K., Gordon, J.I., Huttley, G.A., Kelley, S.T., Knights, D., Koenig, J.E., Ley, R.E., Lozupone, C.A., Mcdonald, D., Muegge, B.D., Pirrung, M., Reeder, J., Sevinsky, J.R., Turnbaugh, P.J., Walters, W.A., Widmann, J., Yatsunenko, T., Zaneveld, J., and Knight, R. (2010). QIIME allows analysis of high-throughput community sequencing data. *Nat. Methods* 7**,** 335-336.

Carpenter, E.J., Anderson, S.J., Harvey, G.R., Miklas, H.P., and Peck, B.B. (1972). Polystyrene spherules in coastal waters. *Science* 178**,** 749.

Carson, H.S., Nerheim, M.S., Carroll, K.A., and Eriksen, M. (2013). The plastic-associated microorganisms of the North Pacific gyre. *Mar. Pollut. Bull.* 75**,** 126-132.

Cartraud, A.E., Le Corre, M., Turquet, J., and Tourmetz, J. (2019). Plastic ingestion in seabirds of the western Indian Ocean. *Mar. Pollut. Bull.* 140**,** 308-314.

Casale, P., Affronte, M., Insacco, G., Freggi, D., Vallini, C., Pino D'astore, P., Basso, R., Paolillo, G., Abbate, G., and Argano, R. (2010). Sea turtle strandings reveal high

anthropogenic mortality in Italian waters. *Aquat. Conserv.: Mar. Freshwat. Ecosyst.* 20**,** 611-620.

Castro, H.F., Williams, N.H., and Ogram, A. (2000). Phylogeny of sulfate-reducing bacteria. *FEMS Microbiol. Ecol.* 31**,** 1-9.

Çetin, D. (2009). Anaerobic biodegradation of poly-3-hydroxybutyrate (PHB) by sulfate reducing bacterium *Desulfotomaculum* sp. *Soil Sediment Contam.* 18**,** 345-353.

Cheung, M.K., Wong, C.K., Chu, K.H., and Kwan, H.S. (2018). Community structure, dynamics and interactions of Bacteria, Archaea and Fungi in subtropical coastal wetland sediments. *Sci. Rep.* 8**,** 14397.

Chinthapalli, R., Skoczinski, P., Carus, M., Baltus, W., D;, D.G., Käb, H., Raschka, A., and Ravenstijn, J. (2019). Biobased building blocks and polymers - global capacities, production and trends 2018–2023. Nova-Institüt, Hürth, Germany.

Choy, C.A., and Drazen, J.C. (2013). Plastic for dinner? Observations of frequent debris ingestion by pelagic predatory fishes from the central North Pacific. *Mar. Ecol. Prog. Ser.* 485**,** 155-163.

Chung, H.C., Lee, O.O., Huang, Y.-L., Mok, S.Y., Kolter, R., and Qian, P.-Y. (2010). Bacterial community succession and chemical profiles of subtidal biofilms in relation to larval settlement of the polychaete *Hydroides elegans*. *ISME J.* 4**,** 817.

Claessens, M., De Meester, S., Van Landuyt, L., De Clerck, K., and Janssen, C.R. (2011). Occurrence and distribution of microplastics in marine sediments along the Belgian coast. *Mar. Pollut. Bull.* 62**,** 2199-2204.

Clark, R.B. (1997). *Marine Pollution.* Clarendon, UK: Oxford University Press.

Clarke, K., and Gorley, R. (2015). PRIMER v7: User manual/tutorial. PRIMER-E Ltd., Plymouth, UK.

Clarke, K.R., Somerfield, P.J., and Gorley, R.N. (2008). Testing of null hypotheses in exploratory community analyses: similarity profiles and biota-environment linkage. *J. Exp. Mar. Biol. Ecol.* 366**,** 56-69.

Cock, P.J.A., Antao, T., Chang, J.T., Chapman, B.A., Cox, C.J., Dalke, A., Friedberg, I., Hamelryck, T., Kauff, F., Wilczynski, B., and De Hoon, M.J.L. (2009). Biopython: freely available Python tools for computational molecular biology and bioinformatics. *Bioinformatics* 25**,** 1422-1423.

Cole, M., Lindeque, P., Fileman, E., Halsband, C., Goodhead, R., Moger, J., and Galloway, T.S. (2013). Microplastic ingestion by zooplankton. *Environ. Sci. Technol.* 47**,** 6646-6655.

Colton, J.B., Burns, B.R., and Knapp, F.D. (1974). Plastic particles in surface waters of the northwestern Atlantic. *Science* 185**,** 491.

Conkle, J.L., Báez Del Valle, C.D., and Turner, J.W. (2018). Are we underestimating microplastic contamination in aquatic environments? *Environ. Manage.* 61**,** 1-8.

Contreras-Moreira, B., and Vinuesa, P. (2013). GET_HOMOLOGUES, a versatile software package for scalable and robust microbial pangenome analysis. *Appl. Environ. Microbiol.* 79**,** 7696-7701.

Convey, P., Barnes, D., and Morton, A. (2002). Debris accumulation on oceanic island shores of the Scotia Arc, Antarctica. *Polar Biol.* 25**,** 612-617.

Courtene-Jones, W., Quinn, B., Gary, S.F., Mogg, A.O.M., and Narayanaswamy, B.E. (2017a). Microplastic pollution identified in deep-sea water and ingested by benthic invertebrates in the Rockall Trough, North Atlantic Ocean. *Environ. Pollut.* 231**,** 271-280.

Courtene-Jones, W., Quinn, B., Murphy, F., Gary, S.F., and Narayanaswamy, B.E. (2017b). Optimisation of enzymatic digestion and validation of specimen preservation methods for the analysis of ingested microplastics. *Anal. Methods* 9**,** 1437-1445.

Crump, B.C., Armbrust, E.V., and Baross, J.A. (1999). Phylogenetic analysis of particle-attached and free-living bacterial communities in the Columbia River, its estuary, and the adjacent coastal ocean. *Appl. Environ. Microbiol.* 65**,** 3192-3204.

Cunningham, D.J., and Wilson, S.P. (2003). Marine debris on beaches of the greater Sydney region. *J. Coast. Res.* 19**,** 421-430.

Dang, H., and Lovell, C.R. (2016). Microbial surface colonization and biofilm development in marine environments. *Microbiol. Mol. Biol. Rev.* 80**,** 91-138.

Dantas, D.V., Barletta, M., and Da Costa, M.F. (2012). The seasonal and spatial patterns of ingestion of polyfilament nylon fragments by estuarine drums (Sciaenidae). *Environ. Sci. Pollut. Res.* 19**,** 600-606.

Davidova, I.A., Wawrik, B., Callaghan, A.V., Duncan, K., Marks, C.R., and Suflita, J.M. (2016). *Dethiosulfatarculus sandiegensis* gen. nov., sp. nov., isolated from a methanogenic paraffin-degrading enrichment culture and emended description of the family *Desulfarculaceae*. *Int. J. Syst. Evol. Microbiol.* 66**,** 1242-1248.

Davison, P., and Asch, R.G. (2011). Plastic ingestion by mesopelagic fishes in the North Pacific subtropical gyre. *Mar. Ecol. Prog. Ser.* 432**,** 173-180.

Dawes, E.A., and Senior, P.J. (1973). "The Role and Regulation of Energy Reserve Polymers in Micro-organisms," in *Adv. Microb. Physiol.,* eds. A.H. Rose & D.W. Tempest. London, UK: Academic Press, 135-266.

De Lucia, G.A., Caliani, I., Marra, S., Camedda, A., Coppa, S., Alcaro, L., Campani, T., Giannetti, M., Coppola, D., Cicero, A.M., Panti, C., Baini, M., Guerranti, C., Marsili, L., Massaro, G., Fossi, M.C., and Matiddi, M. (2014). Amount and distribution of neustonic micro-plastic off the western Sardinian coast (central-western Mediterranean Sea). *Mar. Environ. Res.* 100**,** 10-16.

De Tender, C.A., Devriese, L.I., Haegeman, A., Maes, S., Ruttink, T., and Dawyndt, P. (2015). Bacterial community profiling of plastic litter in the Belgian part of the North Sea. *Environ. Sci. Technol.* 49**,** 9629-9638.

De Witte, B., Devriese, L., Bekaert, K., Hoffman, S., Vandermeersch, G., Cooreman, K., and Robbens, J. (2014). Quality assessment of the blue mussel (*Mytilus edulis*): comparison between commercial and wild types. *Mar. Pollut. Bull.* 85**,** 146-155.

Degange, A.R., and Newby, T.C. (1980). Mortality of seabirds and fish in a lost salmon driftnet. *Mar. Pollut. Bull.* 11**,** 322-323.

Delong, E.F., Franks, D.G., and Alldredge, A.L. (1993). Phylogenetic diversity of aggregate-attached vs. free-living marine bacterial assemblages. *Limnol. Oceanogr.* 38**,** 924-934.

Denier Van Der Gon, H.A., Van Bodegom, P.M., Wassmann, R., Lantin, R.S., and Metra-Corton, T.M. (2001). Sulfate-containing amendments to reduce methane emissions from rice fields: mechanisms, effectiveness and costs. *Mitig. Adapt. Strat. Gl.* 6**,** 71-89.

Denuncio, P., Bastida, R., Dassis, M., Giardino, G., Gerpe, M., and Rodríguez, D. (2011). Plastic ingestion in Franciscana dolphins, *Pontoporia blainvillei* (Gervais and d'Orbigny, 1844), from Argentina. *Mar. Pollut. Bull.* 62**,** 1836-1841.

Derraik, J.G.B. (2002). The pollution of the marine environment by plastic debris: a review. *Mar. Pollut. Bull.* 44**,** 842-852.

Desforges, J.-P.W., Galbraith, M., Dangerfield, N., and Ross, P.S. (2014). Widespread distribution of microplastics in subsurface seawater in the NE Pacific Ocean. *Mar. Pollut. Bull.* 79**,** 94-99.

Desforges, J.P., Galbraith, M., and Ross, P.S. (2015). Ingestion of microplastics by zooplankton in the northeast Pacific ocean. *Arch. Environ. Contam. Toxicol.* 69**,** 320-330.

Devereux, R., Winfrey, M.R., Winfrey, J., and Stahl, D.A. (1996). Depth profile of sulfate-reducing bacterial ribosomal RNA and mercury methylation in an estuarine sediment. *FEMS Microbiol. Ecol.* 20**,** 23-31.

Devriese, L.I., Van Der Meulen, M.D., Maes, T., Bekaert, K., Paul-Pont, I., Frere, L., Robbens, J., and Vethaak, A.D. (2015). Microplastic contamination in brown shrimp (*Crangon crangon*, Linnaeus 1758) from coastal waters of the Southern North Sea and channel area. *Mar. Pollut. Bull.* 98**,** 179-187.

Didier, D., Anne, M., and Alexandra, T.H. (2017). Plastics in the North Atlantic garbage patch: A boat-microbe for hitchhikers and plastic degraders. *Sci. Total Environ.* 599–600**,** 1222-1232.

Dikgang, J., Leiman, A., and Visser, M. (2012). Analysis of the plastic-bag levy in South Africa. *Resources, Conservation and Recycling* 66**,** 59-65.

Dilkes-Hoffman, L.S., Lant, P.A., Laycock, B., and Pratt, S. (2019). The rate of biodegradation of PHA bioplastics in the marine environment: A meta-study. *Mar. Pollut. Bull.* 142**,** 15-24.

E.U. (2018). Directive of the European parliament and of the council on the reduction of the impact of certain plastic products on the environment. European Commission, Brussels, Belgium.

Edgar, R.C. (2004). MUSCLE: multiple sequence alignment with high accuracy and high throughput. *Nucleic Acids Res.* 32**,** 1792-1797.

Edyvane, K.S., Dalgetty, A., Hone, P.W., Higham, J.S., and Wace, N.M. (2004). Long-term marine litter monitoring in the remote Great Australian Bight, South Australia. *Mar. Pollut. Bull.* 48**,** 1060-1075.

Eich, A., Mildenberger, T., Laforsch, C., and Weber, M. (2015). Biofilm and diatom succession on polyethylene (PE) and biodegradable plastic bags in two marine habitats: early signs of degradation in the pelagic and benthic zone? *PLoS One* 10**,** e0137201.

Emadian, S.M., Onay, T.T., and Demirel, B. (2017). Biodegradation of bioplastics in natural environments. *Waste Manage.* 59**,** 526-536.

Enright, A.J., Van Dongen, S., and Ouzounis, C.A. (2002). An efficient algorithm for large-scale detection of protein families. *Nucleic Acids Res.* 30**,** 1575-1584.

Eriksen, M., Lebreton, L.C., Carson, H.S., Thiel, M., Moore, C.J., Borerro, J.C., Galgani, F., Ryan, P.G., and Reisser, J. (2014). Plastic pollution in the world's oceans: more than 5 trillion plastic pieces weighing over 250,000 tons afloat at sea. *PLoS One* 9**,** e111913.

Esmaeili, A., Pourbabaee, A.A., Alikhani, H.A., Shabani, F., and Esmaeili, E. (2013). Biodegradation of low-density polyethylene (LDPE) by mixed culture of L*ysinibacillus xylanilyticus* and *Aspergillus niger* in soil. *PLoS One* 8**,** e71720.

European Bioplastics. (2018). Bioplastics - facts and figures. Berlin, Germany.

Faith, D.P. (1992). Conservation evaluation and phylogenetic diversity. *Biol. Conserv.* 61**,** 1-10.

Fendall, L.S., and Sewell, M.A. (2009). Contributing to marine pollution by washing your face: microplastics in facial cleansers. *Mar. Pollut. Bull.* 58**,** 1225-1228.

Foekema, E.M., De Gruijter, C., Mergia, M.T., Van Franeker, J.A., Murk, A.J., and Koelmans, A.A. (2013). Plastic in North Sea fish. *Environ. Sci. Technol.* 47**,** 8818-8824.

Foulon, V., Le Roux, F., Lambert, C., Huvet, A., Soudant, P., and Paul-Pont, I. (2016). Colonization of polystyrene microparticles by *Vibrio crassostreae*: light and electron microscopic investigation. *Environ. Sci. Technol.* 50**,** 10988-10996.

Gajendiran, A., Krishnamoorthy, S., and Abraham, J. (2016). Microbial degradation of low-density polyethylene (LDPE) by *Aspergillus clavatus* strain JASK1 isolated from landfill soil. *3 Biotech* 6

Galgani, F. (2015). Marine litter, future prospects for research. *Front. Mar. Sci.* 2**,** 87.

Gauci, V., Matthews, E., Dise, N., Walter, B., Koch, D., Granberg, G., and Vile, M. (2004). Sulfur pollution suppression of the wetland methane source in the 20th and 21st centuries. *Proc. Natl. Acad. Sci. U. S. A.* 101**,** 12583-12587.

Gewert, B., Plassmann, M.M., and Macleod, M. (2015). Pathways for degradation of plastic polymers floating in the marine environment. *Environ. Sci.: Process. Impacts* 17**,** 1513-1521.

Geyer, R., Jambeck, J.R., and Law, K.L. (2017). Production, use, and fate of all plastics ever made. *Sci. Adv.* 3**,** e1700782.

Good, T.P., June, J.A., Etnier, M.A., and Broadhurst, G. (2010). Derelict fishing nets in Puget Sound and the Northwest Straits: patterns and threats to marine fauna. *Mar. Pollut. Bull.* 60**,** 39-50.

Gupta, V., and Bashir, Z. (2002). "PET Fibers, Films, and Bottles," in *Handbook of Thermoplastic Polyesters: Homopolymers, Copolymers, Blends, and Composites,* ed. S. Fakirov. Weinheim, Germany: Wiley-VCH, 362-388.

Hai, T., Lange, D., Rabus, R., and Steinbuchel, A. (2004). Polyhydroxyalkanoate (PHA) accumulation in sulfate-reducing bacteria and identification of a class III PHA synthase (PhaEC) in *Desulfococcus multivorans*. *Appl. Environ. Microbiol.* 70**,** 4440-4448.

Harke, M.J., Davis, T.W., Watson, S.B., and Gobler, C.J. (2015). Nutrient-controlled niche differentiation of western Lake Erie cyanobacterial populations revealed via metatranscriptomic surveys. *Environ. Sci. Technol.* 50**,** 604-615.

Harrison, J.P., Schratzberger, M., Sapp, M., and Osborn, A.M. (2014). Rapid bacterial colonization of low-density polyethylene microplastics in coastal sediment microcosms. *BMC Microbiol.* 14**,** 1-15.

Hausmann, B., Pelikan, C., Herbold, C.W., Köstlbacher, S., Albertsen, M., Eichorst, S.A., Glavina Del Rio, T., Huemer, M., Nielsen, P.H., Rattei, T., Stingl, U., Tringe, S.G., Trojan, D., Wentrup, C., Woebken, D., Pester, M., and Loy, A. (2018). Peatland Acidobacteria with a dissimilatory sulfur metabolism. *ISME J.* 12**,** 1729-1742.

Hawas, J., El-Banna, T.E.-S., Belal, E.B.A., and El-Aziz, A. (2016). Production of bioplastic from some selected bacterial strains. *Int. J. Curr. Microbiol. App. Sci* 5**,** 10-22.

Helgason, E., Økstad, O.A., Caugant, D.A., Johansen, H.A., Fouet, A., Mock, M., Hegna, I., and Kolstø, A.-B. (2000). *Bacillus anthracis*, *Bacillus cereus*, and *Bacillus thuringiensis*—one species on the basis of genetic evidence. *Appl. Environ. Microbiol.* 66**,** 2627-2630.

Hollibaugh, J.T., Wong, P.S., and Murrell, M.C. (2000). Similarity of particle-associated and free-living bacterial communities in northern San Francisco Bay, California. *Aquat. Microb. Ecol.* 21**,** 103-114.

Holmes, L.A., Turner, A., and Thompson, R.C. (2014). Interactions between trace metals and plastic production pellets under estuarine conditions. *Mar. Chem.* 167**,** 25-32.

Hotelier, T., Renault, L., Cousin, X., Negre, V., Marchot, P., and Chatonnet, A. (2004). ESTHER, the database of the α/β-hydrolase fold superfamily of proteins. *Nucleic Acids Res.* 32**,** D145-D147.

Hothorn, T., Bretz, F., and Westfall, P. (2008). Simultaneous inference in general parametric models. *Biom. J.* 50**,** 346-363.

Hyatt, D., Chen, G.-L., Locascio, P.F., Land, M.L., Larimer, F.W., and Hauser, L.J. (2010). Prodigal: prokaryotic gene recognition and translation initiation site identification. *BMC Bioinformatics* 11**,** 119-119.

Ishizaki, A., Tanaka, K., and Taga, N. (2001). Microbial production of poly-D-3-hydroxybutyrate from CO2. *Appl. Microbiol. Biotechnol.* 57**,** 6-12.

Jackson, C.R., Churchill, P.F., and Roden, E.E. (2001). Successional changes in bacterial assemblage structure during epilithic biofilm development. *Ecology* 82**,** 555-566.

Jain, C., Rodriguez-R, L.M., Phillippy, A.M., Konstantinidis, K.T., and Aluru, S. (2018). High-throughput ANI analysis of 90K prokaryotic genomes reveals clear species boundaries. *Nat. Commun.* 9**,** 5114.

Jambeck, J.R., Geyer, R., Wilcox, C., Siegler, T.R., Perryman, M., Andrady, A., Narayan, R., and Lavender, L.K. (2015). Plastic waste inputs from land into the ocean. *Science* 347**,** 768-771.

Jendrossek, D., and Handrick, R. (2002). Microbial degradation of polyhydroxyalkanoates. *Annu. Rev. Microbiol.* 56**,** 403-432.

Jensen, M.P., Limpus, C.J., Whiting, S.D., Guinea, M., Prince, R.I.T., Dethmers, K.E.M., Adnyana, I.B.W., Kennett, R., and Fitzsimmons, N.N. (2013). Defining olive ridley turtle

Lepidochelys olivacea management units in Australia and assessing the potential impact of mortality in ghost nets. *Endanger. Species Res.* 21**,** 241-253.

Jiang, P., Zhao, S., Zhu, L., and Li, D. (2018). Microplastic-associated bacterial assemblages in the intertidal zone of the Yangtze Estuary. *Sci. Total Environ.* 624**,** 48-54.

John, J.S. (2011). SeqPrep. https://github.com/jstjohn/SeqPrep.

Jørgensen, B.B. (1977). The sulfur cycle of a coastal marine sediment (Limfjorden, Denmark). *Limnol. Oceanogr.* 22**,** 814-832.

Jørgensen, B.B. (1982). Mineralization of organic matter in the sea bed—the role of sulphate reduction. *Nature* 296**,** 643-645.

Jørgensen, B.B., Findlay, A.J., and Pellerin, A. (2019). The biogeochemical sulfur cycle of marine sediments. *Front. Microbiol.* 10

Kalyaanamoorthy, S., Minh, B.Q., Wong, T.K.F., Von Haeseler, A., and Jermiin, L.S. (2017). ModelFinder: fast model selection for accurate phylogenetic estimates. *Nat. Methods* 14**,** 587.

Kang, D.D., Froula, J., Egan, R., and Wang, Z. (2015). MetaBAT, an efficient tool for accurately reconstructing single genomes from complex microbial communities. *PeerJ* 3**,** e1165.

Kanhai, L.D.K., Gårdfeldt, K., Lyashevska, O., Hassellöv, M., Thompson, R.C., and O'connor, I. (2018). Microplastics in sub-surface waters of the Arctic Central Basin. *Mar. Pollut. Bull.* 130**,** 8-18.

Karner, M., and Herndl, G.J. (1992). Extracellular enzymatic activity and secondary production in free-living and marine-snow-associated bacteria. *Mar. Biol.* 113**,** 341-347.

Kellogg, C.T.E., and Deming, J.W. (2014). Particle-associated extracellular enzyme activity and bacterial community composition across the Canadian Arctic Ocean. *FEMS Microbiol. Ecol.* 89**,** 360-375.

Kenyon, K.W., and Kridler, E. (1969). Laysan albatrosses swallow indigestible matter. *The Auk* 86**,** 339-343.

Keswani, A., Oliver, D.M., Gutierrez, T., and Quilliam, R.S. (2016). Microbial hitchhikers on marine plastic debris: human exposure risks at bathing waters and beach environments. *Mar. Environ. Res.* 118**,** 10-19.

Kim, I.-G., Lee, M.-H., Jung, S.-Y., Song, J.J., Oh, T.-K., and Yoon, J.-H. (2005). *Exiguobacterium aestuarii* sp. nov. and *Exiguobacterium marinum* sp. nov., isolated from a tidal flat of the Yellow Sea in Korea. *Int. J. Syst. Evol. Microbiol.* 55**,** 885-889.

Kint, D., and Muñoz-Guerra, S. (1999). A review on the potential biodegradability of poly(ethylene terephthalate). *Polym. Int.* 48**,** 346-352.

Kirstein, I.V., Kirmizi, S., Wichels, A., Garin-Fernandez, A., Erler, R., Loder, M., and Gerdts, G. (2016). Dangerous hitchhikers? Evidence for potentially pathogenic *Vibrio* spp. on microplastic particles. *Mar. Environ. Res.* 120**,** 1-8.

Kita, K., Mashiba, S.-I., Nagita, M., Ishimaru, K., Okamoto, K., Yanase, H., and Kato, N. (1997). Cloning of poly(3-hydroxybutyrate) depolymerase from a marine bacterium, *Alcaligenes faecalis* AE122, and characterization of its gene product. *Biochim. Biophys. Acta* 1352**,** 113-122.

Kjeldsen, K.U., Loy, A., Jakobsen, T.F., Thomsen, T.R., Wagner, M., and Ingvorsen, K. (2007). Diversity of sulfate-reducing bacteria from an extreme hypersaline sediment, Great Salt Lake (Utah). *FEMS Microbiol. Ecol.* 60**,** 287-298.

Klimke, W., Agarwala, R., Badretdin, A., Chetvernin, S., Ciufo, S., Fedorov, B., Kiryutin, B., O'neill, K., Resch, W., Resenchuk, S., Schafer, S., Tolstoy, I., and Tatusova, T. (2009). The National Center for Biotechnology Information's Protein Clusters Database. *Nucleic Acids Res.* 37**,** D216-223.

Klump, J.V., and Martens, C.S. (1981). Biogeochemical cycling in an organic rich coastal marine basin—II. Nutrient sediment-water exchange processes. *Geochim. Cosmochim. Acta* 45**,** 101-121.

Knoll, M., Hamm, T.M., Wagner, F., Martinez, V., and Pleiss, J. (2009). The PHA Depolymerase Engineering Database: A systematic analysis tool for the diverse family of polyhydroxyalkanoate (PHA) depolymerases. *BMC Bioinformatics* 10**,** 89.

Koch, H.M., and Calafat, A.M. (2009). Human body burdens of chemicals used in plastic manufacture. *Philosophical Transactions of the Royal Society B: Biological Sciences* 364**,** 2063-2078.

Kuever, J. (2014). "The Family Desulfarculaceae," in *The Prokaryotes,* eds. R. E.;, D. E.F.;, L. S.;, S. E.; & T. F. Berlin, Germany: Springer, 41-44.

Laist, D.W. (1987). Overview of the biological effects of lost and discarded plastic debris in the marine environment. *Mar. Pollut. Bull.* 18**,** 319-326.

Laist, D.W. (1997). "Impacts of Marine Debris: Entanglement of Marine Life in Marine Debris Including a Comprehensive List of Species with Entanglement and Ingestion Records," in *Marine Debris: Sources, Impacts, and Solutions,* eds. J.M. Coe & D.B. Rogers. New York, NY: Springer New York, 99-139.

Land, M., Hauser, L., Jun, S.-R., Nookaew, I., Leuze, M.R., Ahn, T.-H., Karpinets, T., Lund, O., Kora, G., Wassenaar, T., Poudel, S., and Ussery, D.W. (2015). Insights from 20 years of bacterial genome sequencing. *Funct. Integr. Gen.* 15**,** 141-161.

Law, K.L., and Thompson, R.C. (2014). Microplastics in the seas. *Science* 345**,** 144.

Lawson, T.J., Wilcox, C., Johns, K., Dann, P., and Hardesty, B.D. (2015). Characteristics of marine debris that entangle Australian fur seals (*Arctocephalus pusillus doriferus*) in southern Australia. *Mar. Pollut. Bull.* 98**,** 354-357.

Lazar, B., and Gračan, R. (2011). Ingestion of marine debris by loggerhead sea turtles, Caretta caretta, in the Adriatic Sea. *Mar. Pollut. Bull.* 62**,** 43-47.

Le Gall, J. (1963). A new species of *Desulfovibrio*. *J. Bacteriol.* 86**,** 1120-1120.

Leathers, T.D., Govind, N.S., and Greene, R.V. (2000). Biodegradation of poly(3-hydroxybutyrate-co-3-hydroxyvalerate) by a tropical marine bacterium, *Pseudoalteromonas* sp. NRRL B-30083. *J. Polym. Environ.* 8**,** 119-124.

Lee, J., Yi, H., and Chun, J. (2011). rRNASelector: A computer program for selecting ribosomal RNA encoding sequences from metagenomic and metatranscriptomic shotgun libraries. *J. Microbiol.* 49**,** 689-691.

Lee, S.Y. (1996). Bacterial polyhydroxyalkanoates. *Biotechnol. Bioeng.* 49**,** 1-14.

Legislative Assembly of Ontario (2015). "Bill 75, Microbead Elimination and Monitoring Act, 2015". (Toronto, Ontario).

León-Zayas, R., Roberts, C., Vague, M., and Mellies, J.L. (2019). Draft genome sequences of five environmental bacterial isolates that degrade polyethylene terephthalate plastic. *Microbiol. Res. Announc.* 8**,** e00237-00219.

Li, D., Liu, C.-M., Luo, R., Sadakane, K., and Lam, T.-W. (2015). MEGAHIT: an ultra-fast single-node solution for large and complex metagenomics assembly via succinct de Bruijn graph. *Bioinformatics* 31**,** 1674-1676.

Li, H., and Durbin, R. (2010). Fast and accurate long-read alignment with Burrows-Wheeler transform. *Bioinformatics* 26**,** 589-595.

Li, L., Stoeckert, C.J., and Roos, D.S. (2003). OrthoMCL: identification of ortholog groups for eukaryotic genomes. *Genome Res.* 13**,** 2178-2189.

Li, W.C., Tse, H.F., and Fok, L. (2016a). Plastic waste in the marine environment: A review of sources, occurrence and effects. *Sci. Total Environ.* 566-567**,** 333-349.

Li, Z., Yang, J., and Loh, X.J. (2016b). Polyhydroxyalkanoates: opening doors for a sustainable future. *Npg Asia Materials* 8**,** e265.

Lindau, C.W., Alford, D.P., Bollich, P.K., and Linscombe, S.D. (1994). Inhibition of methane evolution by calcium sulfate addition to flooded rice. *Plant Soil* 158**,** 299-301.

Liu, Y., Lai, Q., Göker, M., Meier-Kolthoff, J.P., Wang, M., Sun, Y., Wang, L., and Shao, Z. (2015). Genomic insights into the taxonomic status of the *Bacillus cereus* group. *Sci. Rep.* 5**,** 14082.

Lobelle, D., and Cunliffe, M. (2011). Early microbial biofilm formation on marine plastic debris. *Mar. Pollut. Bull.* 62**,** 197-200.

Lozupone, C., Lladser, M.E., Knights, D., Stombaugh, J., and Knight, R. (2011). UniFrac: an effective distance metric for microbial community comparison. *ISME J.* 5**,** 169-172.

Lusher, A.L., Hernandez-Milian, G., O'brien, J., Berrow, S., O'connor, I., and Officer, R. (2015). Microplastic and macroplastic ingestion by a deep diving, oceanic cetacean: The True's beaked whale *Mesoplodon mirus*. *Environ. Pollut.* 199**,** 185-191.

Mabrouk, M.M., and Sabry, S.A. (2001). Degradation of poly (3-hydroxybutyrate) and its copolymer poly (3-hydroxybutyrate-co-3-hydroxyvalerate) by a marine *Streptomyces* sp. SNG9. *Microbiol. Res.* 156**,** 323-335.

Magoc, T., and Salzberg, S.L. (2011). FLASH: fast length adjustment of short reads to improve genome assemblies. *Bioinformatics* 27**,** 2957-2963.

Martin, M. (2011). Cutadapt removes adapter sequences from high-throughout sequencing reads. *EMB.net Journal* 17**,** 10-12.

Mas-Castellà, J., Urmeneta, J., Lafuente, R., Navarrete, A., and Guerrero, R. (1995). Biodegradation of poly-β-hydroxyalkanoates in anaerobic sediments. *Int. Biodeterior. Biodegrad.* 35**,** 155-174.

Mathalon, A., and Hill, P. (2014). Microplastic fibers in the intertidal ecosystem surrounding Halifax Harbor, Nova Scotia. *Mar. Pollut. Bull.* 81**,** 69-79.

Mato, Y., Isobe, T., Takada, H., Kanehiro, H., Ohtake, C., and Kaminuma, T. (2001). Plastic resin pellets as a transport medium for toxic chemicals in the marine environment. *Environ. Sci. Technol.* 35**,** 318-324.

Matsusaki, H., Abe, H., and Doi, Y. (2000). Biosynthesis and properties of poly(3-hydroxybutyrate-co-3-hydroxyalkanoates) by recombinant strains of *Pseudomonas* sp. 61-3. *Biomacromolecules* 1**,** 17-22.

Mayer, J.M. (1990). "Degradation Kinetics of Polymer Films in Marine and Soil Systems under Accelerated Conditions," in *Novel Biodegradable Microbial Polymers,* ed. E.A. Dawes. Dordrecht, Germany: Springer.

Mccormick, A., Hoellein, T.J., Mason, S.A., Schluep, J., and Kelly, J.J. (2014). Microplastic is an abundant and distinct microbial habitat in an urban river. *Environ. Sci. Technol.* 48**,** 11863-11871.

Mcmurdie, P.J., and Holmes, S. (2013). phyloseq: an R package for reproducible interactive analysis and graphics of microbiome census data. *PLoS One* 8**,** e61217.

Mergaert, J., Webb, A., Anderson, C., Wouters, A., and Swings, J. (1993). Microbial degradation of poly(3-hydroxybutyrate) and poly(3-hydroxybutyrate-co-3-hydroxyvalerate) in soils. *Appl. Environ. Microbiol.* 59**,** 3233-3238.

Mergaert, J., Wouters, A., Swings, J., and Anderson, C. (1995). *In situ* biodegradation of poly(3-hydroxybutyrate) and poly(3-hydroxybutyrate-co-3-hydroxyvalerate) in natural waters. *Can. J. Microbiol.* 41**,** 154-159.

Minh, B.Q., Nguyen, M.a.T., and Von Haeseler, A. (2013). Ultrafast approximation for phylogenetic bootstrap. *Mol. Biol. Evol.* 30**,** 1188-1195.

Mitchell, A., Bucchini, F., Cochrane, G., Denise, H., Hoopen, P.T., Fraser, M., Pesseat, S., Potter, S., Scheremetjew, M., Sterk, P., and Finn, R.D. (2016). EBI metagenomics in 2016 - an expanding and evolving resource for the analysis and archiving of metagenomic data. *Nucleic Acids Res.* 44**,** D595-D603.

Mohamed Nor, N.H., and Obbard, J.P. (2014). Microplastics in Singapore's coastal mangrove ecosystems. *Mar. Pollut. Bull.* 79**,** 278-283.

Moore, C.J. (2008). Synthetic polymers in the marine environment: A rapidly increasing, long-term threat. *Environ. Res.* 108**,** 131-139.

Moore, C.J., Moore, S.L., Leecaster, M.K., and Weisberg, S.B. (2001). A comparison of plastic and plankton in the North Pacific Central Gyre. *Mar. Pollut. Bull.* 42**,** 1297-1300.

Morais-Silva, F.O., Rezende, A.M., Pimentel, C., Santos, C.I., Clemente, C., Varela–Raposo, A., Resende, D.M., Da Silva, S.M., De Oliveira, L.M., and Matos, M. (2014). Genome sequence of the model sulfate reducer *Desulfovibrio gigas*: a comparative analysis within the *Desulfovibrio* genus. *Microbiologyopen.* 3**,** 513-530.

Moser, M.L., and Lee, D.S. (1992). A fourteen-year survey of plastic ingestion by western north Atlantic seabirds. *Colonial Waterbirds* 15**,** 83-94.

Mukai, K., Yamada, K., and Doi, Y. (1993). Enzymatic degradation of poly(hydroxyalkanoates) by a marine bacterium. *Polym. Degradation Stab.* 41**,** 85-91.

Mukherjee, S., Roy Chowdhuri, U., and Kundu, P.P. (2016). Bio-degradation of polyethylene waste by simultaneous use of two bacteria: *Bacillus licheniformis* for production of bio-surfactant and *Lysinibacillus fusiformis* for bio-degradation. *RSC Advances* 6**,** 2982-2992.

Müller, A.L., Kjeldsen, K.U., Rattei, T., Pester, M., and Loy, A. (2014). Phylogenetic and environmental diversity of DsrAB-type dissimilatory (bi)sulfite reductases. *ISME J.* 9**,** 1152-1165.

Müller, R.-J., Kleeberg, I., and Deckwer, W.-D. (2001). Biodegradation of polyesters containing aromatic constituents. *J. Biotechnol.* 86**,** 87-95.

Murray, F., and Cowie, P.R. (2011). Plastic contamination in the decapod crustacean *Nephrops norvegicus* (Linnaeus, 1758). *Mar. Pollut. Bull.* 62**,** 1207-1217.

Murrell, M., Hollibaugh, J., Silver, M., and Wong, P. (1999). Bacterioplankton dynamics in northern San Francisco Bay: Role of particle association and seasonal freshwater flow. *Limnol. Oceanogr.* 44**,** 295-308.

Muyzer, G., and Stams, A.J.M. (2008). The ecology and biotechnology of sulphate-reducing bacteria. *Nature Reviews Microbiology* 6**,** 441.

Nadal, M.A., Alomar, C., and Deudero, S. (2016). High levels of microplastic ingestion by the semipelagic fish bogue *Boops boops* (L.) around the Balearic Islands. *Environ. Pollut.* 214**,** 517-523.

Nanda, S., Sahu, S., and Abraham, J. (2010). Studies on the biodegradation of natural and synthetic polyethylene by *Pseudomonas* spp. *J. Appl. Sci. Environ. Manage.* 14**,** 57-60.

National Association for Pet Container Resources. (2018). Postconsumer PET Container Recycling Activity in 2017. National Association for PET Container Resources, Florence, Kentucky.

Nauendorf, A., Krause, S., Bigalke, N.K., Gorb, E.V., Gorb, S.N., Haeckel, M., Wahl, M., and Treude, T. (2016). Microbial colonization and degradation of polyethylene and biodegradable plastic bags in temperate fine-grained organic-rich marine sediments. *Mar. Pollut. Bull.* 103**,** 168-178.

Nehra, K., Jamdagni, P., and Lathwal, P. (2017). "Bioplastics: A Sustainable Approach Toward Healthier Environment," in *Plant Biotechnology: Recent Advancements and Developments,* eds. S.K. Gahlawat, R.K. Salar, P. Siwach, J.S. Duhan, S. Kumar & P. Kaur. Singapore: Springer Singapore, 297-314.

Neilson, J.L., Straley, J.M., Gabriele, C.M., and Hills, S. (2009). Non-lethal entanglement of humpback whales (*Megaptera novaeangliae*) in fishing gear in northern Southeast Alaska. *J. Biogeogr.* 36**,** 452-464.

Nelms, S.E., Duncan, E.M., Broderick, A.C., Galloway, T.S., Godfrey, M.H., Hamann, M., Lindeque, P.K., and Godley, B.J. (2015). Plastic and marine turtles: a review and call for research. *ICES J. Mar. Sci.* 73**,** 165-181.

Nguyen, L.-T., Schmidt, H.A., Von Haeseler, A., and Minh, B.Q. (2015). IQ-TREE: A fast and effective stochastic algorithm for estimating maximum-likelihood phylogenies. *Mol. Biol. Evol.* 32**,** 268-274.

Notredame, C., Higgins, D.G., and Heringa, J. (2000). T-Coffee: A novel method for fast and accurate multiple sequence alignment. *J. Mol. Biol.* 302**,** 205-217.

O'brien, J., and Thondhlana, G. (2019). Plastic bag use in South Africa: Perceptions, practices and potential intervention strategies. *Waste Manage.* 84**,** 320-328.

Obbard, R.W., Sadri, S., Wong, Y.Q., Khitun, A.A., Baker, I., and Thompson, R.C. (2014). Global warming releases microplastic legacy frozen in Arctic Sea ice. *Earth's Future* 2**,** 315-320.

Oberbeckmann, S., Kreikemeyer, B., and Labrenz, M. (2018). Environmental factors support the formation of specific bacterial assemblages on microplastics. *Front. Microbiol.* 8

Oberbeckmann, S., Loeder, M.G., Gerdts, G., and Osborn, A.M. (2014). Spatial and seasonal variation in diversity and structure of microbial biofilms on marine plastics in Northern European waters. *FEMS Microbiol. Ecol.* 90**,** 478-492.

Oberbeckmann, S., Osborn, A.M., and Duhaime, M.B. (2016). Microbes on a bottle: substrate, season and geography influence community composition of microbes colonizing marine plastic debris. *PLoS One* 11**,** e0159289.

Obruca, S., Sedlacek, P., Koller, M., Kucera, D., and Pernicova, I. (2018). Involvement of polyhydroxyalkanoates in stress resistance of microbial cells: biotechnological consequences and applications. *Biotechnol. Adv.* 36**,** 856-870.

Oehlmann, J., Schulte-Oehlmann, U., Kloas, W., Jagnytsch, O., Lutz, I., Kusk, K.O., Wollenberger, L., Santos, E.M., Paull, G.C., Look, K.J.W.V., and Tyler, C.R. (2009). A

critical analysis of the biological impacts of plasticizers on wildlife. *Philosophical Transactions of the Royal Society B: Biological Sciences* 364**,** 2047-2062.

Oksanen, J., Blanchet, F.G., Friendly, M., Kindt, R., Legendre, P., Mcglinn, D., Minchin, P.R., O'hara, R.B., Simpson, G.L., Solymos, P., Stevens, M.H.H., Szoecs, E., and Wagner, H. (2019). vegan: Community Ecology Package. https://CRAN.R-project.org/package=vegan.

Ondov, B.D., Treangen, T.J., Melsted, P., Mallonee, A.B., Bergman, N.H., Koren, S., and Phillippy, A.M. (2016). Mash: fast genome and metagenome distance estimation using MinHash. *Genome Biol.* 17**,** 132.

Orr, I.G., Hadar, Y., and Sivan, A. (2004). Colonization, biofilm formation and biodegradation of polyethylene by a strain of *Rhodococcus ruber*. *Appl. Microbiol. Biotechnol.* 65**,** 97-104.

Ortiz-Álvarez, R., Fierer, N., De Los Ríos, A., Casamayor, E.O., and Barberán, A. (2018). Consistent changes in the taxonomic structure and functional attributes of bacterial communities during primary succession. *ISME J.* 12**,** 1658-1667.

Overbeek, R., Olson, R., Pusch, G.D., Olsen, G.J., Davis, J.J., Disz, T., Edwards, R.A., Gerdes, S., Parrello, B., Shukla, M., Vonstein, V., Wattam, A.R., Xia, F., and Stevens, R. (2014). The SEED and the Rapid Annotation of microbial genomes using Subsystems Technology (RAST). *Nucleic Acids Res.* 42**,** D206-D214.

Page, B., Mckenzie, J., Mcintosh, R., Baylis, A., Morrissey, A., Calvert, N., Haase, T., Berris, M., Dowie, D., Shaughnessy, P.D., and Goldsworthy, S.D. (2004). Entanglement of Australian sea lions and New Zealand fur seals in lost fishing gear and other marine

debris before and after government and industry attempts to reduce the problem. *Mar. Pollut. Bull.* 49**,** 33-42.

Parks, D.H., Imelfort, M., Skennerton, C.T., Hugenholtz, P., and Tyson, G.W. (2015). CheckM: assessing the quality of microbial genomes recovered from isolates, single cells, and metagenomes. *Genome Res.* 25**,** 1043-1055.

Parks, D.H., Rinke, C., Chuvochina, M., Chaumeil, P.-A., Woodcroft, B.J., Evans, P.N., Hugenholtz, P., and Tyson, G.W. (2017). Recovery of nearly 8,000 metagenome-assembled genomes substantially expands the tree of life. *Nat. Microbiol.* 2**,** 1533-1542.

Parsons, G.R., Kang, A.K., Legget, C.G., and Boyle, K.J. (1984). Valuing beach closures on the Padre Island National Seashore. *Mar. Resour. Econ.* 24**,** 213-235.

Patel, V.K., Srivastava, R., Sharma, A., Srivastava, A.K., Singh, S., Srivastava, A.K., Kashyap, P.L., Chakdar, H., Pandiyan, K., Kalra, A., and Saxena, A.K. (2018). Halotolerant *Exiguobacterium profundum* PHM11 tolerate salinity by accumulating L-proline and fine-tuning gene expression profiles of related metabolic pathways. *Front. Microbiol.* 9

Pauli, N.-C., Petermann, J.S., Lott, C., and Weber, M. (2017). Macrofouling communities and the degradation of plastic bags in the sea: an *in situ* experiment. *Royal Soc. Open Sci.* 4**,** e170549.

Pedrotti, M.L., Petit, S., Elineau, A., Bruzaud, S., Crebassa, J.C., Dumontet, B., Marti, E., Gorsky, G., and Cozar, A. (2016). Changes in the floating plastic pollution of the Mediterranean Sea in relation to the distance to land. *PLoS One* 11**,** e0161581.

Pham, C.K., Rodríguez, Y., Dauphin, A., Carriço, R., Frias, J.P.G.L., Vandeperre, F., Otero, V., Santos, M.R., Martins, H.R., Bolten, A.B., and Bjorndal, K.A. (2017). Plastic ingestion in

oceanic-stage loggerhead sea turtles (*Caretta caretta*) off the North Atlantic subtropical gyre. *Mar. Pollut. Bull.* 121**,** 222-229.

Pinnell, L.J., Conkle, J.L., and Turner, J.W. (2019). Microbial succession during the biodegradation of bioplastic in coastal marine sediment. *(manuscript under review)*

Pinnell, L.J., and Turner, J.W. (2019). Shotgun metagenomics reveals the benthic microbial community response to plastic and bioplastic in a coastal marine environment. *Front. Microbiol.* 10

Plastics Industry Association. (2018). 2018 Size and Impact Report of U.S. Plastics Indusry. Plastics Industry Association,

Ploug, H., Grossart, H.-P., Azam, F., and Jørgensen, B.B. (1999). Photosynthesis, respiration, and carbon turnover in sinking marine snow from surface waters of Southern California Bight: implications for the carbon cycle in the ocean. *Mar. Ecol. Prog. Ser.* 179**,** 1-11.

Poortinga, W., Whitmarsh, L., and Suffolk, C. (2013). The introduction of a single-use carrier bag charge in Wales: Attitude change and behavioural spillover effects. *J. Environ. Psychol.* 36**,** 240-247.

Possatto, F.E., Barletta, M., Costa, M.F., Do Sul, J.A., and Dantas, D.V. (2011). Plastic debris ingestion by marine catfish: an unexpected fisheries impact. *Mar. Pollut. Bull.* 62**,** 1098-1102.

Purdy, K., Munson, M., Cresswell-Maynard, T., Nedwell, D., and Embley, T. (2003). Use of 16S rRNA-targeted oligonucleotide probes to investigate function and phylogeny of sulphate-reducing bacteria and methanogenic archaea in a UK estuary. *FEMS Microbiol. Ecol.* 44**,** 361-371.

Purdy, K.J., Embley, T.M., and Nedwell, D.B. (2002). The distribution and activity of sulphate reducing bacteria in estuarine and coastal marine sediments. *Antonie Van Leeuwenhoek* 81**,** 181-187.

Purdy, K.J., Nedwell, D.B., Embley, T.M., and Takii, S. (1997). Use of 16S rRNA-targeted oligonucleotide probes to investigate the occurrence and selection of sulfate-reducing bacteria in response to nutrient addition to sediment slurry microcosms from a Japanese estuary. *FEMS Microbiol. Ecol.* 24**,** 221-234.

Quast, C., Pruesse, E., Yilmaz, P., Gerken, J., Schweer, T., Yarza, P., Peplies, J., and Glöckner, F.O. (2013). The SILVA ribosomal RNA gene database project: improved data processing and web-based tools. *Nucleic Acids Res.* 41**,** D590-D596.

R Core Team (2017). "R: A language and environment for statistical computing". (Vienna, Austria: R Foundation for Statistical Computing).

Rai, R., Keshavarz, T., Roether, J.A., Boccaccini, A.R., and Roy, I. (2011). Medium chain length polyhydroxyalkanoates, promising new biomedical materials for the future. *Materials Science and Engineering: R: Reports* 72**,** 29-47.

Rasko, D.A., Altherr, M.R., Han, C.S., and Ravel, J. (2005). Genomics of the *Bacillus cereus* group of organisms. *FEMS Microbiol. Rev.* 29**,** 303-329.

Reddy, C.S.K., Ghai, R., Rashmi, and Kalia, V.C. (2003). Polyhydroxyalkanoates: an overview. *Bioresour. Technol.* 87**,** 137-146.

Redford, D.P., Trulli, H.K., and Trulli, W.R. (1997). "Sources of Plastic Pellets in the Aquatic Environment," in *Marine Debris: Sources, Impacts, and Solutions,* eds. J.M. Coe & D.B. Rogers. New York, NY: Springer New York, 335-343.

Rho, M., Tang, H., and Ye, Y. (2010). FragGeneScan: predicting genes in short and error-prone reads. *Nucleic Acids Res.* 38**,** e191-e191.

Ribic, C.A., Sheavly, S.B., Rugg, D.J., and Erdmann, E.S. (2010). Trends and drivers of marine debris on the Atlantic coast of the United States 1997–2007. *Mar. Pollut. Bull.* 60**,** 1231-1242.

Rios, L.M., Moore, C., and Jones, P.R. (2007). Persistent organic pollutants carried by synthetic polymers in the ocean environment. *Mar. Pollut. Bull.* 54**,** 1230-1237.

Rjeb, A., Tajounte, L., El Idrissi, M.C., Letarte, S., Adnot, A., Roy, D., Claire, Y., Périchaud, A., and Kaloustian, J. (2000). IR spectroscopy study of polypropylene natural aging. *J. Appl. Polym. Sci.* 77**,** 1742-1748.

Rochman, C.M., Hentschel, B.T., and Teh, S.J. (2014). Long-term sorption of metals is similar among plastic types: implications for plastic debris in aquatic environments. *PLoS One* 9**,** e85433.

Rochman, C.M., Hoh, E., Kurobe, T., and Teh, S.J. (2013). Ingested plastic transfers hazardous chemicals to fish and induces hepatic stress. *Sci. Rep.* 3**,** 3263.

Romeo, T., Pietro, B., Pedà, C., Consoli, P., Andaloro, F., and Fossi, M.C. (2015). First evidence of presence of plastic debris in stomach of large pelagic fish in the Mediterranean Sea. *Mar. Pollut. Bull.* 95**,** 358-361.

Ryan, P.G. (2008). Seabirds indicate changes in the composition of plastic litter in the Atlantic and south-western Indian Oceans. *Mar. Pollut. Bull.* 56**,** 1406-1409.

Ryan, P.G., Moore, C.J., Van Franeker, J.A., and Moloney, C.L. (2009). Monitoring the abundance of plastic debris in the marine environment. *Philosophical Transactions of the Royal Society B: Biological Sciences* 364**,** 1999-2012.

Salim, Y.S., Sharon, A., Vigneswari, S., Mohamad Ibrahim, M.N., and Amirul, A.A. (2012). Environmental degradation of microbial polyhydroxyalkanoates and oil palm-based composites. *Appl. Biochem. Biotechnol.* 167**,** 314-326.

Salta, M., Wharton, J.A., Blache, Y., Stokes, K.R., and Briand, J.F. (2013). Marine biofilms on artificial surfaces: structure and dynamics. *Environ. Microbiol.* 15**,** 2879-2893.

Santos, A.A., Venceslau, S.S., Grein, F., Leavitt, W.D., Dahl, C., Johnston, D.T., and Pereira, I.a.C. (2015). A protein trisulfide couples dissimilatory sulfate reduction to energy conservation. *Science* 350**,** 1541.

Schnell, S., Wondrak, C., Wahl, G., and Schink, B. (1991). Anaerobic degradation of sorbic acid by sulfate-reducing and fermenting bacteria: pentanone-2 and isopentanone-2 as byproducts. *Biodegradation* 2**,** 33-41.

Schrey, E., and Vauk, G.J.M. (1987). Records of entangled gannets (*Sula bassana*) at Helgoland, German Bight. *Mar. Pollut. Bull.* 18**,** 350-352.

Schuyler, Q., Hardesty, B.D., Wilcox, C., and Townsend, K.A. (2014). Global analysis of anthropogenic debris ingestion by sea turtles. *Conserv. Biol.* 28**,** 129-139.

Schuyler, Q.A., Wilcox, C., Townsend, K.A., Wedemeyer-Strombel, K.R., Balazs, G., Van Sebille, E., and Hardesty, B.D. (2016). Risk analysis reveals global hotspots for marine debris ingestion by sea turtles. *Glob. Chang. Biol.* 22**,** 567-576.

Secchi, E.R., and Zarzur, S. (1999). Plastic debris ingested by a Blainville's beaked whale, *Mesoplodon densiostris*, washed ashore in Brazil. *Aquat. Mamm.* 25**,** 21-24.

Seemann, T. (2014). Prokka: rapid prokaryotic genome annotation. *Bioinformatics* 30**,** 2068-2069.

Seymour, J.R., Amin, S.A., Raina, J.-B., and Stocker, R. (2017). Zooming in on the phycosphere: the ecological interface for phytoplankton–bacteria relationships. *Nat. Microbiol.* 2**,** 17065.

Shah, A.A., Hasan, F., Hameed, A., and Ahmed, S. (2007). Isolation and characterization of poly(3-hydroxybutyrate-co-3-hydroxyvalerate) degrading bacteria and purification of PHBV depolymerase from newly isolated *Bacillus* sp. AF3. *Int. Biodeterior. Biodegrad.* 60**,** 109-115.

Sharon, C., and Sharon, M. (2017). Studies on biodegradation of polyethylene terephthalate: A synthetic polymer. *Journal of Microbiology and Biotechnology Research* 2**,** 10.

Shaw, D.G., and Mapes, G.A. (1979). Surface circulation and the distribution of pelagic tar and plastic. *Mar. Pollut. Bull.* 10**,** 160-162.

Singh, J., and Gupta, K. (2014). Screening and identification of low density polyethylene (LDPE) degrading soil fungi isolated from polythene polluted sites around Gwalior City (MP). *Int. J. Curr. Microbiol. App. Sci.* 3**,** 443-448.

Sivan, A., Szanto, M., and Pavlov, V. (2006). Biofilm development of the polyethylene-degrading bacterium *Rhodococcus ruber*. *Appl. Microbiol. Biotechnol.* 72**,** 346-352.

Skennerton, C.T., Haroon, M.F., Briegel, A., Shi, J., Jensen, G.J., Tyson, G.W., and Orphan, V.J. (2016). Phylogenomic analysis of *Candidatus* 'Izimaplasma'species: free-living representatives from a *Tenericutes* clade found in methane seeps. *ISME J.* 10**,** 2679-2692.

Solaiman, D.K.Y., and Ashby, R.D. (2005). Rapid genetic characterization of poly(hydroxyalkanoate) synthase and its applications. *Biomacromolecules* 6**,** 532-537.

Sorokin, D.Y., Tourova, T.P., Sukhacheva, M.V., and Muyzer, G. (2012). *Desulfuribacillus alkaliarsenatis* gen. nov. sp. nov., a deep-lineage, obligately anaerobic, dissimilatory

sulfur and arsenate-reducing, haloalkaliphilic representative of the order Bacillales from soda lakes. *Extremophiles* 16**,** 597-605.

Sridewi, N., Bhubalan, K., and Sudesh, K. (2006). Degradation of commercially important polyhydroxyalkanoates in tropical mangrove ecosystem. *Polym. Degradation Stab.* 91**,** 2931-2940.

Stamatakis, A. (2014). RAxML version 8: a tool for phylogenetic analysis and post-analysis of large phylogenies. *Bioinformatics* 30**,** 1312-1313.

Stelfox, M., Hudgins, J., and Sweet, M. (2016). A review of ghost gear entanglement amongst marine mammals, reptiles and elasmobranchs. *Mar. Pollut. Bull.* 111**,** 6-17.

Sudhakar, M., Doble, M., Murthy, P.S., and Venkatesan, R. (2008). Marine microbe-mediated biodegradation of low- and high-density polyethylenes. *Int. Biodeterior. Biodegrad.* 61**,** 203-213.

Sun, H., Spring, S., Lapidus, A., Davenport, K., Del Rio, T.G., Tice, H., Nolan, M., Copeland, A., Cheng, J.-F., Lucas, S., Tapia, R., Goodwin, L., Pitluck, S., Ivanova, N., Pagani, I., Mavromatis, K., Ovchinnikova, G., Pati, A., Chen, A., Palaniappan, K., Hauser, L., Chang, Y.-J., Jeffries, C.D., Detter, J.C., Han, C., Rohde, M., Brambilla, E., Göker, M., Woyke, T., Bristow, J., Eisen, J.A., Markowitz, V., Hugenholtz, P., Kyrpides, N.C., Klenk, H.-P., and Land, M. (2010). Complete genome sequence of *Desulfarculus baarsii* type strain (2st14). *Stand Genomic Sci* 3**,** 276-284.

Sun, X., Li, Q., Zhu, M., Liang, J., Zheng, S., and Zhao, Y. (2017). Ingestion of microplastics by natural zooplankton groups in the northern South China Sea. *Mar. Pollut. Bull.* 115**,** 217-224.

Talavera, G., and Castresana, J. (2007). Improvement of phylogenies after removing divergent and ambiguously aligned blocks from protein sequence alignments. *Syst. Biol.* 56**,** 564-577.

Tarpley, R., and Marwitz, S. (1993). Plastic debris ingestion by cetaceans along the Texas coast: two case reports. *Aquat. Mamm.* 19**,** 93-98.

Teuten, E.L., Rowland, S.J., Galloway, T.S., and Thompson, R.C. (2007). Potential for plastics to transport hydrophobic contaminants. *Environ. Sci. Technol.* 41**,** 7759-7764.

Thellen, C., Coyne, M., Froio, D., Auerbach, M., Wirsen, C., and Ratto, J.A. (2008). A processing, characterization and marine biodegradation study of melt-extruded polyhydroxyalkanoate (PHA) films. *J. Polym. Environ.* 16**,** 1-11.

Thompson, R.C., Moore, C.J., Vom Saal, F.S., and Swan, S.H. (2009a). Plastics, the environment and human health: current consensus and future trends. *Philos. Trans. R. Soc. Lond. B Biol. Sci.* 364**,** 2153-2166.

Thompson, R.C., Olsen, Y., Mitchell, R.P., Davis, A., Rowland, S.J., John, A.W.G., Mcgonigle, D., and Russell, A.E. (2004). Lost at sea: where is all the plastic? *Science* 304**,** 838.

Thompson, R.C., Swan, S.H., Moore, C.J., and Vom Saal, F.S. (2009b). Our plastic age. *Philosophical Transactions of the Royal Society B: Biological Sciences* 364**,** 1973-1976.

Tunnell, J.W. (2002). "Geography, Climate, and Hydrography," in *The Laguna Madre of Texas and Tamaulipas,* eds. J.W. Tunnell & F.W. Judd. College Station, Texas: Texas A&M University Press, 7-27.

U.N.E.P. (2018). Single-use plastics: A roadmap for sustainability. United Nations Environment Programme, Nairobi, Kenya.

United States Congress (2015). "H.R.1321 - Microbead-Free Waters Act of 2015". (Washington, DC).

Urmeneta, J., Mas-Castella, J., and Guerrero, R. (1995). Biodegradation of poly-(beta)-hydroxyalkanoates in a lake sediment sample increases bacterial sulfate reduction. *Appl. Environ. Microbiol.* 61**,** 2046-2048.

Van Cauwenberghe, L., Devriese, L., Galgani, F., Robbens, J., and Janssen, C.R. (2015). Microplastics in sediments: a review of techniques, occurrence and effects. *Mar. Environ. Res.* 111**,** 5-17.

Van Cauwenberghe, L., and Janssen, C.R. (2014). Microplastics in bivalves cultured for human consumption. *Environ. Pollut.* 193**,** 65-70.

Van Cauwenberghe, L., Vanreusel, A., Mees, J., and Janssen, C.R. (2013). Microplastic pollution in deep-sea sediments. *Environ. Pollut.* 182**,** 495-499.

Van Der Meulen, M., Devriese, L., Lee, J., Maes, T., Van Dalfsen, J., Huvet, A., Soudant, P., Robbens, J., and Vethaak, A. (2014). Socio-economic impact of microplastics in the 2 Seas, Channel and France Manche Region: an initial risk assessment. *MICRO Interreg project IVa*

Van Franeker, J.A., Blaize, C., Danielsen, J., Fairclough, K., Gollan, J., Guse, N., Hansen, P.L., Heubeck, M., Jensen, J.K., Le Guillou, G., Olsen, B., Olsen, K.O., Pedersen, J., Stienen, E.W., and Turner, D.M. (2011). Monitoring plastic ingestion by the northern fulmar Fulmarus glacialis in the North Sea. *Environ. Pollut.* 159**,** 2609-2615.

Vendel, A.L., Bessa, F., Alves, V.E.N., Amorim, A.L.A., Patrício, J., and Palma, A.R.T. (2017). Widespread microplastic ingestion by fish assemblages in tropical estuaries subjected to anthropogenic pressures. *Mar. Pollut. Bull.* 117**,** 448-455.

Verlinden, R.a.J., Hill, D.J., Kenward, M.A., Williams, C.D., and Radecka, I. (2007). Bacterial synthesis of biodegradable polyhydroxyalkanoates. *J. Appl. Microbiol.* 102**,** 1437-1449.

Vethaak, A.D., and Leslie, H.A. (2016). Plastic debris is a human health issue. *Environ. Sci. Technol.* 50**,** 6825-6826.

Vigneron, A., Cruaud, P., Alsop, E., De Rezende, J.R., Head, I.M., and Tsesmetzis, N. (2018). Beyond the tip of the iceberg; a new view of the diversity of sulfite- and sulfate-reducing microorganisms. *ISME J.* 12**,** 2096-2099.

Vigneswari, S., Lee, T.S., Bhubalan, K., and Amirul, A.A. (2015). Extracellular polyhydroxyalkanoate depolymerase by *Acidovorax* sp. DP5. *Enzyme Research* 2015**,** 8.

Vishnivetskaya, T.A., Kathariou, S., and Tiedje, J.M. (2009). The *Exiguobacterium* genus: biodiversity and biogeography. *Extremophiles* 13**,** 541-555.

Volova, T.G., Boyandin, A.N., Vasiliev, A.D., Karpov, V.A., Prudnikova, S.V., Mishukova, O.V., Boyarskikh, U.A., Filipenko, M.L., Rudnev, V.P., Bá Xuân, B., Việt Dũng, V., and Gitelson, I.I. (2010). Biodegradation of polyhydroxyalkanoates (PHAs) in tropical coastal waters and identification of PHA-degrading bacteria. *Polym. Degradation Stab.* 95**,** 2350-2359.

Volova, T.G., Prudnikova, S.V., Vinogradova, O.N., Syrvacheva, D.A., and Shishatskaya, E.I. (2017). Microbial degradation of polyhydroxyalkanoates with different chemical compositions and their biodegradability. *Microb. Ecol.* 73**,** 353-367.

Votier, S.C., Archibald, K., Morgan, G., and Morgan, L. (2011). The use of plastic debris as nesting material by a colonial seabird and associated entanglement mortality. *Mar. Pollut. Bull.* 62**,** 168-172.

Wagner, M., Loy, A., Klein, M., Lee, N., Ramsing, N.B., Stahl, D.A., and Friedrich, M.W. (2005). "Functional Marker Genes for Identification of Sulfate-Reducing Prokaryotes," in *Methods Enzymol.*: Academic Press, 469-489.

Walters, W., Hyde, E.R., Berg-Lyons, D., Ackermann, G., Humphrey, G., Parada, A., Gilbert, J.A., Jansson, J.K., Caporaso, J.G., Fuhrman, J.A., Apprill, A., and Knight, R. (2016). Improved bacterial 16S rRNA gene (V4 and V4-5) and fungal internal transcribed spacer marker gene primers for microbial community surveys. *mSystems* 1**,** e00009-00015.

Wang, S., Lydon, K.A., White, E.M., Grubbs, J.B., Lipp, E.K., Locklin, J., and Jambeck, J.R. (2018). Biodegradation of poly(3-hydroxybutyrate-co-3-hydroxyhexanoate) plastic under anaerobic sludge and aerobic seawater conditions: gas evolution and microbial diversity. *Environ. Sci. Technol.* 52**,** 5700-5709.

Wattam, A.R., Davis, J.J., Assaf, R., Boisvert, S., Brettin, T., Bun, C., Conrad, N., Dietrich, E.M., Disz, T., Gabbard, J.L., Gerdes, S., Henry, C.S., Kenyon, R.W., Machi, D., Mao, C., Nordberg, E.K., Olsen, G.J., Murphy-Olson, D.E., Olson, R., Overbeek, R., Parrello, B., Pusch, G.D., Shukla, M., Vonstein, V., Warren, A., Xia, F., Yoo, H., and Stevens, R.L. (2017). Improvements to PATRIC, the all-bacterial bioinformatics database and analysis resource center. *Nucleic Acids Res.* 45**,** D535-d542.

Wei, R., and Zimmermann, W. (2017). Microbial enzymes for the recycling of recalcitrant petroleum-based plastics: how far are we? *Microb. Biotechnol.* 10**,** 1308-1322.

Wickham, H. (2016). ggplot2: Elegant graphics for data analysis. Springer-Verlag, New York, NY.

Wilbanks, E.G., Jaekel, U., Salman, V., Humphrey, P.T., Eisen, J.A., Facciotti, M.T., Buckley, D.H., Zinder, S.H., Druschel, G.K., Fike, D.A., and Orphan, V.J. (2014). Microscale

sulfur cycling in the phototrophic pink berry consortia of the Sippewissett Salt Marsh. *Environ. Microbiol.* 16**,** 3398-3415.

Wilcox, C., Van Sebille, E., and Hardesty, B.D. (2015). Threat of plastic pollution to seabirds is global, pervasive, and increasing. *Proc. Natl. Acad. Sci. U. S. A.* 112**,** 11899-11904.

Winn, H.E., Beamish, P., and Perkins, P.J. (1979). Sounds of two entrapped humpback whales (*Megaptera novaeangliae*) in Newfoundland. *Mar. Biol.* 55**,** 151-155.

Witt, V., Wild, C., and Uthicke, S. (2011). Effect of substrate type on bacterial community composition in biofilms from the Great Barrier Reef. *FEMS Microbiol. Lett.* 323**,** 188-195.

Wöhlbrand, L., Jacob, J.H., Kube, M., Mussmann, M., Jarling, R., Beck, A., Amann, R., Wilkes, H., Reinhardt, R., and Rabus, R. (2013). Complete genome, catabolic sub-proteomes and key-metabolites of *Desulfobacula toluolica* Tol2, a marine, aromatic compound-degrading, sulfate-reducing bacterium. *Environ. Microbiol.* 15**,** 1334-1355.

Woodall, L.C., Sanchez-Vidal, A., Canals, M., Paterson, G.L.J., Coppock, R., Sleight, V., Calafat, A., Rogers, A.D., Narayanaswamy, B.E., and Thompson, R.C. (2014). The deep sea is a major sink for microplastic debris. *Royal Soc. Open Sci.* 1**,** 140317.

World Economic Forum - Ellen Macarthur Foundation. (2016). The new plastics economy - rethinking the future of plastics. World Economic Forum, Ellen MacArthur Foundation, World Economic Forum, Ellen MacArthur Foundation.

Xanthos, D., and Walker, T.R. (2017). International policies to reduce plastic marine pollution from single-use plastics (plastic bags and microbeads): A review. *Mar. Pollut. Bull.* 118**,** 17-26.

Yang, Y., Yang, J., Wu, W.M., Zhao, J., Song, Y., Gao, L., Yang, R., and Jiang, L. (2015). Biodegradation and mineralization of polystyrene by plastic-eating mealworms: Part 2. role of gut microorganisms. *Environ. Sci. Technol.* 49**,** 12087-12093.

Yoshida, S., Hiraga, K., Takehana, T., Taniguchi, I., Yamaji, H., Maeda, Y., Toyohara, K., Miyamoto, K., Kimura, Y., and Oda, K. (2016). A bacterium that degrades and assimilates poly(ethylene terephthalate). *Science* 351**,** 1196-1199.

Zecchin, S., Mueller, R.C., Seifert, J., Stingl, U., Anantharaman, K., Von Bergen, M., Cavalca, L., and Pester, M. (2018). Rice paddy *Nitrospirae* carry and express genes related to sulfate respiration: proposal of the new genus "*Candidatus* Sulfobium". *Appl. Environ. Microbiol.* 84**,** e02224-02217.

Zerbino, D.R., and Birney, E. (2008). Velvet: algorithms for de novo short read assembly using de Bruijn graphs. *Genome Res.* 18**,** 821-829.

Zettler, E.R., Mincer, T.J., and Amaral-Zettler, L.A. (2013). Life in the "plastisphere": microbial communities on plastic marine debris. *Environ. Sci. Technol.* 47**,** 7137-7146.

Zhou, J., Bruns, M.A., and Tiedje, J.M. (1996). DNA recovery from soils of diverse composition. *Appl. Environ. Microbiol.* 62**,** 316-322.

APPENDICES.

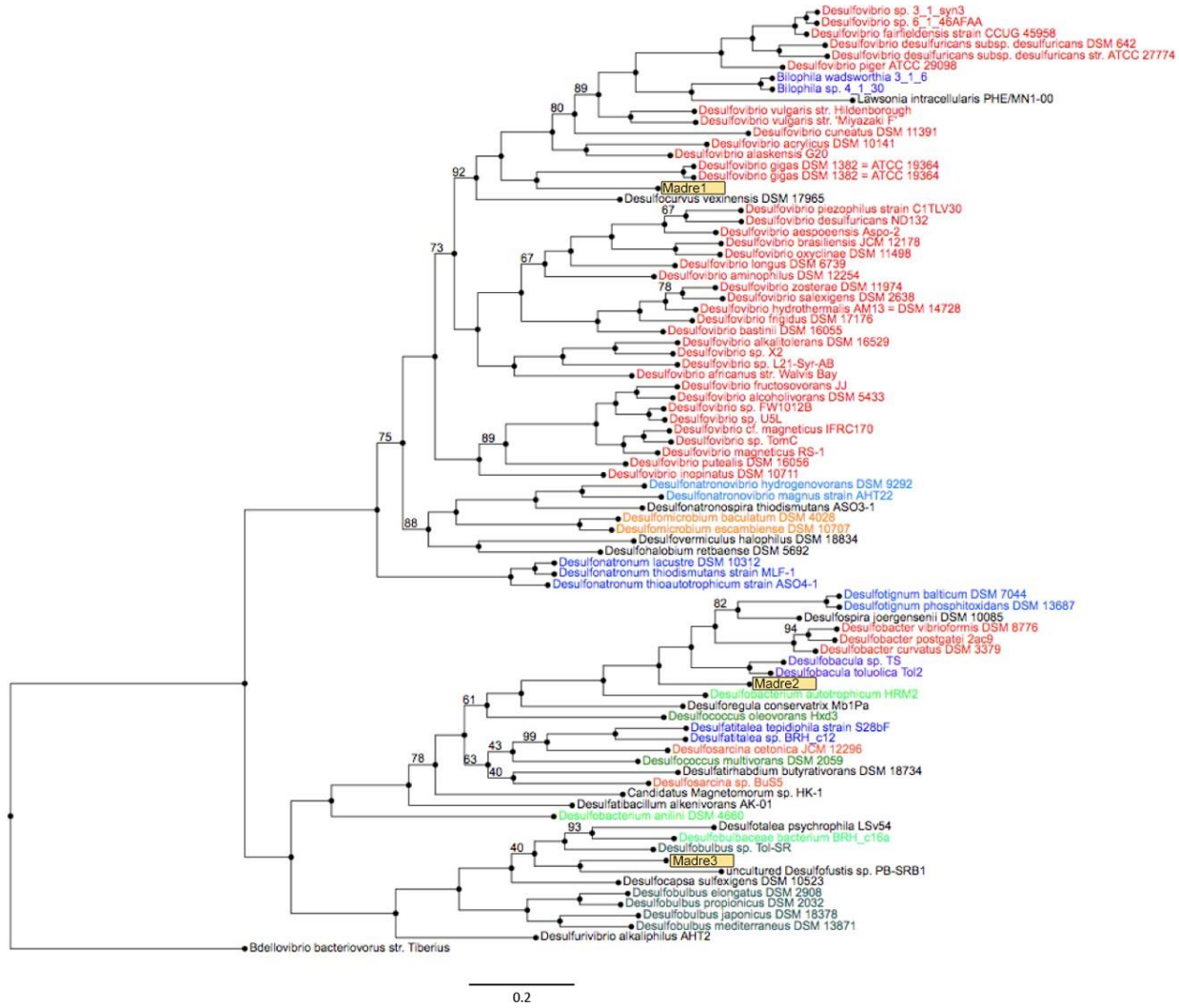

Appendix 1. The complete phylogenetic tree containing the three PHA biofilm SRMs recovered in this study (highlighted in yellow). The coloration of labels corresponds to different taxa contained within the tree. Branch labels show the bootstrap support values. Unlabeled nodes have support values of 100. Branch lengths represent the average number of substitutions per site. The tree is rooted to a distantly related Deltaproteobacteria (*Bdellovibrio bacteriovorans*).

Appendix 2. The complete phylogenetic tree containing the two isolates (SRB1LM and SRB3LM) from the PHA biofilm community classified as species of *Bacillus*. Branch labels show the bootstrap support values. Branch lengths represent the average number of substitutions per site. The tree is rooted to a distantly related Bacillaceae (*B. clausii* KSM-K16).

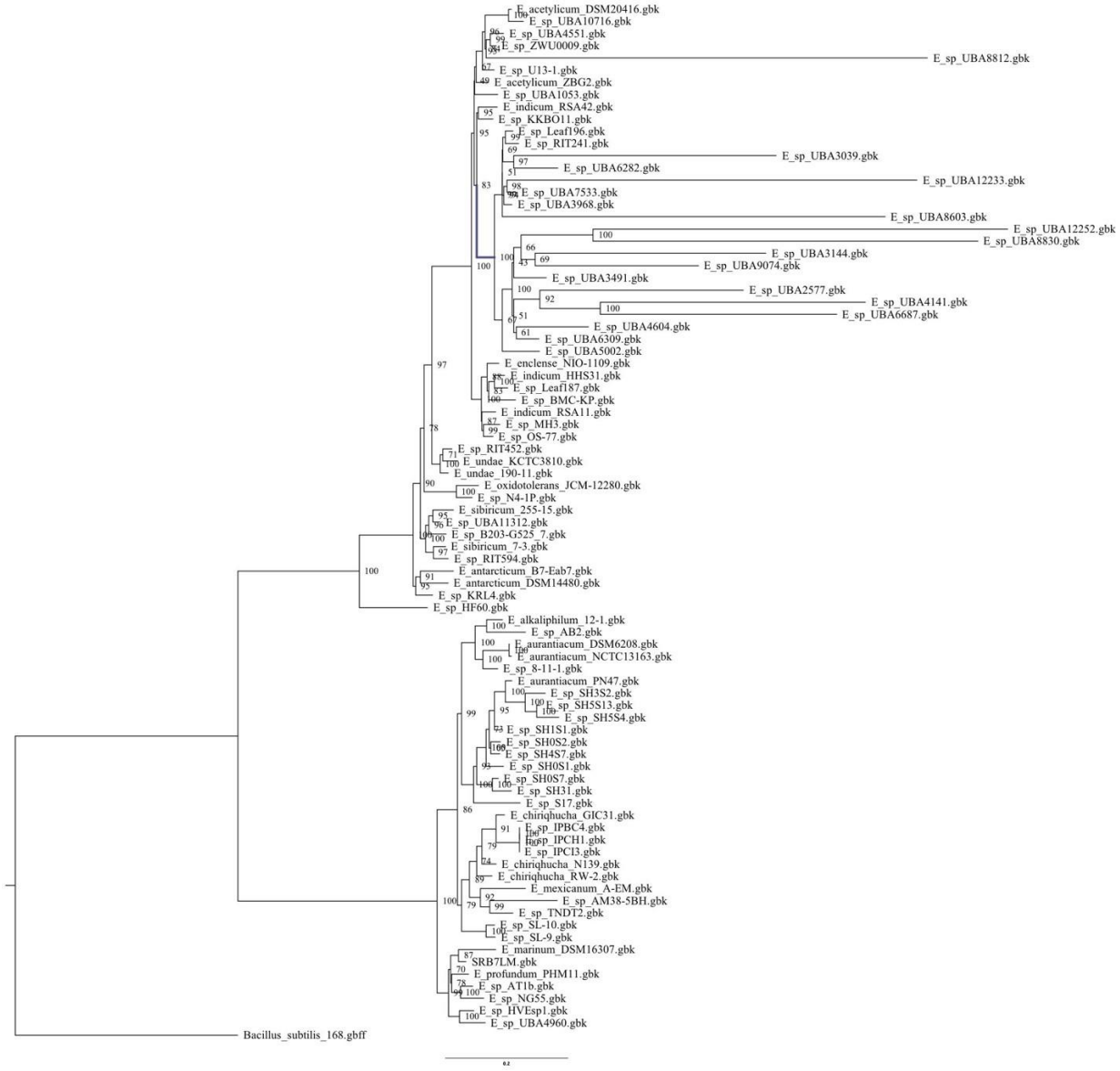

Appendix 3. The complete phylogenetic tree containing the isolate (SRB7LM) from the PHA biofilm community classified as a species of *Exiguobacterium.* Branch labels show the bootstrap support values. Branch lengths represent the average number of substitutions per site. The tree is rooted to a distantly related Bacillaceae (*B. subtilis* 168).